UNIVERSITEIT•STELLENBOSCH•UNIVERSITY
jou kennisvennoot • your knowledge partner

Towards a Practical Resource Assessment of the Extractable Energy in the Agulhas Ocean Current

Can the Agulhas Current be considered for a base-load supply of electricity?

Imke Meyer

Project presented in partial fulfilment of the requirements for the degree of Master of Engineering (Mechanical) in the Faculty of Engineering at Stellenbosch University

Supervisor: Prof J. L. Van Niekerk

December 2015

Departement Meganiese en Megatroniese Ingenieurswese

Department of Mechanical and Mechatronic Engineering

DECLARATION

By submitting this assignment electronically, I declare that the entirety of the work contained therein is my own, original work, that I am the sole author thereof (save to the extent explicitly otherwise stated), that reproduction and publication thereof by Stellenbosch University will not infringe any third party rights and that I have not previously in its entirety or in part submitted it for obtaining any qualification.

Signature: .....
I. Meyer

Date: .....

ABSTRACT

The Agulhas Current is South Africa's swift flowing western boundary current. To analyse this current, two ADCP deployment series are examined: the first from an exploratory mission to find an energetic site and the second for a detailed assessment to quantify the resource at the found site. The found energetic region lies approximately 32.51˚ S and 28.83˚ E. In this region a mid-shelf location (91 m depth) and an off-shore location (255 m depth) are evaluated. It is found that the current core boarders on the mid-shelf location and passes over the off-shore location with mean velocities of 1.34 m/s and 1.59 m/s respectively at a 30 m depth. The presence of one Natal Pulse is seen in the dataset, this is lower than the published average of 1.6 pulses a year. It was found that Natal Pulses can be tracked through the use of remote sensing. This is advantageous as up to 15 days warning can be established prior to the Pulse arriving at a potential ocean current power plant.

The most suited, developed technology found to potentially deploy in this current are Minesto Deep Green turbines. The found capacity factor and specific yield for one Minesto (DG-12) 500 kW turbine at 30 m depth was estimated to be 62% and 4 886 kWh/kW for the mid-shelf location and 76% and 5 416 kWh/kW for the off-shore location. Although the 500 kW turbine performs well, there is still scope to optimise this turbine for the specific Agulhas Current conditions. Through a simplified analysis, the capacity credit of a possible 2 000 MW array is analysed. It is found that an ocean current power plant can add to the load carrying capacity of the country and outperforms wind power plants in this respect. Environmental, economic and social aspects of installing an ocean current plant in the selected area are considered. The selected sites are well positioned with respect to grid connectivity as the nearest medium voltage substation is 30 km from the point of contact at the coastline. Further the sites are not located within any existing or proposed marine protected areas or prime fishing grounds, however a detailed environmental assessment will have to be carried out to ensure no harmful impacts results if such a plant is commissioned. The largest barriers at present are the cost and mooring challenges and there is a need for a detailed economic assessment to determine if associated cost of working in deeper waters (off-shore site) is justified. If the mooring challenges in water depths of 250 m or greater are overcome then such a turbine array can make a significant contribution to the South African electricity grid.

UITTREKSEL

Die Agulhas seestroom is ‘n vinnige vloeiende stroom wat langs die Oos-Kus van Suid Afrika vloei. Die sterkte van die stroom is deur middel van twee afsonderlike stelle akoestiese meetinstrumente wat die vloei tempo en rigting bepaal, gemeet. Eerstens is ‘n ligging gesoek waar die meeste energie gevind kan word, en tweedens is ‘n in-diepte waardebepaling gedoen om die hulpbron by die betrokke ligging te bepaal. Die grootste energiebron lê by ongeveer 32.51°S and 28.83°O. In hierdie area is ‘n analise op ‘n posisie halfpad op die kontinentale bank (91 m waterdiepte) en ‘n posisie in die diepsee van die bank af (255 m waterdiepte) gedoen. Daar is bevind dat die seestroom kern aan die mid-bank posisie grens en vloei oor die diepsee ligging teen ‘n gemiddelde snelheid van 1.34 m/s en 1.59 m/s by ‘n waterdiepte van 30 m. Volgens die data kom daar net een Natal Puls in die gemoniteerde tydperk in die area voor teenoor die voorheen gepubliseerde gemiddeld van 1.6 pulse per jaar. Daar is gevind dat die Natal Pulse gemeet kan word met behulp van afstand sensore. Hierdie inligting is voordelig as gevolg van die feit dat daar tot 15 dae vooraf waarskuwings gegee kan word voordat ‘n Natal Puls by ‘n potensiële kragopwekker opdaag.

Die mees geskikte, ontwikkelde tegnologie wat potensieel in die Agulhas seestroom ontplooi kan word, is die Minesto Deep Green seestroom turbines. Dit word beraam dat die kapasiteit-faktor sowel as die spesifieke energie opbrengs van een Minesto (DG-12) 500 kW turbine op ‘n diepte van 30 m 62% en 4 886 kWh/kW by die mid-bank ligging beloop en 76% en 5 416 kWh/kW in die diepsee posisie. Alhoewel hierdie 500 kW turbine goed presteer is daar wel geleentheid vir verbetering en optimering met betrekking tot die spesifieke stroom kondisies van die Agulhas seestroom. Deur middel van ‘n vereenvoudigde analise is die kapasiteit krediet van ‘n moontlike 2 000 MW groep turbines geanaliseer. Daar is bevind dat ‘n seestroom kragstasie ‘n positiewe bydrae kan lewer tot die elektrisiteit opwekkings-kapasiteit van die land en lewer ‘n selfs beter opbrengs as windenergie in hierdie sin. Omgewings, ekonomiese en sosiale aspekte met betrekking tot die installering van ‘n seestroom kragopwekker in die bogenoemde liggings is in ag geneem. Met betrekking tot konnektiwiteit tot die nasionale krag netwerk is die posisies goed geplaas want die naaste medium-spanning substasie lê 30 km van die landings punt op die kuslyn af. Verder is die bepaalde liggings nie naby enige bestaande of toekomstige mariene reservate of visvang gebiede geleë nie. Daar sal wel ‘n omgewingsimpakstudie gedoen moet word. Die grootste hindernis tans is die koste van so ‘n kragstasie sowel as die uitdagings met betrekking to die verankering van die turbines. Daar sal ‘n in-diepte ekonomiese beraming gedoen moet word om te bepaal of die kostes verbonde aan ‘n dieper verankering-posisie haalbaar is. As die ander uitdagings in diep waters van 250 m of dieper, oorkombaar is, sal ‘n turbine van hierdie aard ‘n substansiële bydrae kan lewer tot die Suid Afrikaanse kragnetwerk.

ACKNOWLEDGEMENTS

I would like to acknowledge the South African national utility Eskom for making the data available without which this research would not have been possible.

I would like to thank my supervisor Prof. J. L. Van Niekerk for the guidance I received during the course of this work. Further I would like to acknowledge my parents for the continual support and encouragement during this endeavor.

TABLE OF CONTENTS

LIST OF FIGURES

LIST OF TABLES

NOMENCLATURE

CC	Capacity credit
EFC	Equivalent firm capacity
PF	Packing factor
V	Velocity
A_i	Swept area
A_o	Operating area
C_f	Capacity factor
C_p	Turbine efficiency
P_d	Power density
P_r	Rated power
$\bar{V}_E$	mean eastward component of velocity
$\overline{V}_N$	mean northward component of velocity
d_i	Turbine diameter
v_{ins}	Instantaneous velocity
v_{rated}	Rated turbine speed
θ_i	Instantaneous flow direction
θ_{std}	Standard deviation of direction
$\bar{\theta}$	Mean flow direction
ρ	Water density
σ	Time varying velocity

1. INTRODUCTION

South Africa is a resource rich country in respect to both fossil fuels (coal) and renewable energy (solar, wind, biomass and ocean resources). Currently South Africa's energy generation is very carbon intensive, and increased international pressure calling for South Africa to reduce its carbon emissions, has stimulated interest in renewable energy. The Department of Energy is facilitating the implementation of utility scale renewable energy power plants through the Renewable Energy Independent Power Producers Procurement Programme. This programme mainly focuses on solar, wind and biomass conversion technologies. These technologies are well developed and the resources well documented. Ocean energy resources are not as well documented, and on a global scale the technology is yet to converge. The ocean wave resource along the South African coast has been documented by Stellenbosch University in the past (Joubert, 2008); however the ocean current resource is yet to be explored. The aim of this report is to characterise the ocean current resource along the South African coast towards a resource assessment for the purpose of marine energy extraction.

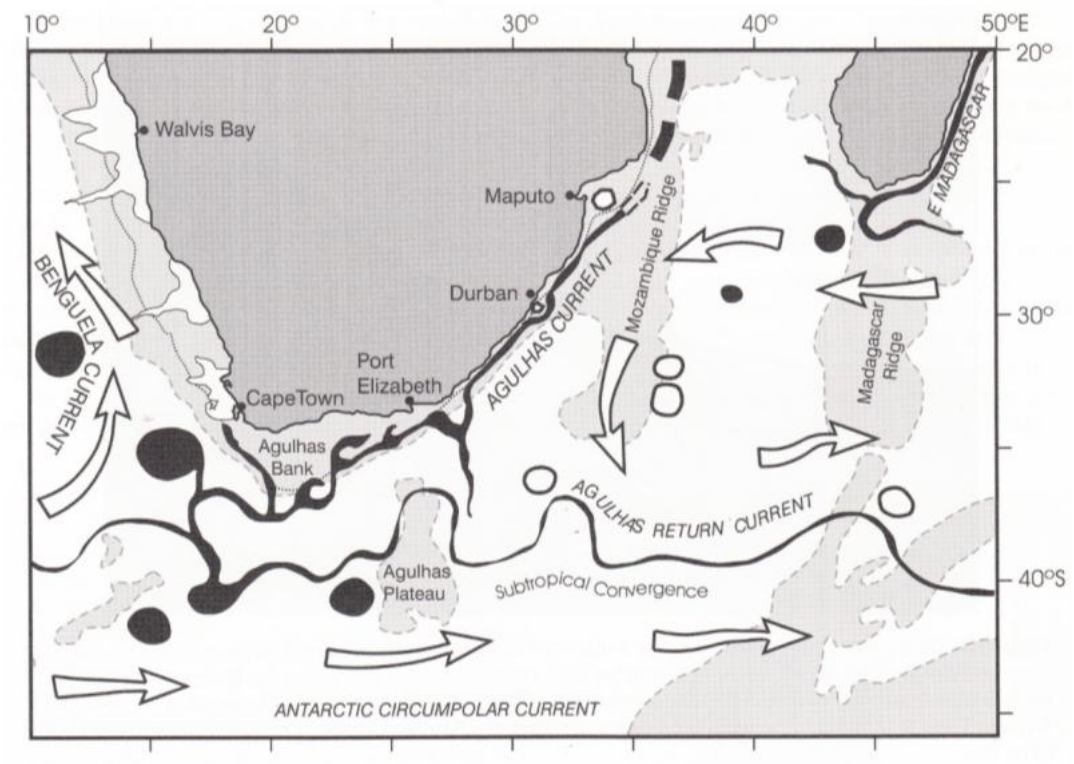

Figure 1: Schematic of ocean currents around South Africa. Areas shallower than 3000 m are shaded; edge of the continental shelf is circumscribed by a 500 m isobaths, indicated by a dotted line. (Lutjeharms, 2006)

The ocean currents around the world carry great potential for energy extraction and electricity generation. Looking at South Africa there are two predominant currents which flank the coastline. The Agulhas Current flanks the western boundary of the Indian Ocean and the Benguela Current the eastern boundary of the Atlantic Ocean, as shown in Figure 1. Figure 1 illustrates the positioning and the flow of these currents and as illustrated, the Agulhas Current flows towards the South Pole and the Benguela Current towards the Equator. It has been proposed in the past that the energy contained in these currents can be harnessed to generate electricity.

This report examines the Agulhas Current characteristics and attempts to quantify how the found behaviour will impact potential for power production. In the following section, a detailed literature survey is carried out to examine past oceanographic work and published methods on quantification of ocean current resources. In section 3, the resource assessment methodology used for the quantification of the Agulhas Current is presented. Section 4 presents a technology review for the purpose of finding an appropriate technology to harness the energy of the Agulhas Current. The results of the assessment are presented in Section 5 and followed by a conclusion. Section 5 presents results on the technical aspects of harnessing energy from the Agulhas Current as well as considering the environmental and social impacts of such an endeavour. The analysis of the Current is achieved through the examination of *in situ* ADCP (Acoustic Doppler Current Profiler) measurements taken from 2006 to 2013. The focus area of the analysis lies between the latitudes of 31˚S and 34˚S as indicated by Figure 2.

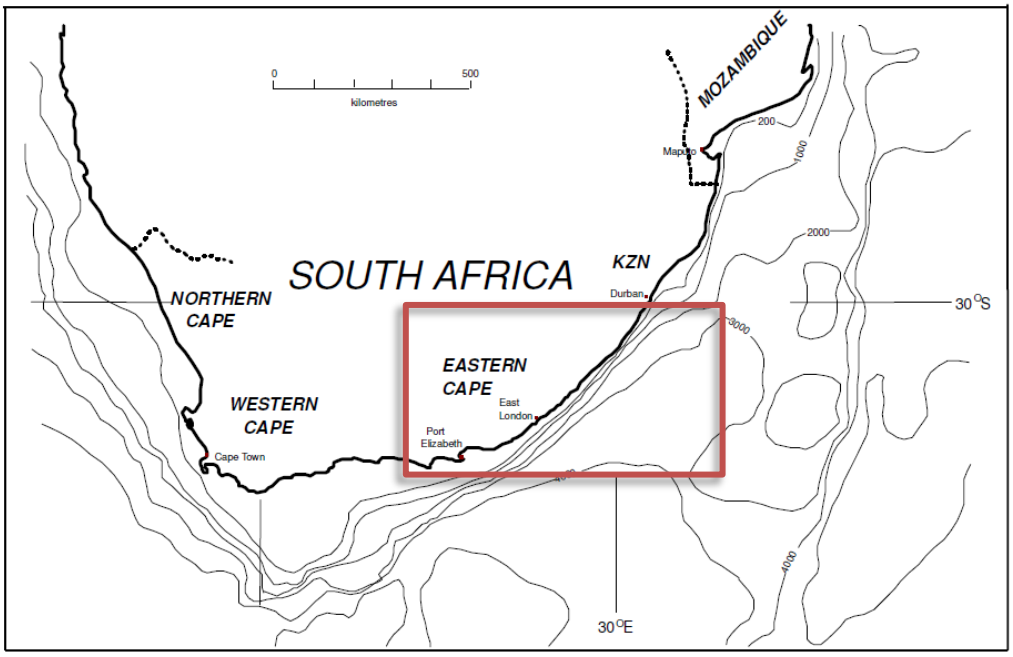

Figure 2: Position of ADCP deployments

2. LITERATURE SURVEY

2.1. Ocean Currents

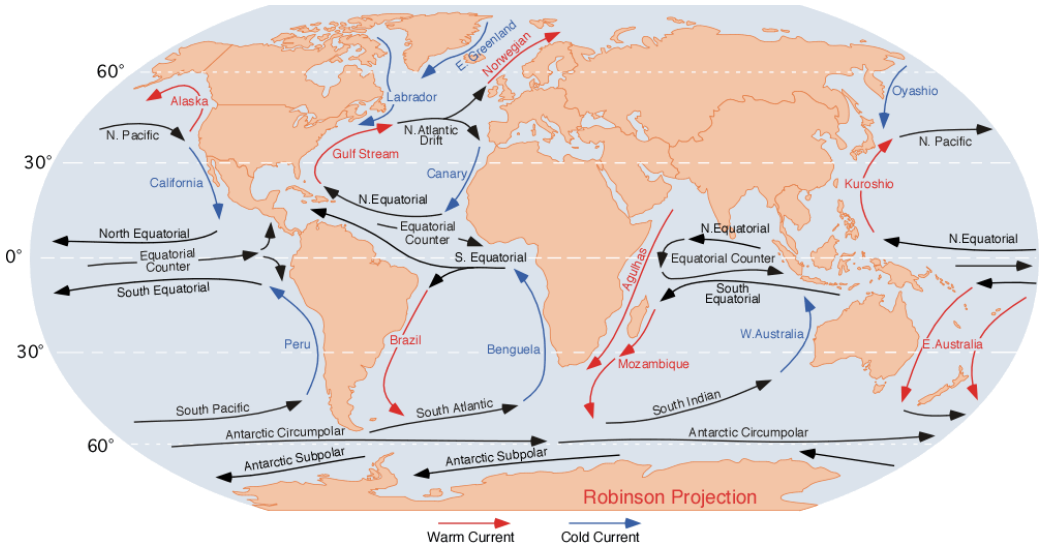

Figure 3: Global ocean current circulation (Pidwirny, 2006)

Figure 3 shows the global ocean current circulation with the major currents highlighted. It is seen that the Agulhas Current is a warm western boundary current. Each current has its own features but most western boundary currents have similar characteristics. Western boundary currents are narrow, intense, flow poleward and are driven by the zonally integrated wind stress curl of the adjacent basins (Lutjeharms, 2006). These characteristics make the Agulhas Current, the Gulf Stream, the Kuroshio, the Brazil Current and East Austrian Current of interest to the marine energy industry.

2.2. The Agulhas Current

The focus of this ocean current assessment is on the Agulhas Current since it has been found that the Benguela Current has mean flow speeds that are too low to drive marine turbines. The mean speeds of the Benguela Current range from 0.11 to 0.23 m/s and transports between 15 and 20 Sv[1] (Gyory, et al., 2012), too low to drive marine turbines and thus the Benguela Current is not further analysed. The Agulhas Current is stronger than the Benguela Current and it has been found to have approximate transport values of 70 Sv (Bryden, et al., 2005).

The Agulhas Current has been studied spatially by mariners since it lies in the path of one of the world's busiest trade routes and ships need to avoid it on the

[1] A Sv is a Sverdrup, a unit to measure current flow. 1 Sv = 10^6 m^3/s

way out to the East and use it to their advantage coming from the East (Beal & Bryden, 1999). However the vertical structure of the current is poorly documented. For the purpose of marine energy extraction, the vertical structure of the water column is important as the velocity of the current depends on depth. Many studies have been carried out that focus on the oceanographic properties of the current. However the focus on this resource assessment is rather on the directionality and velocity structure of the current. The vertical volumetric and velocity transport properties of the Agulhas current has been researched with predominant findings published by Beal and Bryden (1999) and Bryden, Beal, and Duncan (2005). Each of these analyses is done at a low resolution covering hundreds of kilometres and focus on the oceanographic properties of the current. Furthermore, the variability of the current is of interest with publications seen by Rouault and Penven (2011) and Krug and Tournadre (2012).

2.2.1. Macro effects

Situated to the east of South Africa, the Agulhas Current forms the western boundary of the Indian Ocean subtropical gyre carrying warm tropical and sub-tropical water southward (Lutjeharms, 2006) . It has been found by Bryden, Beal and Duncan (2005) that the Agulhas current is the largest western boundary current in the Southern hemisphere, indicating that this current holds a large amount of untapped energy that has the potential to be harnessed through the use of suitable ocean turbines.

The Agulhas current is a surface current which is wind driven. It is instrumental in the meridional overturning circulation and the effects of deploying turbines in the current's path need to be assessed. The largest source of water mass contribution to the Agulhas Current is the Agulhas Current recirculation water followed by the Mozambique Current and the East Madagascar Current. The current becomes fully formed somewhere north of Durban (-29.87°, 31.10°) and as it travels south closely follows the South African continental shelf. The continental shelf between Maputo (-25.96°, 32.61°) and Port Elizabeth (-33.95°, 25.67°) is narrow, never exceeding 25 km from the coast to the 200 m isobath (Lutjeharms, 2006). This narrow continental shelf results in the current flowing near the shore with a high velocity. Such characteristics make the Agulhas Current attractive for marine energy extraction.

The narrow shelf with a steep continental slope and uncomplicated topography helps stabilize the Agulhas Current in this region and thus no regular wide meanderings are present. However, there is one area of exception – The Natal Bight, situated between Durban and Richards Bay (-28.81, 32.12). This area has a wider continental shelf and the shelf's morphology change destabilizes the Agulhas Current, resulting in infrequent formation of cyclonic meanders known as Natal Pulses (Lutjeharms, 2006). These solitary meanders propagate southward,

growing in diameter as they travel, with recorded diameters of up to 200 km near Port Elizabeth. This results in the core of the current being displaced seaward the distance of the meander's diameter. Further discussion on these perturbations is carried out in section 2.2.3.

2.2.2. Velocity Structure and Volume Transport

Making use of Acoustic Doppler Current Profilers (ADCP) detailed vertical structural analysis of the Agulhas Current was carried out by Beal and Bryden (1999) and Bryden, Beal, and Duncan (2005). Further Rouault (2010) made use of satellite altimetry data to examine behavioural characteristics that influence the volume transport of the Agulhas Current.

In the article *The Velocity and Vorticity structure of the Agulhas Current at 32°S* (Beal & Bryden, 1999), 14 hydrographic stations were placed perpendicular to the coastline spanning a distance of 230 km from shore, as shown in Figure 4. Also seen in Figure 4 the area of investigation lies beside the continental shelf with the near shore ADCP deployed on the sea side of the 200 m isobaths. The aim of this investigation was to better understand the deep velocity structure of the current.

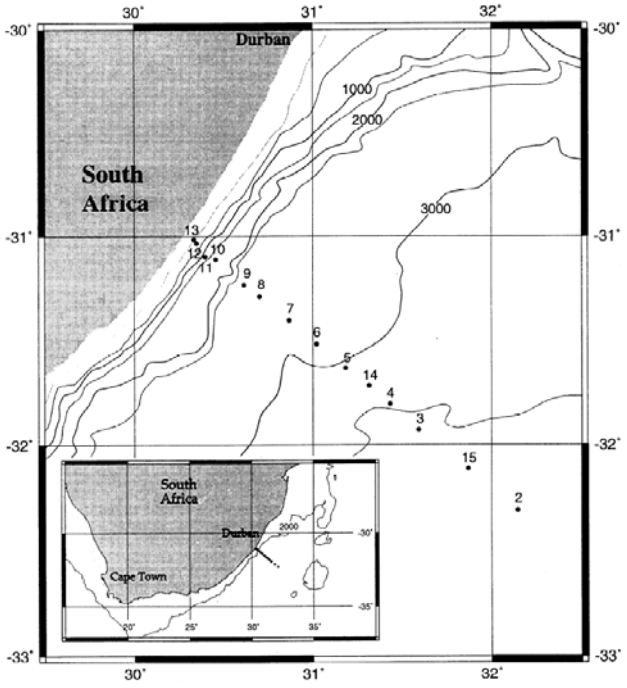

Figure 4: Hydrographic station placement (Beal & Bryden, 1999)

Beal and Bryden(1999) compare direct and geostrophic velocity profiles. In order to determine the geostrophic velocity profiles, the method of zero velocity surface based on water mass distribution is used. With this method a volume transport of

82 Sv is found. This value is then compared to the direct velocity measurements whereby a volume transport of 73 Sv is found. The difference in volume transport is due to the measurements captured by the ADCPs that quantify the presence of the Agulhas undercurrent. Through the direct velocity analysis it is found that the current lies 20 km from the coast, is approximately 90 km wide and has maximum measured surface velocities of 1.8 m/s. In order to achieve a comprehensive velocity profile the measured ADCP data is extrapolated; firstly vertically at each station then to the zero velocity edge on the continental slope. During data analysis Beal and Bryden attempt to minimize the effects of velocity averaging when presenting the velocity profile through the use of water mass considerations. In this investigation temporal averaging conditions were not considered.

The achieved 'v' shaped velocity profile is seen in Figure 5. It has been found that the core of the current moves increasingly offshore with depth and that the current possesses large vertical shears at the zero velocity contour between the depths of 300 and 800 m at station 11, Figure 6.

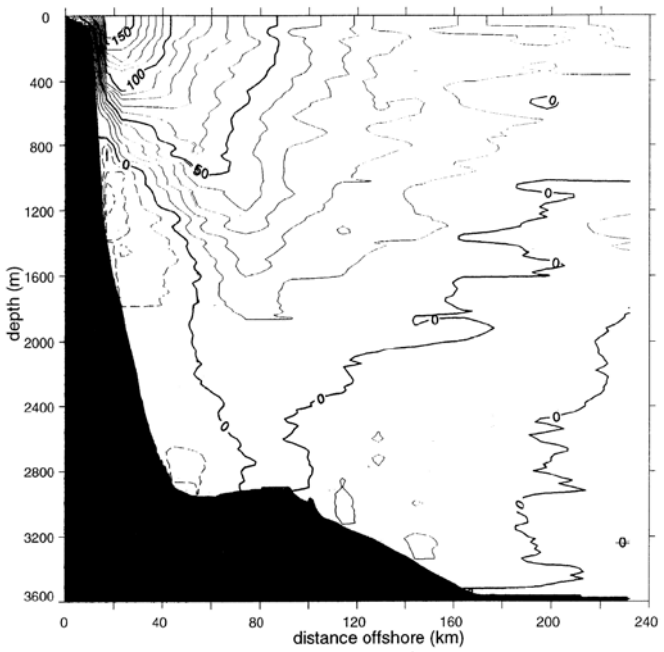

Figure 5: Velocity structure [cm/s] (Beal & Bryden, 1999)

This shows the presence of the Agulhas undercurrent travelling in a north westerly direction. Owing to the area of investigation, this research is useful in characterising the overall volume transport of the Agulhas Current but it will not be useful in determining current velocities in shallow enough areas for marine energy extraction. This research also shows that the presence of the Agulhas undercurrent will not hamper the deployment or output of turbines as the undercurrent only becomes a significant feature at depths below 800 m.

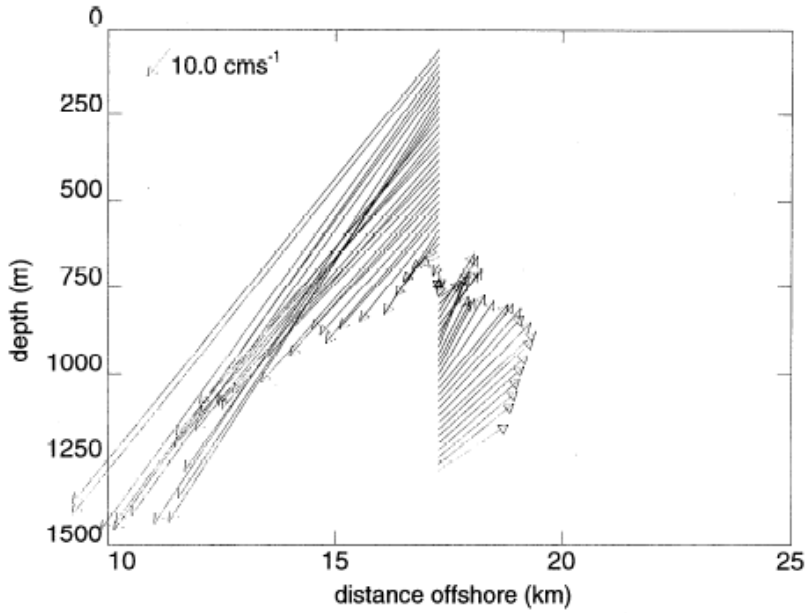

Figure 6: Velocity vectors at station 11 (Beal & Bryden, 1999)

Further investigation into the structure, transport and temporal variability of the Agulhas Current was carried out in 2005 by Bryden, Beal, and Duncan, (2005). The Agulhas Current was measured with the use of 6 moorings perpendicular to the coast of Port Edward, as seen in Figure 7. The six mooring were placed 13.4, 18.8, 32.4, 61.7, 101.9 and 152.8 km from the coast. Mooring A was completely lost and mooring B damaged, resulting in the velocity data for the water column ranging between 400 m and 50 m below the surface from mooring B and C. This dataset was part of the World Ocean Circulation Experiment, (the same data as Beal and Bryden (1999) used) but in this analysis temporal conditions were taken into consideration with a greater sensitivity to the variability of the current.

In order for a comprehensive representation of the behaviour of the Agulhas Current to be realised, the values obtained at specific depths at each of the moorings have been interpolated vertically and extrapolated laterally. This method of data manipulation has resulted in reliable values being achieved for the velocity of the Agulhas Current. Owing to the vast area that has been covered, the resolution of the data is coarse, where only daily values are taken from the temporal data. Bryden et al (2005) took the variability into account when examining the mean characteristics of the Agulhas Current through the use of composite spectral analysis. With the use of this analysis, the mean structure of the Agulhas Current was developed as seen in Figure 8.

Through the use of this mean structure, Bryden et al (2005) examined the total transport that is achieved by the Agulhas Current. It was concluded in the study that a transport of -69.7 Sv ± 4.3 Sv is achieved by the Agulhas Current at 31^{o} S, where the negative sign indicates the southward direction in which the current

flows. The transport value was found by integrating the velocity from the coast to 203 km offshore, and from 2 400 m below the surface to the sea surface for each day recorded. This value is 5% less than the value found by Beal and Bryden (1999).

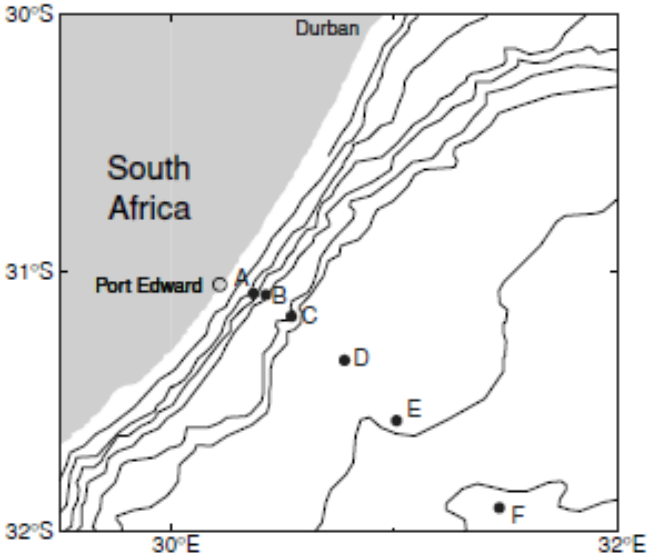

Figure 7: Mooring placement used by Bryden, Beal and Duncan (2005)

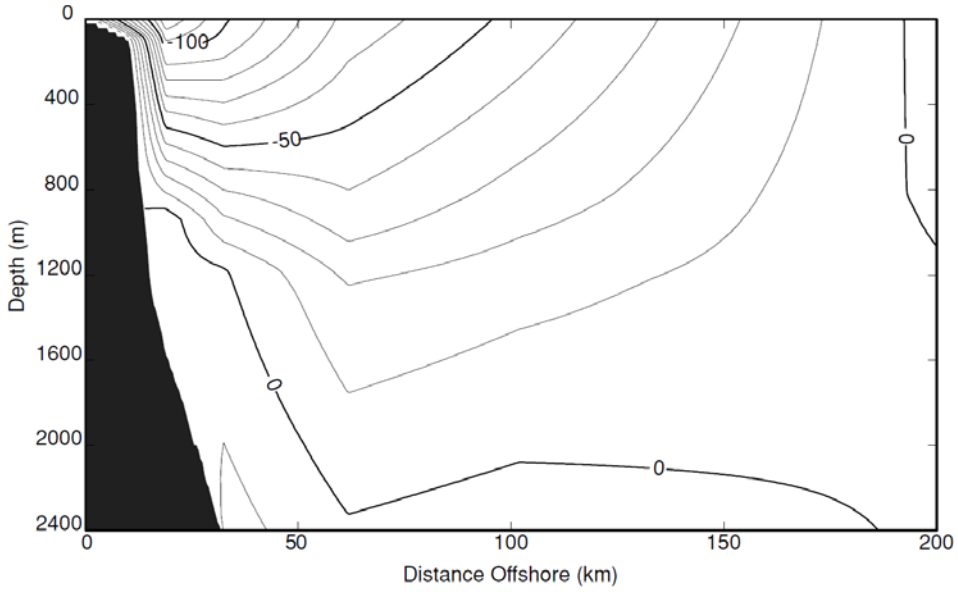

Figure 8: Mean structure of the Agulhas Current presented by Bryden et al (Bryden, et al., 2005)

Further this research did not see the prominent ‘v’ shaped profile of the zero velocity contour as discovered by Beal and Bryden (1999). Again the focus area of this research is too far off shore to be applicable for marine energy research, but the found transportation values indicate the power of the current, with velocity

magnitudes being the most promising at the surface near the continental shelf edge.

The presence of the Agulhas Undercurrent cannot be ignored when examining the overall transport and velocity profiles of the Agulhas Current. The undercurrent flows towards the equator along the continental shelf. The depth of the undercurrent varies with distance from shore but the undercurrent is found at deeper depths as the distance from the shore increases. Bryden et al. (2005) states that the average depth of the undercurrent is 2 218 m in regions further than 60 km from the shore.

The volume transport of the Agulhas Undercurrent can be seen in Figure 9 where a comparison is made between the transport of the Undercurrent and the Agulhas Current. It is seen that the Agulhas Current has a far larger transport capacity and larger variability compared to the Undercurrent's much smaller transport capacity but less variability. It has been calculated that the undercurrent transport is an average of 6±1 Sv (Beal & Bryden, 1999). This average transport in the north east direction shows that there is a persistent undercurrent.

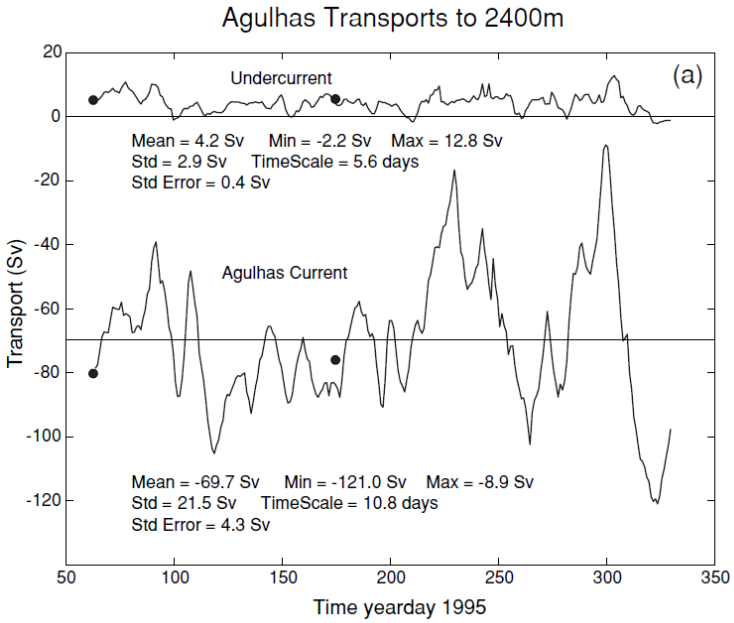

Figure 9: Agulhas Current transports (Bryden, et al., 2005)

The Undercurrent always flanks this zero velocity contour where one component of the undercurrent runs alongside the continental slope and the other on the offshore side of the Agulhas Current profile (Beal, 2003). This formation is clearly seen in Figure 10 where the blue contours indicate the undercurrent. The Agulhas Undercurrent is relatively independent of the Agulhas Current for the undercurrent does not affect the velocity of the Agulhas Current (Bryden, et al., 2005). The Undercurrent will affect power extraction technology performance if

the technology is situated in the undercurrent's sphere of influence, due to the opposite direction in which the Agulhas Current and Undercurrent flow.

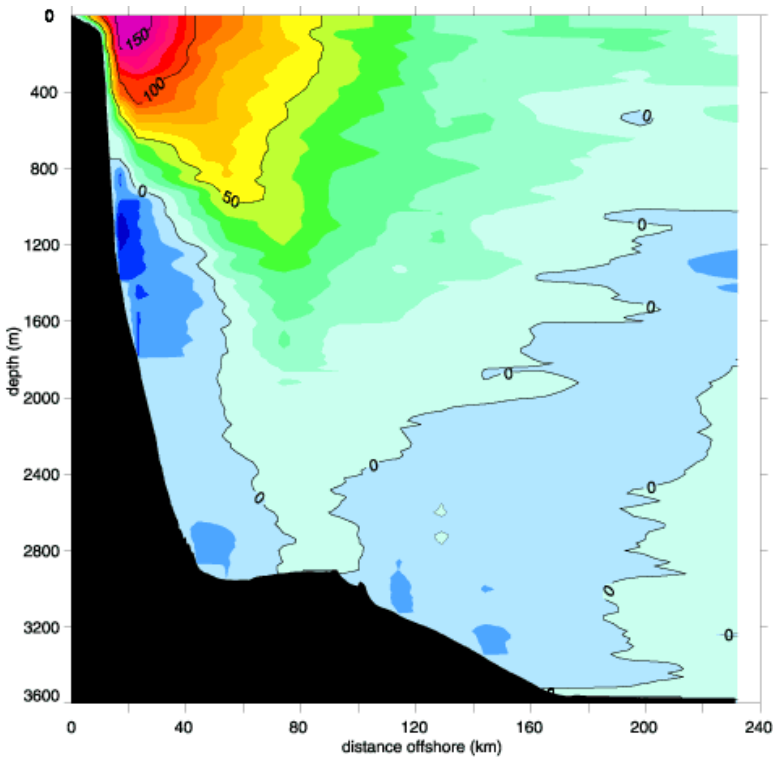

Figure 10: The undercurrent can be seen in blue (negative flow direction) and the Agulhas Current in red (positive flow direction) (Beal, 2003)

2.2.3. Variability

The effects of the Agulhas Current variability must be carefully examined to help understand the nature of this resource. The dominant form of variability is the presence of the Natal Pulses, which form in the region of the Natal Bight (Lutjeharms, 2006). Other factors include wind forcing from the Indian Anticyclone, and forcing from source regions, namely the southern branch of the East Madagascar Current flowing through the Mozambique channel and recirculation of the Agulhas Current. There are also daily meanders which can displace the Current's core.

Natal Pulses are "large solitary meanders in the Agulhas Current associated with a cold-water core and a cyclonic circulation inshore of the current" (Rouault, 2011). The formation of the Natal Pulse is attributed to the change in slope of the continental shelf in the Durban region, which causes the instability of the current and the formation of these pulses. The pulses grow steadily in diameter as they move south-westward along the continental slope, with a typical diameter of 150 km. The pulses have a phase velocity of approximately 10 to 20 km per day (Rouault, 2011). The pulses cause the Agulhas Current to move off course, so by

the time the pulse passes the Port Elisabeth region, it has moved the Agulhas Current core approximately 200 km seaward from its normal location (Lutjeharms, 2006).

Rouault and Penven (2011) presented the research, *New perspectives on Natal Pulses from satellite observations* making use of Sea Surface Temperature (SST) data in order to evaluate the variability of Agulhas Current. Rouault and Penven (2011) identified Natal Pulses in the dataset analysed as follows: “that the Agulhas Current inshore front meander is displaced more than 30 km from its mean position and that the pulse lasts for more than 10 days”. This is based on the results of Bryden et al. (2005), where the average found timescale associated with alongshore fluctuation is 10.2 days. With these criteria, it is found that Natal Pulses occur at the latitude of Port Elizabeth with a mean frequency of 1.6 times a year, with irregular time intervals of 50 to 240 days. Although the mean frequency is only 1.6 times a year, it has been found that the Current can be affected by the presence of Natal Pulses for up to 110 days a year. This is significant in respect to power production and will negatively impact the capacity factor of the resource.

It was found that once the Natal Pulse was formed, one of three actions can occur: meander dissipation, meander merging or meander occlusion. Ideally if meander dissipation occurs before the pulse reaches a potential turbine array, the power output from the array will remain relatively unchanged. If meander merging takes place, a Natal Pulse will merge with an offshore meander, forming a larger Natal Pulse. Such a formation is illustrated in Figure 11. Lastly, if meander occlusion occurs, the Natal pulse becomes unstable and an enclosed cyclonic eddy forms and detaches from the current moving offshore. Such occurrences are very infrequent.

The long periods of satellite data used in remote sensing is valuable, however this data only considers surface behaviour and traits and cannot be used to establish the characteristics of the current below the surface. It is these characteristics that are required when assessing a resource for marine current turbines.

The presence of a Natal Pulse in the water column is seen as the sharp decrease in velocity at the location of the current’s core (indicating that the core has been displaced) and the direction of the current reversing as the current passes over a specific point. The pulse can also cause upstream retroflection near Port Elizabeth and early shedding of warm water Agulhas rings, which generally propagate into the Atlantic Ocean, upsetting the normal flow regime. However, it has been found that the pulses are not present when the minima and maxima in transport are seen. Bryden et al (2005) noted that although weak transport is seen in the early stages of the Natal Pulse, near normal overall southward transport is experienced when the strongest cyclonic circulation occurs.

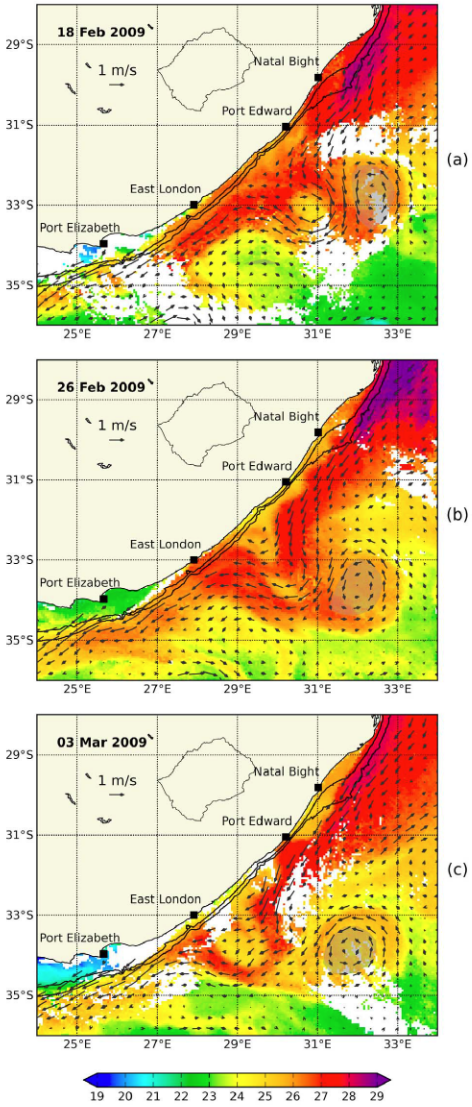

Figure 11: Evolution of a merging meander. A large Natal Pulse centred at 31°E, 33°S (b) merges with an upstream instability located at 29.5°E, 32.5°S and (c) evolves into a single cyclonic meander (Rouault & Penven, 2011)

The presence of the Natal Pulses in the Agulhas Current will impact the power extraction over an extended period of time as the presence of the Natal Pulse can reduce the velocity of the Agulhas Current to near zero and even reverse the direction of flow in an area. This phenomenon must be carefully considered in order to determine the severity of the impact on the potential for resource extraction.

There has been no proof published in literature that there is seasonal variability in the Agulhas Current or variability due to neap or spring tides. More detailed research needs to be carried out for a longer period of time to establish any annual or seasonal variability (Rouault, 2011).

2.3. Characterisation of the Ocean Current Resources for Energy Extraction

The characterization of ocean energy currents for the purpose of energy extraction is a relatively new field with little published work seen on the Gulf Stream, Kuroshio and the Agulhas Current. More significant bodies of work have been published on these currents from an oceanographic point of view and often with the focus on deep sea research rather than high resolution models focusing on the continental shelf region. Further, coastal regions for tidal energy extraction have also been explored with focus areas off the United Kingdom coast and the Eastern Canadian coast. The characterisation methodology of tidal currents together with the published literature on characterization of ocean currents will be used to form a methodology to characterise the Agulhas Current.

2.3.1. Ocean current characteristics

Some resource assessments for the purpose of marine energy extraction have been carried out on the Agulhas Current, Gulf Stream and Kuroshio Current.

a. Agulhas Current

The resource assessment presented by Marais, et al, (2011) focuses on the near shore (less than 50 km from the coastline) of the Agulhas Current. The methodology used to analyse the data is questionable at this resolution as Marais et al, (2011) did not take the variability of the Agulhas Current into account and presented a very coarse area approximation of the Agulhas Current, shown in Figure 12 to achieve a power estimate.

In order to achieve the graphs presented in Figure 12, Marais et al, (2011) averaged the velocity values of the ADCP measurements to a weekly temporal resolution, with little sensitivity analysis regarding the variability of the current. By disregarding the variability, no change in direction of local velocity vectors was taken into consideration and the outliers present in the dataset can skew the average value. With this course approximation, there is little indication of a velocity gradient and sensitivity towards the depth velocity relationship limiting the information that can be deduced from the graphs as to the most promising depth of deployment. The gross velocity approximation up to the sea surface also disregards all interactions between the waves and tides and the current. Further, no spatial integration method was given and thus the possibility of an inaccurate prediction of power with this methodology is great.

Making use of the same dataset as Marais, et al. (2011), Wright, et al. (2011) presented a more feasible analysis of the data. Wright et al (2011) assessed the data by first finding the optimum depth of the current, and finding the depth with

the greatest velocity for each site of ADCP deployment. The optimum depths found for an energetic site are approximately 45 m below the surface. This finding is at odds with past research as the Agulhas Current is a surface current and the most energetic waters flow closest to the surface. The method used to find the optimum depths are not described thus the integrity of these results cannot be verified. Further, a temporal analysis was carried out at these depths in order to evaluate the variability and standard deviation of the current at that point. Wright, et al. (2011) did not attempt to extrapolate spatially nor average the data temporally establishing credibility of the analysis.

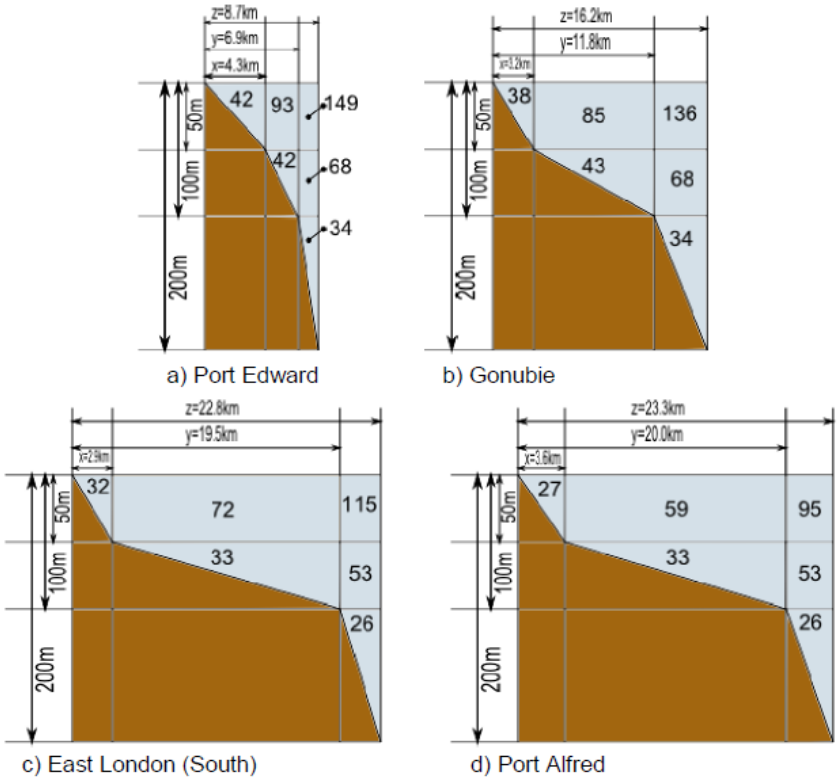

Figure 12: Velocity graphs presented by Marais et al, (2011) in [cm/s]

The resource assessments published by Marais et al, (2011) and Wright, et al. (2011) show that there is scope for an in depth resource analysis of the Agulhas Current for marine energy extraction and that the methodologies used have not been successful in accurately quantifying the potential power of this resource.

b. Gulf Stream

Researchers from North Carolina A&T State University and Florida Atlantic University are investigating the Gulf Stream for the purpose of marine energy extraction. The methodology presented attempts to minimise the effects of temporal and spatial averaging.

Duerr and Dhanak (2012) consider the theoretical power density and the practically extractable power with the use of a number of different turbine parameters and packing factors. In order to find the theoretical power density, the following equation is used:

$$P_d(y,z,t) = \frac{1}{2}\rho V^2\left(\vec{V}\cdot\vec{n}\right) \cong \frac{1}{2}\rho V^3 \qquad (1)$$

Where ρ is the water density and $V = \left|\vec{V}\right|\cdot\vec{n}$ is the unit vector to the cross sectional plane y,z.

This approximation assumes that the principle velocity component is in the streamwise direction and the cross stream components are small. For the most accurate results, the velocity component must be instantaneous and not temporally averaged. However if the velocity is averaged over a period of time, the power will be under-predicated due to the cubed power velocity relationship. In order to overcome this error, the time averaged velocity is rewritten as follows:

$$V(y,z,t) = \bar{V}(y,z) + \sigma(y,z,t) \qquad (2)$$

If this is substituted into equation (1), the power density can be described as follows:

$$\overline{P_d} = \frac{1}{2}\bar{\rho}(\bar{V}^3 + 3\bar{V}\overline{\sigma^2}) \qquad (3)$$

This expression shows that the expected value of power density will be larger than the cube of the average velocity and thus this under prediction must be noted when working with time averaged velocity values. Duerr and Dhanak used both *in situ* measurement and ocean model outputs to quantify the velocity of the Gulf Stream. The data was presented in time series format where the relationship between depth, velocity and time was illustrated together with plots of probability of velocity occurrence histograms throughout the water column.

In order to find the practically extractable power, the location of the turbines must first be determined. Similar to the Agulhas Current, the Gulf Stream is also a surface current; however Duerr and Dhanak (2012) make a conservative estimate in respect to turbine interference with other marine users stating that the turbines should be deployed at 50 m or deeper in the water column. Additionally the cut-in speed of the turbine, the turbine diameter and turbine array density will also impact the chosen location and extractable power.

The array density is dependent on the packing factor deployed at the site and the packing factor is found as follows:

$$PF = \frac{\sum A_i}{A_o} \qquad (4)$$

Where

$$A_i = \frac{\pi {d_i}^2}{4} \quad (5)$$

is the swept area of a horizontal turbine and A_o is the operating area.

Thus the packing factor is the total area occupied by turbines divided by the operating area. With this ratio the maximum theoretical packing factor can be calculated. If the operational area is square with a side length of d then the packing factor results in a ratio of $\frac{\pi}{4}$ that is 79%. This is the maximum packing factor that can be achieved for horizontal axis turbines that are fixed to a stationary mounting (Duerr & Dhanak, 2012). It is important for this ratio to be taken into consideration when calculating the total extractable power at a location.

In order to find the optimum power harnessing device, practically extractable power from turbines with cut-in speeds of 0.5 – 1.5 m/s and diameters of 10, 20 and 30 m were analysed (Duerr & Dhanak, 2012).Through the use of these variables the design parameters of a turbine ideally suited for operation in the Gulf Stream is achieved. Through this analysis it was found that a turbine with the largest diameter and lowest cut-in speed, 0.5 m/s cut-in speed and 30 m diameter, would theoretically extract the most energy. However, such a turbine is not necessarily already developed and the manufacturability is yet to be determined. One aspect of the current that Duerr and Dhanak (2012) failed to examine is the current directionality and the impact that the change of direction can possibly have on power production.

Further analysis of the Gulf Stream was carried out by Kabir et al. (2014) with greater focus on the velocity and the directionality of the current. Kabir et al. (2014) make use of directional rose plots to show the predominant direction with the most frequently occurring velocity. A rose plot is an effective way of presenting ADCP data as the velocity and directional data is not averaged in any way, but rather binned to indicate a prominent direction and the associated velocity. This plot also gives a sense of the variability of the current as changes in current direction and velocity fluctuations are indicated. Kabir et al. (2014) also used a probability density function to analyse the velocity characteristics to determine how the trends at different sites compare.

In the Gulf Stream region, the Hybrid Coordinate Ocean Model (HYCOM) is well developed with a 1/12° degree resolution. This model is a 3-dimensional, real time, ocean prediction simulator and used by Van Zwieten et al. (2014) to analyse the characteristics of the Gulf Stream. Van Zwieten et al. (2014) consider the power density, probability of exceedance for velocity and percentage current reversals to describe the current. The percentage current reversals will be useful in the context of the Agulhas Current as this parameter will help determine the

impact of Natal Pulses on energy extraction. A current reversal is defined as a current which is flowing in a direction that is more than 90° from the average current direction (VanZwieten, et al., 2014).

If the directional rose plots, together with power density and percentage current reversals are used as the indicators for the current characteristics, a holistic view of the current's behaviour can be found.

c. Kuroshio

The other western boundary current of interest is the Kuroshio Current that flanks the Taiwanese and Japanese coast. Published data on the energy density of the current is limited as is the methodology used to investigate this parameter. Researchers from Energy Research Centre and Institute of Applied Mathematics, National Taiwan University (Chen, 2010) have examined the possibility of a power plant that makes use of the energy contained in the current. This investigation focuses on a high level overview of the parameters that are considered when developing an ocean current power plant with specific focus on the available technology.

The volume transport together with the monsoon and seasonal variation is used to characterise the potential theoretical power of the Kuroshio Current. It was found that the seasonal variation greatly impacts the potential power of the current with a 6 GW difference between winter and summer, where winter sees a power of 4 GW and summer possibly 10 GW (Chen, 2010). With the established potential theoretical power, the following aspects are considered that will impact the practically extractable power: type of turbine, density of turbine deployment, flow characteristics in the sea of power plant, seabed topography and geological features and environmental and sea usage considerations.

Figure 13: Schematic of the proposed Kuroshio power plant (Chen, 2010)

Figure 13 shows a schematic of the Kuroshio power plant, it is proposed that there are three groups of turbines, with each cluster containing 25 turbines with a transformer attached to the platform. The proposed mooring depth is 30 m to

avoid interaction from typhoons and surface waves. This 30 m is not as conservative as Duerr and Dhanak's (2012) 50 m proposed mooring depth and will result in a higher power output for such surface currents. The proposed design aims to achieve anchoring at 500 m or more. The technical aspects of this design is still to be established and no such system is fully designed as of yet. For the successful extraction of energy this proposed design indicates the need for floating turbines within the ocean current atmosphere.

The environmental aspects considered include geological investigation of the seabed, marine ecological investigation and surveys of ancient Kuroshio and geological stability. An investigation into the geological characteristics of the seabed and a marine ecological investigation will be pertinent when examining the Agulhas Current for marine energy extraction. The bedrock and stability of the seabed will largely impact the type of mooring that can be used as well as the survivability of the plant. The use of ocean current energy to generate electricity is renewable; however the sustainability of the plant must also be determined with respect to the environmental impacts on the ecosystem surrounding the plant. The warm water of western boundary currents allow for a rich and diverse marine environment (Chen, 2010). The presence of an ocean current turbine plant can affect the ocean ecosystem, the fishery resources and the benthic ecosystem. The impacts of a turbine array in the Agulhas Current on the marine ecology will need to be considered for a holistic resource assessment.

2.3.2. Tidal Characterisation parameters for energy extraction

The tidal energy industry is more developed than the ocean current industry and is closest related to the ocean current industry. Some lessons learnt and methodology applied can be transferred between the two industries.

Extensive work has been done on this topic by the University of Edinburgh, with Couch and Bryden (2006) outlining the parameters essential for establishing the hydrodynamic resource characteristics for tidal energy extraction. The parameters of importance as identified by Couch and Bryden (2006) are: the local water depth, the location of the nearest exploitable grid connection and an energetic and persistent resource. All three these parameters are applicable to the ocean current industry as the local depth will have mooring implications, the distance from the nearest exploitable grid will have financial implications for the project and need for an energetic and persistent resource ensures that the site will be able to consistently produce power. These three primary parameters will help with the site section criteria and if a site meets these three criteria there is potential for further investigation (Couch & Bryden, 2006).

Equimar published a guide to the assessment of marine energy sites and converters in 2011. This guide describes protocols for the resource assessment of tidal sites and identifies the following site characteristics to be noted:

bathymetry, tidal range, tidal constituents and wind (Ingram, et al., 2011). The only two characteristics that may affect the potential power of an ocean current site are bathymetry and wind, however since ocean current sites are significantly deeper and unconstrained by a channel, the bathymetry will have minimal affects with respect to drag. Another factor that is of significance to tidal resource assessment is the presence of extreme waves, however since ocean current turbines need to be located deep enough not to interfere with shipping vessels this should not affect an ocean current site.

The key parameters identified in the quantification of a tidal resource are:

1. *Tidal stream power* at the locations, established through survey and measurement
2. *Power exceedence* curve showing generating availability at the locations
3. *Direction of axes* of the tidal ellipses at the locations
4. *Vertical velocity profile* of the stream at the locations

These parameters will also help quantify the resource at an ocean current site and should be applied to the resource assessment of the Agulhas Current.

2.4. Conclusion

From this literature survey, it is found that some preliminary work has been done in respect to resource assessments for ocean current with the majority of the work focusing on the Gulf Stream. This shows that there is scope for a resource assessment of the Agulhas Current for the purpose of marine energy extraction. The carried out assessments focus on the resource characteristics in respect to magnitude and direction with an attempt to quantify the available power in the analysed current. The pitfalls of using averaged velocity values are recognized and the need for high resolution temporal data is prevalent. Industry practices from the more developed tidal industry are relevant to transfer to the ocean current resource assessments with the emphasis on vertical velocity profiles.

The oceanographic work done on the Agulhas Current is on a large scale with low resolution. The area of interest in the Agulhas Current for marine energy extraction is on the edge of the continental shelf, in general a small region of the published oceanographic studies. Furthermore, because of the sensitivity of power output to the velocity of the current, high resolution models are needed to predict the potential power output. The oceanographic studies are a good starting point for a resource assessment, with studies on macro effects such as the Natal Pulse being valuable inputs, however the need for a detailed resource assessment of the Agulhas Current is established.

3. RESOURCE ASSESSMENT METHODOLOGY

The resource assessment focuses predominantly on the technical characteristics, concentrating specifically on the behavioural features of the current which characterise the potential power output from a turbine array, namely, power density, directionality and availability of the current.

3.1. ADCP Measurements

In situ measured data of the Agulhas Current is available and the resource assessment is based on this data. ADCPs have been used to collect this data resulting in the documentation of the water column at deployment locations. An ADCP employs the acoustic Doppler principle whereby a transducer transmits an acoustic signal into the water column and current velocity is then calculated from measured frequency changes in the return pulse. Reflected pulses from pre-determined layers (called bins) throughout the water column can be recorded and processed, resulting in the acquisition of the vertical velocity structure (Meyer, et al., 2013).

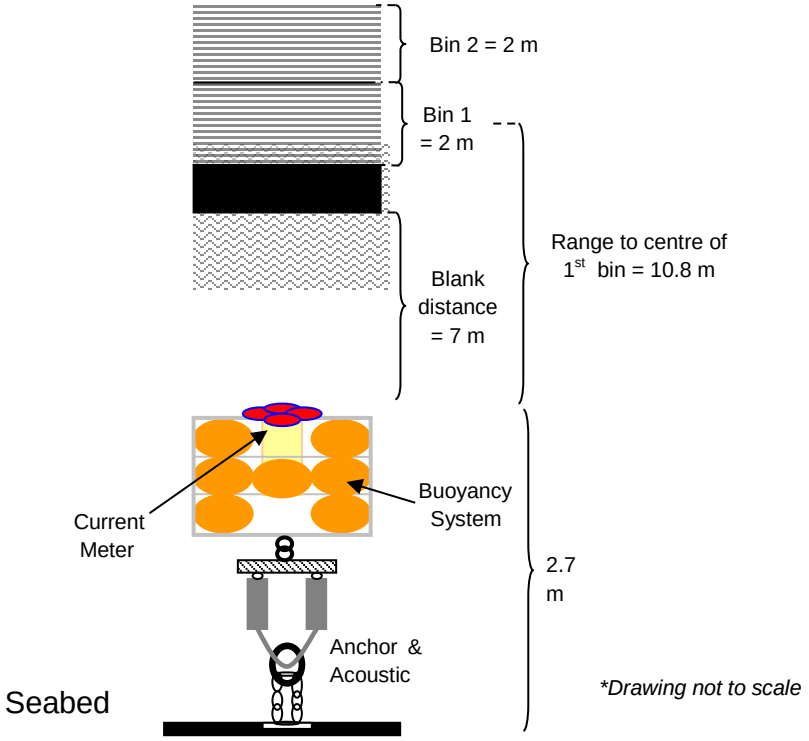

Figure 14: Typical mooring configuration for an ADCP current meter and the transducer heads and pressure sensor (Meyer, et al., 2013).

ADCPs collect both velocity and directional data at different bin depths throughout the water column allowing the relationship between current velocity and depth below the sea surface to be examined. However there are limitations

to using ADCPs as this technology cannot accurately record data close to the sea surface due to inference caused by air bubbles from waves. Further, an ADCP only records the water column directly above its mooring location and thus limited spatial data can be inferred from a single ADCP dataset. A typical mooring configuration is shown in Figure 14.

From 2005 to 2010 ADCPs were deployed along the South African coastline as part of an exploratory mission. From these measurements 4 locations have been identified where continuous time series of longer than one year have been recorded. This minimum time period was chosen so that the presence of seasonal variability, if present, would be taken into consideration. The metadata of all these deployments can be found in Appendix A. As published in the Equimar protocols, the required sample size of data used to determine the occurrence of extreme events depends on the confidence interval and return period. The Equimar protocols suggest that the minimum dataset requirement is a duration of 20% of the return period (Ingram, et al., 2011). Thus it is pertinent to compare the results from the one year ADCP dataset to long term satellite data in order to establish how the found results compare to long term trends.

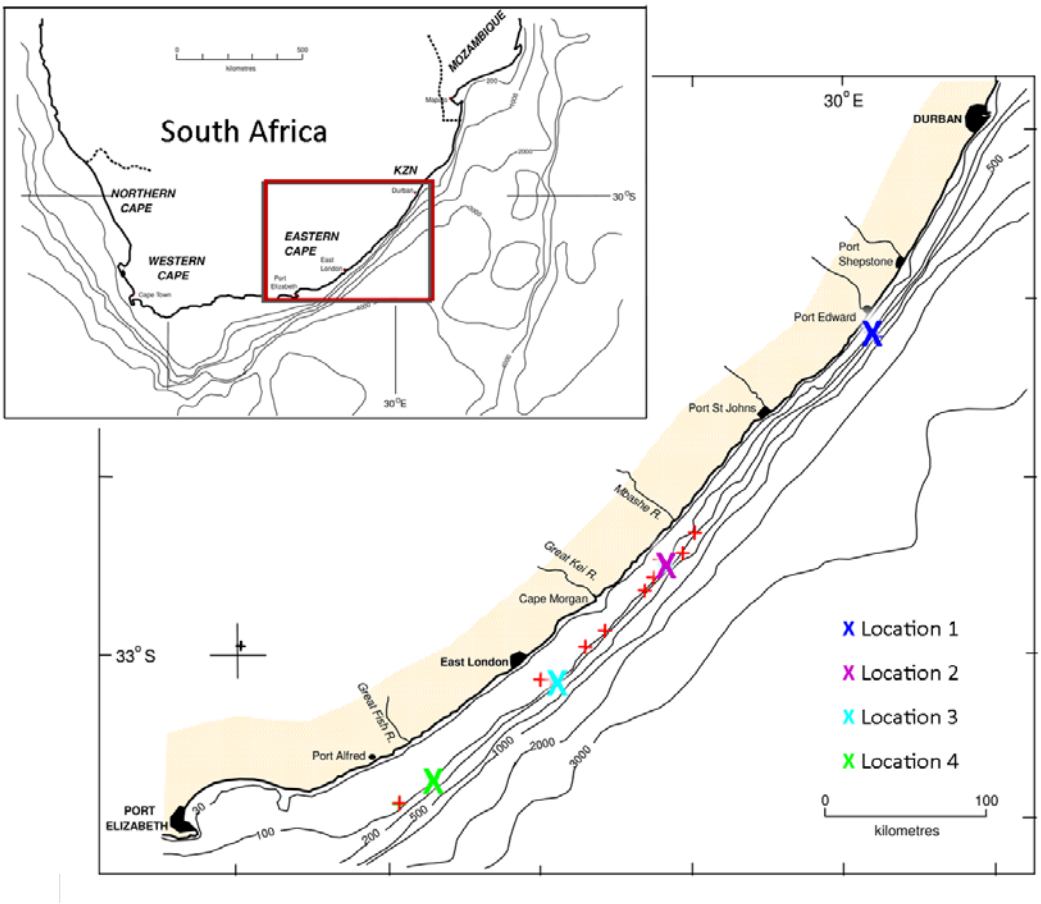

Figure 15: Position of ADCP deployments. Large 'X's indicate datasets longer than 1 year. Red crosses indicate other ADCP deployments of less than 1 year.

Figure 15 shows the large area over which the ADCP data has been collected and the metadata for the four usable datasets, named Deployment Series 1 is given in Table 1. All the measurements have been taken at locations where the sounding depth is less than 100 m, as at the time of measurement this was considered the limiting depth for mooring energy extraction technology. Rouault and Penven (2011) have found that the core of the current is located between 20 and 50 km from the shore and approximately above the 200 m isobath, thus it is observed that measurements were taken at the periphery of the current. It must be noted that the dates each dataset was recorded do not coincide and this can possibly lead to a bias towards one site.

Table 1: Deployment Series 1: Metadata for the South African ADCP deployments

Dataset	ADCP Type/ Bin Resolution	Location	Distance to shore	Time Period	Sounding Depth
Location 1 *Port Edward*	RDI 600 2 m	31.198 S 30.175 E	6 km	08/09/2005-09/09/2006	~60 m
Location 2a *Cape Morgan*	Nortek/ 2 m	32.507 S 28.831 E	15 km	11/04/2006-12/07/2008	~85 m
Location 2b *Cape Morgan*	RDI 300/ 2 m	32.507 S 28.831 E	15 km	12/07/2008-13/09/2010	~85 m
Location 3 *East London*	RDI 300/ 2 m	33.150 S 28.099 E	21 km	18/08/2007-10/12/2008	~85 m
Location 4 *Fish River*	RDI 300/ 2 m	33.703 S 27.298 E	26 km	01/04/2008-04/03/2010	~90 m

Table 2: Deployment Series 2: Details of Available ADCP data

	Location	ADCP Type/ Bin Resolution	Distance from Shore	Time Period	Sounding Depth
I.	**Mid-shelf**	RDI 300/ 2 m	14 km	2012/01/24 - 2013/06/30	91 m
II.	**Off-shore** (edge of shelf)	RDI 150/ 6 m	18 km	2012/01/24 - 2013/06/30	255 m

Further two ADCPs were deployed between 2012 and mid 2013 at a mid-shelf and off-shore location resulting in an 18 month period of continuous data in the region of Location 2. This dataset will be referred to as Deployment Series 2. The details of the captured data are outlined in Table 2. The data was collected using Teledyne RDI ADCPs with a 60 minute temporal resolution. The Teledyne ADCP automatically runs a quality assessment on the collected data and only data collected with a quality assessment of greater than 75% is used for the analysis. Owing to this quality assessment, viable data for the mid-shelf location ranges from 84 m to 10 m below the sea surface and for the off-shore location, from

238 m to 22 m below the sea surface. The exact location of the ADCPs deployed mid-shelf and off-shore may not be disclosed due to a confidentiality agreement.

3.2. Predicting Available Power

3.2.1. Magnitude

Making use of the collected ADCP data the power density of the current can be found. The power density of a fluid stream across a unit cross-section is given by:

$$P_d = \frac{1}{2}\rho {v_{ins}}^3 \quad (6)$$

where ρ is the density of the fluid and v_{ins} is the instantaneous velocity of the fluid stream. All power density calculations will make use of the instantaneous velocity obtained through the use of the ADCPs, as using an average velocity can lead to the under prediction of the resource (Duerr & Dhanak, 2012). Power density does not give the total available power of the resource but rather indicates what power can possibly be extracted using an array of turbines. It is important to note that this parameter indicates the theoretical power density of the resource, where the practically extractable power is dependent on the specific technology chosen to harness the energy and the achievable array density.

To find the theoretical power output from a designed turbine, a quadratic equation is developed to follow the published power curve of the turbine with instantaneous velocity as the input and instantaneous power as the output, as follows:

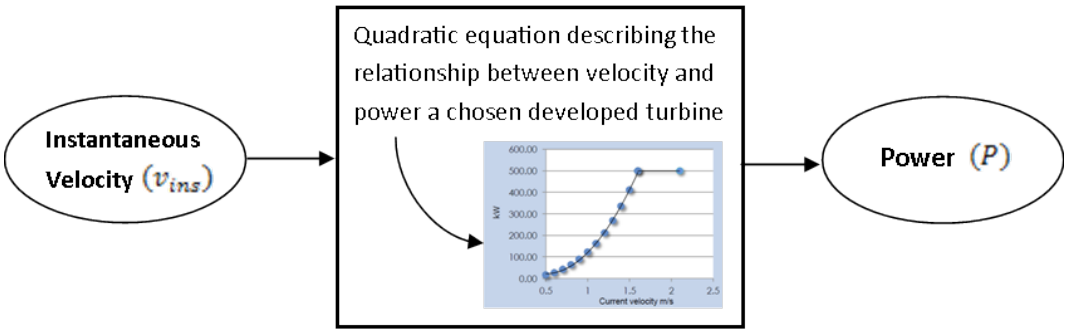

Figure 16: Calculation method for instantaneous power output from with the use of a published power curve

Since the achievable power is highly dependent on the velocity of the resource, the velocity characteristics are interrogated. A 15%, 50% and 75% probability of occurrence curve versus depth will be presented as part of the results to determine the potential optimum operating range of a turbine to be deployed in this resource. This plot will also highlight the ideal deployment depth.

3.2.2. Direction

Temporal velocity plots are presented together with directional analysis to determine the predominant flow direction variability. The prominent direction of the current is found through the use of directional roses. The velocity magnitude is taken into consideration in the directional rose plots with the velocity range divided up into bins of 0.5 m/s. These current roses are polar histograms showing the percentage of occurrence of the current in a specific direction with an indication of velocity magnitude.

To examine the directional properties throughout the water column, the mean flow direction is defined as:

$$\bar{\theta} = \tan^{-1}\left(\frac{\bar{V}_E}{\bar{V}_N}\right), \quad (7)$$

where $\tan^{-1}$ is the inverse tangent function, $\overline{()}$ indicates the mean, $\bar{V}_E$ is the mean eastward component of velocity, and $\bar{V}_N$ is the mean northward component of velocity.

To quantify the directional variability of the resource, the percentage of current reversals is presented. The percentage of current reversals can allude to the presence of Natal Pulses in the dataset. The percentage current reversals are determined as follows:

To find the percentage current reversals, a current reversal is defined as a current stream that is flowing in a direction that is more than $\frac{\pi}{2}$ radians (90°) from $\bar{\theta}$. The percentage of current reversals is found though the following expression:

$$\frac{\sum_{i=1}^{N}|\theta_i - \bar{\theta}| > \frac{\pi}{2}}{N}, \quad (8)$$

where || indicates the absolute value. This definition was presented by Van Zwieten et al. (2014). Another parameter of interest is the standard deviation of the flow direction and for a single location is calculated from:

$$\theta_{std} = \sqrt{\overline{\left((\theta_\iota - \bar{\theta})\big|_{-\pi}^{\pi}\right)^2}}, \quad (9)$$

where $()|_{-\pi}^{\pi}$ indicates that the angle is unwrapped to its equivalent radial value between $-\pi$ and π (VanZwieten, et al., 2014).

3.2.3. Identifying Natal Pulses

A methodology must be established to distinguish between daily variability, such as the presence of eddies, and the occurrence of Natal Pulses. The criteria used by Rouault and Penven (2010) to identify a Natal Pulse are presented here.

1. The Agulhas Current inshore front meander is more than 30 km from its mean position

2. A Natal Pulse persists for a period of 10 days or longer

The ADCP data available for analysis is point data and thus the spatial criterion 1, will not be useful in analysing the point, time series data. However with the occurrence of a Natal Pulse the current's path is displaced seawards, thus the velocity measured by the ADCP will drop to near zero since the current has moved away from this location. Further the directionality measurements will also indicate the presence of a Natal Pulse since, as when Natal Pulse travels over an ADCP, there will not be one distinct direction recorded but the cyclic motion of the Natal Pulse. Thus criteria 2 from Rouault and Penven (2011) coupled with a drop to near zero velocity throughout the water column and change in direction will be the criteria used to identify a Natal Pulse.

3.3. Capacity Factor

To quantify the variability of the Agulhas Current resource, a suitable turbine is selected and from the practically extractable power a capacity factor is obtained. Array configuration and spacing is not considered in this research and the capacity factor of a single turbine is presented. The capacity factor is described by the following expression:

$$C_f = \frac{\sum_{i=1}^{N} C_p \frac{1}{2} \rho A {v_{ins}}^3}{\sum_{i=1}^{N} C_p \frac{1}{2} \rho A {v_{rated}}^3} \quad (10)$$

Or

$$C_f = \frac{\sum_{i=1}^{N} Power\ produced}{\sum_{i=1}^{N} Turbine\ rated\ power} \quad (11)$$

where the C_p is the efficiency of the turbine, ρ is the density of sea water, A the swept area, v_{ins} is the instantaneous current velocity and v_{rated} is the rated speed of the turbine. The capacity factor is calculated over the available data period. As discussed in section 2.2.3, there is no seasonal variation seen in the Agulhas Current thus calculating the capacity factor over a period of longer than a year remains accurate. To achieve a high capacity factor the rated speed of the turbine must be well matched to the mean speed of the current. The results of the current magnitude analysis will help guide the choice of turbine used to determine this parameter.

3.4. Capacity Credit

Capacity factor is a good parameter to use to compare with other renewable energy resources. It has been hypothesised that power extracted from ocean currents can possibly add to the base-load electricity supply of the country. With this hypothesis there is a need for a parameter that can quantify the impact a potential ocean current plant can have on the electricity security of the country especially during the peak usage times. Capacity credit is a parameter that can give this indication. Capacity credit will indicate if any thermal or conventional power capacity investment can be deferred through the installation of an ocean current power plant.

The capacity credit of a system is a certain percentage of the installed renewable energy generation capacity which is considered as a contribution to the firm capacity of the system whilst the reliability of the overall system remains unchanged (Pöller, 2011). In order to calculate this parameter, a potential system size needs to be chosen for a theoretical ocean current power plant. The instantaneous output power from this plant then needs to be compared to the system capacity with specific focus on peak hours of the day. The peak hours of the day and peak season is the focus as this is when unserved periods would potentially occur and in turn affect the reliability of the system.

Capacity credit is found through the following formula:

$$CC = \frac{ELCC}{P_r} \times 100\% \quad (12)$$

Where:
CC is capacity credit (%)
$ELCC$ is equivalent load carrying capacity (MW)
P_r is the rated power of the total installed intermittent power generator

The equivalent load carrying capacity is found through comparing the probability curve for the conventional energy supply system and the conventional energy supply system with the renewable energy plant output added. The curves are compared at 99% confidence level and difference between the two curves at this interval is the equivalent load carrying capacity. This method assumes that predominantly the peak level contributes to the average loss of load probability of the system (Pöller, 2011).

Such an analysis has been carried out for the wind power plants in South Africa and the scenario examined was for 2 000 MW of installed wind power. This same capacity will be used for the potential ocean current plant for sake of comparison. System data from Eskom (Bowen, 2015) has been obtained during the same period that the ocean current data is available in order to find the equivalent load

carrying capacity of the potential ocean current system through the use of a hind cast model.

3.5. Other contributing Factors

Other contributing factors that must be taken into consideration when selecting a site for turbine deployment and finding the practically extractable power include:

1. *Geotechnical and Mooring Considerations*: The seabed bottom types at the point of deployment will impact the type of moorings that can be used. The presence of the shifting subaqueous dunes on the eastern South African continental shelf may prove to be problematic in this regard.
2. *Commercial Fishing Activities*: Fishing activities, commercial and subsistence would impact the location of turbines and the turbines should have minimal impact on the local fishing community.
3. *Shipping Routes*: The presence of the Agulhas shipping route must be taken into consideration when analysing the resources for any technology installed for energy extraction. This technology must be located at least 30 m below the surface to allow sufficient clearance from the ship drafts.
4. *Existing Infrastructure that can Consume the Generated Electricity*: the existing power grid will play a large role in determining the placement of the turbine farm as, if there is no take-off consumer on land further infrastructure will need to be developed to connect the array to the national grid.
5. *Environmental Impact:* Marine Protected Areas cannot be used as suitable sites and must be avoided including for shore access for undersea power cabling. Further, the global effects of placing energy extraction devices within a current which is instrumental in the meridional overturning circulation must be considered.
6. *Regulatory Environment in South Africa:* Established standards and regulations within South Africa's waters must be taken into consideration with concern for other sea users. Owing to South Africa's lack of experience in the marine energy sphere there is uncertainty regarding the implementation processes and required permits for deployment offshore.

4. TECHNOLOGY READINESS

The practically extractable power depends on the technology used to harness the current's energy and the density at which this technology can be deployed. The ocean energy industry as a whole is still immature with respect to commercial technology success with the largest barriers being cost and device survivability.

Owing to the immature nature of ocean current energy industry, ocean current energy extraction devices are still in the research and development stage, with technology readiness levels ranging between TRL 1 and TRL 5 (Mofor, et al., 2014). See Appendix B for technology readiness levels definitions.

At the time of this study, a proposed test site for ocean current turbines is located in the Gulf Stream and championed by the Southeast National Marine Renewable Energy Centre at Florida Atlantic University (FAU). FAU has designed a turbine to test at this berth, however this turbine is not connected to the grid and is not utilised for generation purposes, but rather as exploratory research. Minesto, a Swedish based firm (turbines originally designed for tidal applications) has also expressed interest in deploying the Deep Green turbine in the Gulf Stream at this same test site. This technology holds promise with a design that accelerates the flow velocity through the use of relative motion as the turbine flies through the water in a figure of eight. A schematic of this technology is seen in Figure 17.

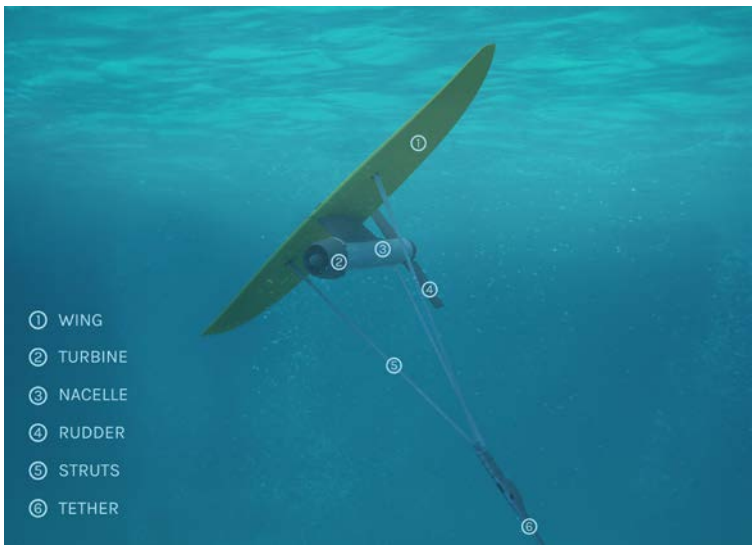

Figure 17: Schematic of the Minesto Deep Green Turbine (Minesto, 2015)

The Aquantis 2.5 MW C-Plane (Figure 18) is another tethered turbine that has especially been designed to operate in ocean currents (specifically the Gulf Stream) with a rated speed of 1.6 m/s, making this device suitable for energy extraction in the Agulhas Current. However at the time of this study no sea trials have been carried out on the C-Plane, thus the success of the device is still to be

verified. Similarly IHI Corporation and Toshiba, are currently developing a tethered turbine for deployment in Kuroshio Current. This device is still in the simulation phase with construction yet to begin. A schematic is seen in Figure 19.

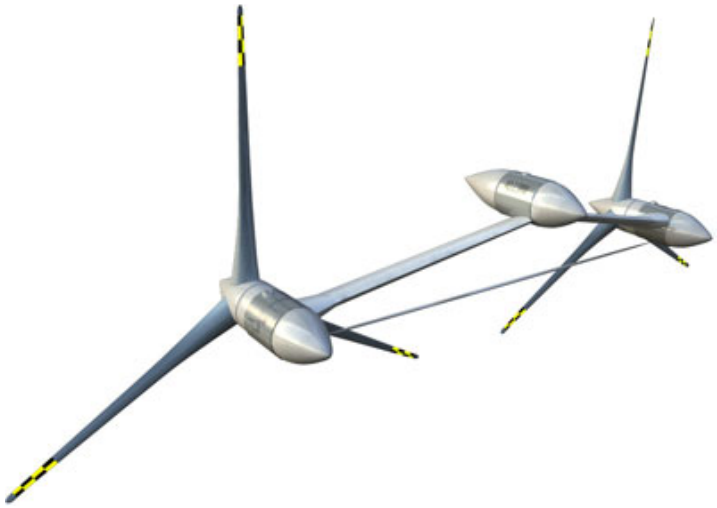

Figure 18: Schematic of the Aquantis C-plane (Ecomerit Technologies, 2012)

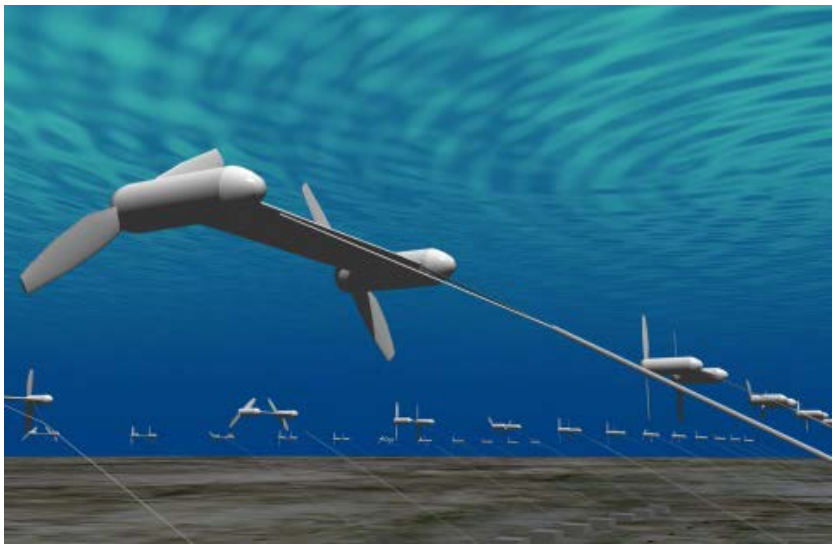

Figure 19: Schematic of IHI Corporation and Toshiba's tethered turbine (Subsea World News , 2014)

Opposed to a horizontal axis tethered turbine, Vortex Power Drive has designed an oscillating device for harnessing energy from ocean currents. This technology has been especially designed to operate in current speeds of less than 3 m/s which is ideal for ocean currents. The technology makes use of the principle of vortex shedding to drive the oscillation, and through a power take-off mechanism, produces electricity (Kane, 2014). Only tank testing has been carried out on a single device, thus survivability and success in ocean currents is not proven. A schematic of an array of Vortex Power Drives is seen in Figure 20. The pile

mounted structure of this technology will be problematic for installation in the Agulhas Current which is a surface current.

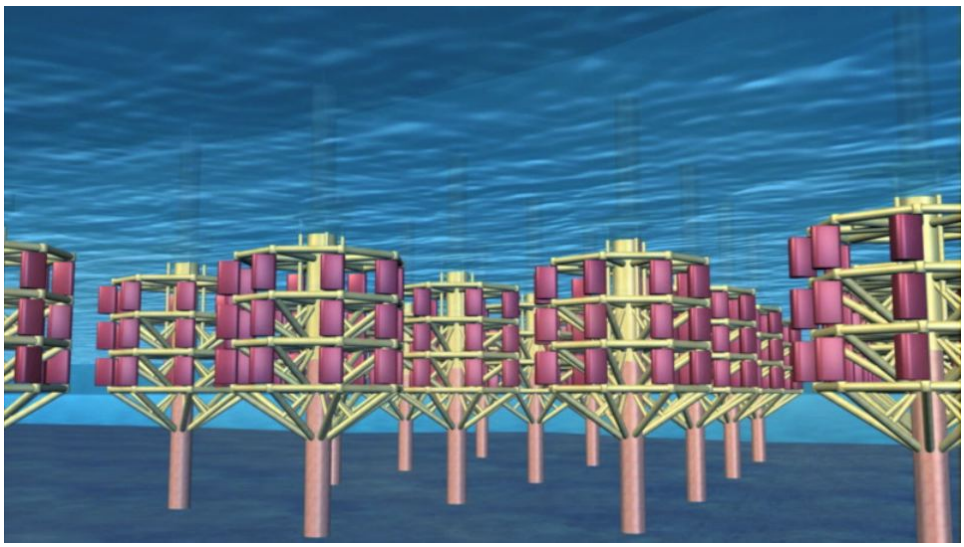

Figure 20: Schematic of the Vortex Power Drive technology (Vortex Power Drive, 2014)

The closest technology to that of ocean current turbines is the technology developed to harness tidal energy. This technology is more advanced than ocean current technology with sea trials conducted on successful designs with some turbines developed up to commercial status. There are many tidal current turbines developed and according to Kempener and Neumann (2014) up to 40 different devices were introduced between 2006 and 2013. However not many of the devices have made it up until commercial deployment status, and few devices surviving the harsh sea conditions.

The tidal energy industry is making progress towards commercial status with plans to deploy the first commercial scale tidal array, MeyGen, off the Scottish Coast by the early 2020s. MeyGen Limited intends to deploy up to 398 MW of offshore tidal stream turbines connected to the UK National grid. The project will be done in a modular fashion; with phase 1 consisting of a maximum of 86 turbines (86 MW). This phase will be monitored closely with respect to environmental considerations as the plant is the first of this scale (MeyGen, 2015). Onshore construction at the site started on the 21st January 2015. MeyGen Limited is working together with Atlantis Resources Limited and Andritz Hydro Hammerfest to design a technology most appropriate for the site conditions. Both these technology developers have a gravity moored turbine with three blades. A photograph Atlantis Resources Limited turbine is seen in Figure 21.

Another consented tidal array is the Anglesey Skerries Tidal Array, however this array is significantly smaller than the MeyGen array with a proposed 10 MW installed capacity. The 10 MW capacity will be achieved by the installation of five 2 MW Marine Current Turbines Siemens' SeaGen turbines. Installation of these turbines was planned for late 2016, but is currently suspended with no indication as to when the project will be restarted. Minesto, interested in both ocean current and tidal current projects, plan to deploy a 10 MW array by 2019 at Holyhead Deep off the coast of Anglesey with support from the Welsh government.

Figure 21: Atlantis Resources Limited turbine (Tethys, 2015)

Figure 22: Photograph of the SeaGen technology (Tidal Energy Today, 2015)

Another notable turbine developer is Open Hydro. Open Hydro deployed a prototype in 2006 at the European Marine Energy Centre (EMEC) test site and proved successful during testing but failed when deployed in the Bay of Fundy off

the east Canadian coast. Adjustments have been made to the Open Hydro turbine and a retest of the device's survivability is underway. Other mentionable turbines are listed in Table 3. All the turbines listed in Table 3 have under gone or are currently undergoing sea trials. All these devices analysed that have been developed up to commercial prototype testing status, are horizontal axis turbines showing the convergence of the industry towards this design. It is noted that Table 3 is in no way an exhaustive list but rather used as an indication of the specifications of a range of tidal technologies that have technology readiness levels of 8 or higher.

Table 3: Some Tidal Turbine Specifications

Company	Mooring Type	Maximum Mooring Depth [m]	Rotor Diameter [m]	Rated Speed [m/s]	Rated Power [kW]
Alstom	Gravity base	~50	18	2.7	1 400
Andritz Hydro Hammerfest	Gravity base	100	21	2.7	1 000
Atlantis Resources Limited.	Gravity base/ Pile Mounted Floating	-	18	2.65	1 000
Marine Current Turbines	Pile Mounted	50	20	2.5	1 000
Minesto	Tethered	120	1.15	1.7	850
Scot Renewables	Tethered	120	unknown	2.5	250
Nautricity Limited	Tethered	500	14	2.5	500
Verdant Power	Gravity Base/ Pile Mounted	50	10	2-4	500
Voith Hydro Ocean Current Technologies	Gravity base/ Pile Mounted	60	13-16	2.9	1 000

The rated operating speed of the stationary (gravity or pile mounted) horizontal axis turbines is greater than 2.5 m/s. From past investigations of the Agulhas Current (Beal & Bryden, 1999), (Bryden, et al., 2005), the mean speed at the current core is approximately 1.5 m/s making these turbines unsuitable for deployment in this resource. Further the pile mounting or gravity base will prove problematic due to the mooring depth in energetic ocean current sites. A tethered device will be more sensible to harness the power from ocean currents as suggested by the three technology developers, FAU, Minesto, Aquantis and IHI Corporation and Toshiba. From these technologies only Minesto has undergone sea trials. Although these sea trials are in a tidal energy context, such testing will add to the progress in the ocean current sphere. From the listed turbines in Table 3 it is seen that, Minesto's turbine has a rated speed 1.7 m/s indicating that this device can possibly be paired with the Agulhas Current for energy extraction.

5. RESULTS

5.1. Deployment Series 1

The purpose of the Deployment Series 1 was to determine an area of energetic flow of the Agulhas Current along the South African coastline. As seen in Figure 15 the four locations with a time series of longer than a year are spread out over 400 km along the coastline. Individual mooring analysis for all ADCP deployments in this series can be found in Appendix C.

5.1.1. Current Magnitude

Figure 23 evaluates the current magnitude showing the current flow speed statistics measured by the ADCPs at each location. The depth and location largely impacts the velocity seen at a site. Location 1 performs poorly since its sounding depth is only 60 m indicating that the current core will be further seaward from the measurement location, hence low velocities are seen at this site. Both datasets analysed at Location 2, Location 2a and Location 2b, and Location 3 perform well with mean velocities exceeding 1 m/s 50% of the time at depths between 50 m to 20 m. Location 4 has a poor performance indicating that the current core moves seawards as it travels south with the widening continental shelf (see Figure 15 for bathymetry lines) with the mean velocity at this site never exceeding 1 m/s.

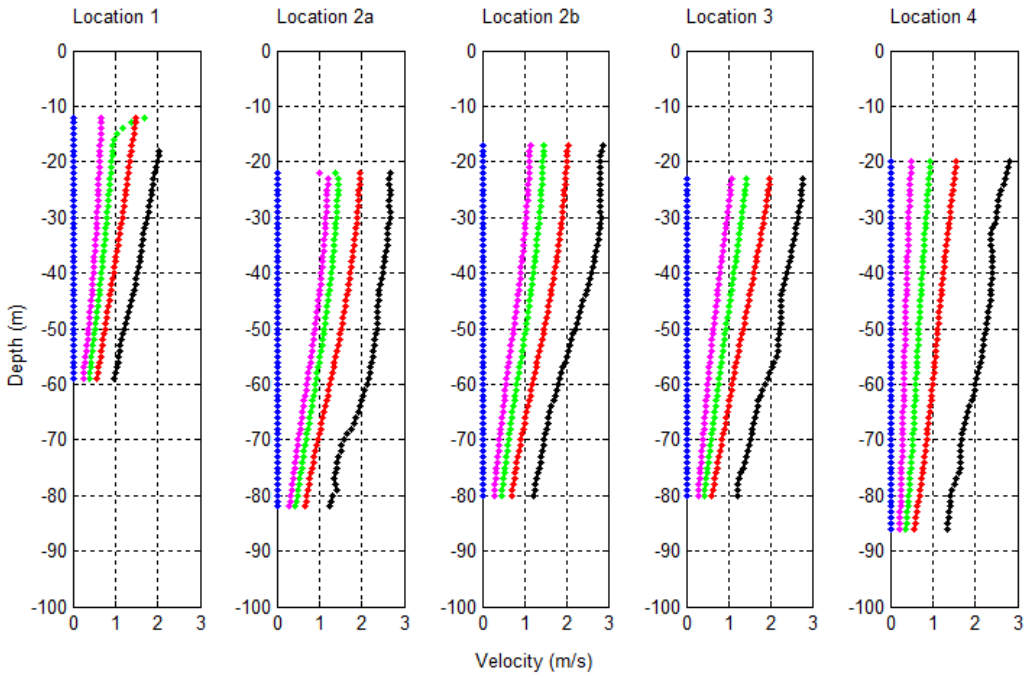

Figure 23: Velocity magnitude plot. Minimum (blue), 75% (magenta), mean (green), 15% (red), and maximum (black) flow speeds

The Agulhas Current is the most energetic at Location 2 with the best velocity performance of the four examined sites with a maximum velocity of 2.82 m/s and mean velocity of 1.45 m/s at 20 m depth seen during the second measurement period at this site.

5.1.2. Power Density

The relationship between power density and velocity is described by equation (6). The mean power density at each site is shown in Figure 24. This figure reiterates the findings of Figure 23, indicating Location 2 is the most energetic site. Shown in Figure 24 at 50 m and 20 m depth the mean power density Location 2b is 868 W/m^2 and 2346 W/m^2 respectively. This is closely followed by Location 3 with a mean power density of 659 W/m^2 and 2164 W/m^2 at the same depths. The velocities at these two sites are very comparable but the cube relationship between velocity and power means that a fractionally faster site contains significantly more power. The dependence of possible power extraction on depth is clearly illustrated in Figure 23 and Figure 24. As Figure 23 shows, the Agulhas current is a surface current and thus the closer to the surface the energy extraction devices are located, the greater amount of energy will possibly be extracted. Owing to the large difference in power density at 20 m and 50 m depth, the discrepancy between the advised deployment depth, i.e: the difference between Duerr and Dhanak (2012) and Chen's (2010) deployment depth, must be resolved though the engagement of other sea users in the area of interest.

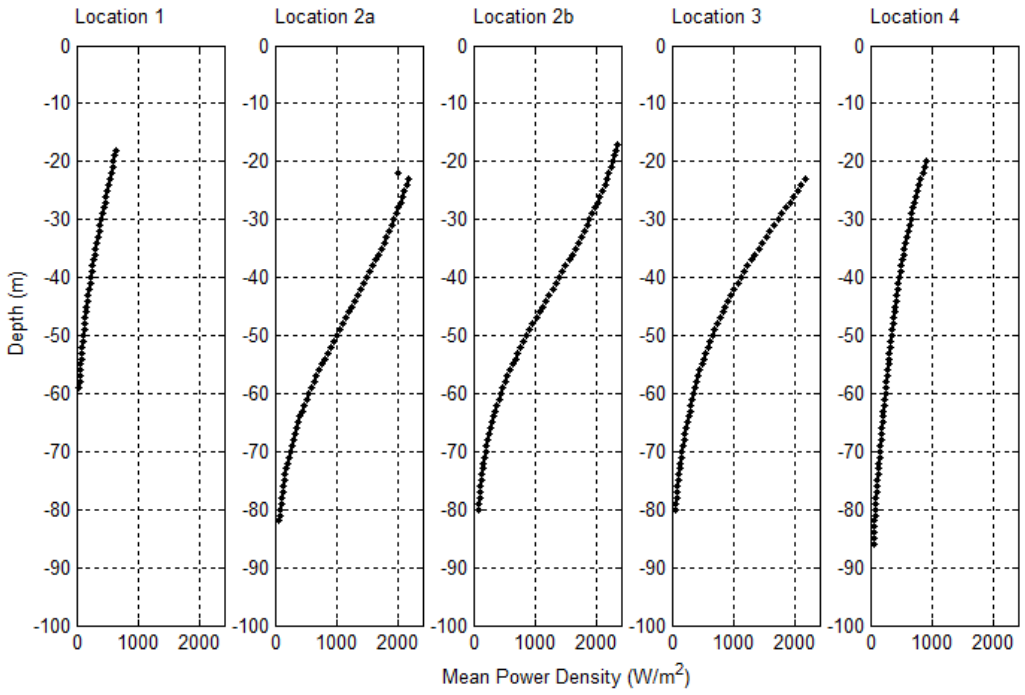

Figure 24: Mean power density at each location

5.1.3. Current Direction

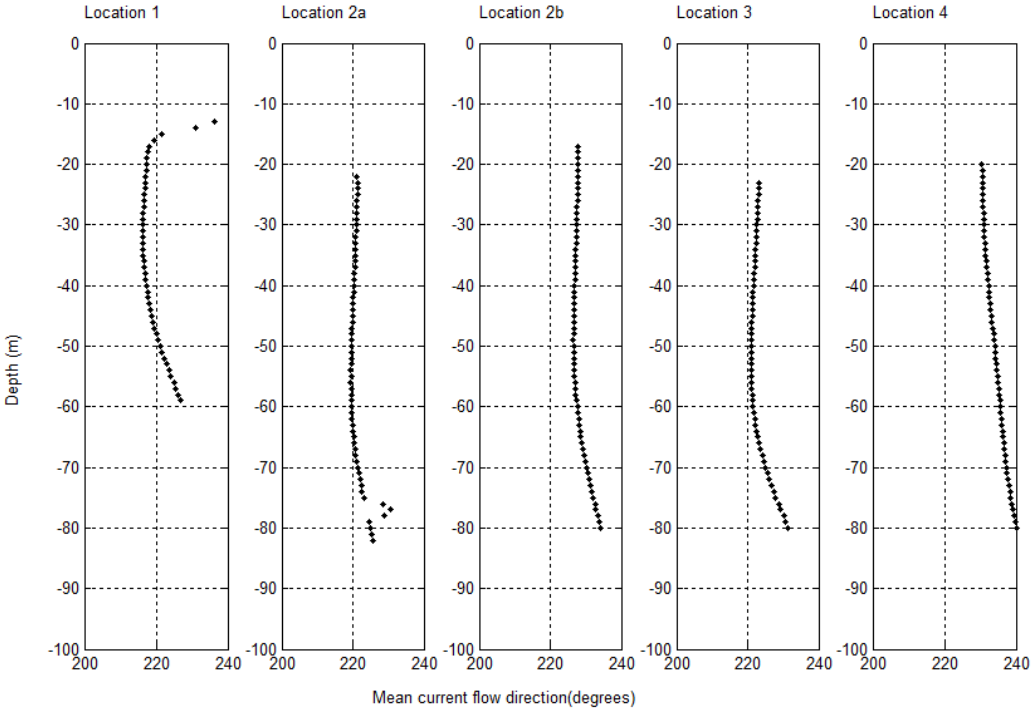

Figure 25: Mean flow direction versus depth

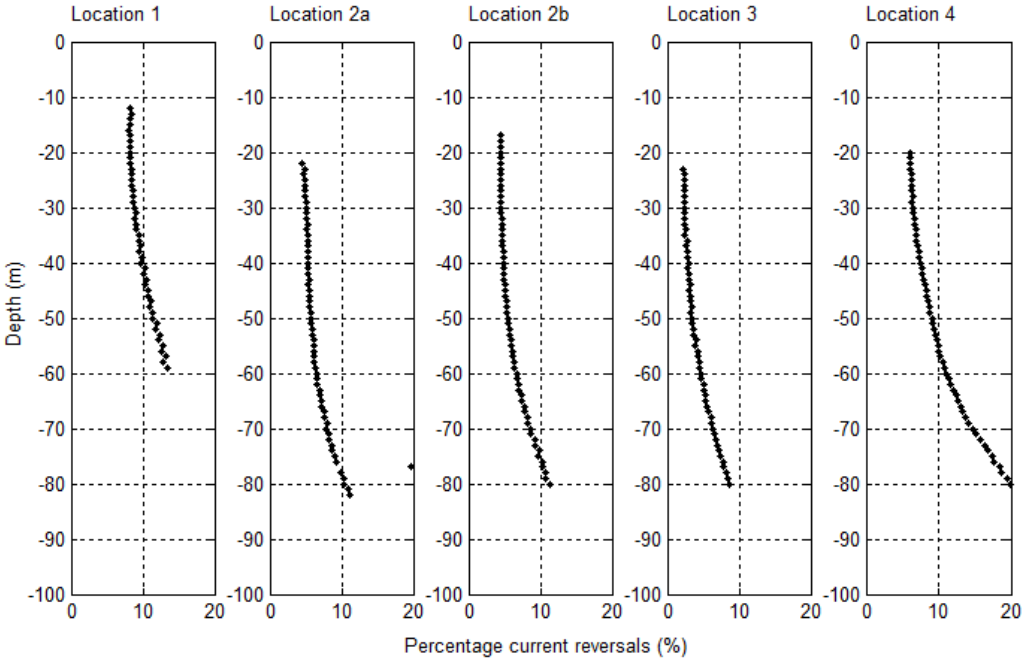

Figure 26: Percentage current reversals versus depth

Figure 25 illustrates the mean flow direction and Figure 26 the percentage of current reversals that occur at each location throughout the water column. Figure 25 shows that the current flows in a south westerly direction tending to a more westerly direction as it moves further south along the cost as seen at Location 4. A general trend shows that the currents variability decreases towards the surface, as observed in Figure 26. This trend is the result of the high velocity magnitudes closer to the surface forcing the current to flow in a more regular direction. Location 3 has the lowest variability with percentage current reversals of 2.3% and 3.3% at 50 m and 20 m, respectively. As indicated the measurements were not collected over the same time period thus the erratic presence of Natal Pulses in one time series can skew these results in dataset's favour. The presence of Natal Pulses is evaluated in section 5.1.4.

5.1.4. Occurrence of Natal Pulses

Temporal plots of the velocity magnitude at each location are evaluated with the use of the criteria presented in section 3.2.3 to find the number of Natal Pulses present in each dataset at each location. Table 4 summarises the number of Natal Pulses at each location during the measured period.

Figure 27 shows time series plots of the flow speed which highlights the variability of the current. The presence of a Natal Pulse is recognized as a drop in the current speed to near zero throughout the water column for longer than 10 continuous days. This indicates that the current core has been displaced from its original course by the Natal Pulse meander seawards. All 5 measurements have been plotted on the same temporal axis so that the different time periods over which that the data was collected are recognised and the propagation of a Pulse southward along the coastline can be identified.

Table 4: Number of Natal Pulses present in each measurement at each location

Dataset	Duration of Measurement (days)	Number of Natal Pulses	Number of Natal Pulses per Year
Location 1 *Port Edward*	365	2	2
Location 2a *Cape Morgan*	811	3	1.3
Location 2b *Cape Morgan*	692	5	2.6
Location 3 *East London*	477	2	1.5
Location 4 *Fish River*	650	4	2.3

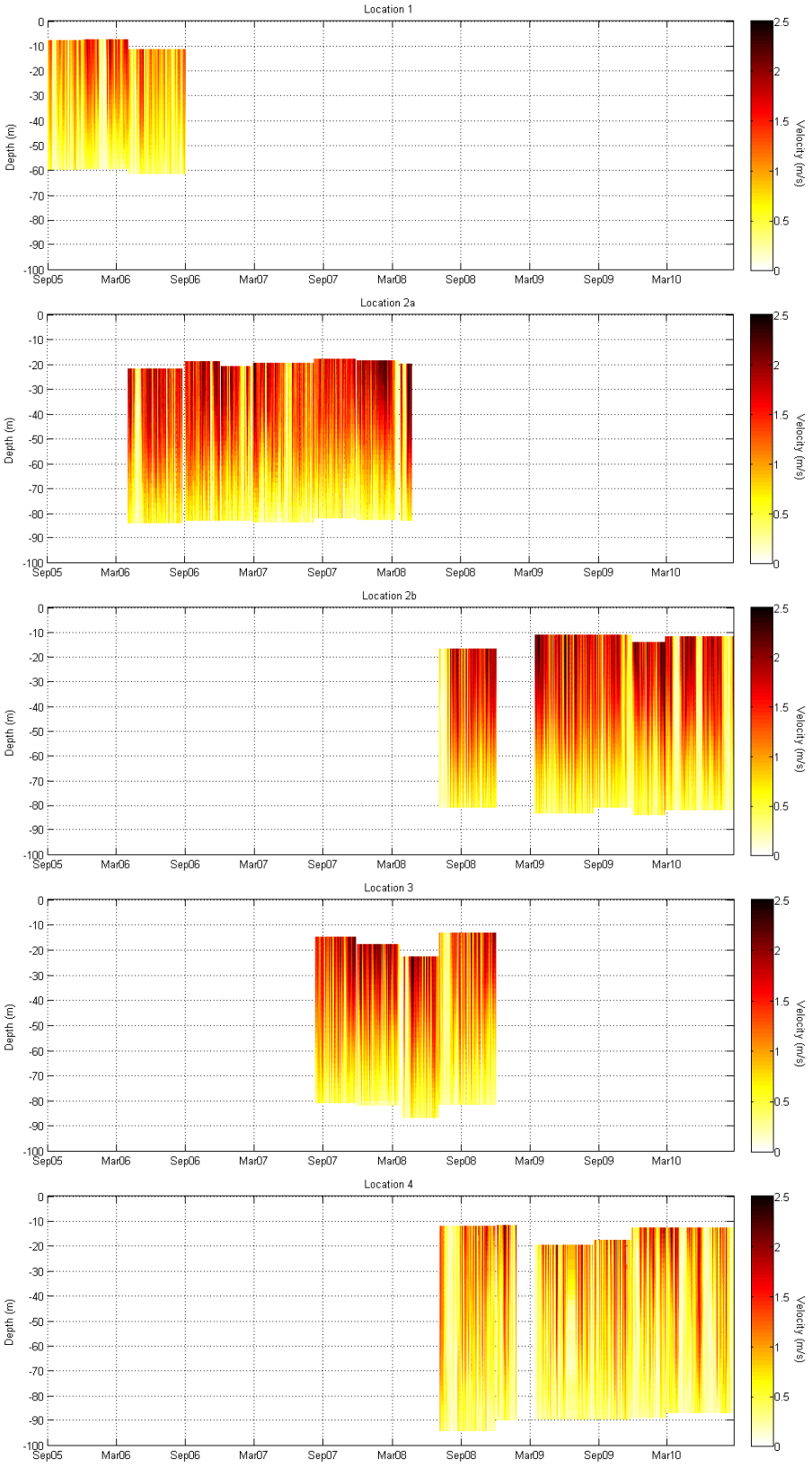

Figure 27: Temporal plots of velocity versus depth at all 5 datasets

In Figure 27, Location 2b, the presence of 4 Pulses (occurring Nov 09, Mar 10, May 10 and Aug 10) each persisting for at least 20 days are seen from November 2009 to September 2010. The average number of Natal Pulses per year found for this measurement period in Table 4 is 2.6. However if the measurement period were taken from November 2009 to November 2010 then the average number of Natal Pulses per year would be found to be 4. Such average skewing must be noted when regarding these results.

Considering Location 4 it is seen that the Natal Pulses of November 2009-September 2010 at Location 2b did not dissipate as they travelled southward as the presence of these pulses are seen in the dataset at Location 4. These pulses arrive at Location 4 approximately 15 to 20 days after being seen Location 2b.

Similarly the Natal Pulse which occurred in July of 2008 travelled down the coast growing in size, as the pulse is first seen in the dataset captured at Location 2b, then again in the Location 3 dataset and lastly in the Location 4 dataset. As with the 4 Natal Pulses from November 2009 to September 2010, this Natal pulse also takes approximately 15 days to arrive at Location 4 from Location 2. This attests to the sluggish velocity at which the pulses propagate taking a fortnight to travel 200 km.

Figure 27, Location 2a, also shows measurements taken at Location 2 but at an earlier time period to that the dataset Location 2b. However when the two datasets are compared, Location 2a only sees 3 pulses of approximately a 10 day duration during the time period of 24 months from April 2008 to May 2008. The difference in occurrence of Natal Pulses at the same location over different time periods shows the erratic and unpredictable nature of this phenomenon.

The results found in the temporal velocity plots compare well to the results found by Rouault and Penven (2011). Figure 28 shows the position of the Agulhas Current inshore front relative to the shore at 6 locations along the coastline in order to determine the presence and propagation of Natal Pulses. It is promising to see the correlation between the *in situ* data presented in Figure 27 and the satellite data used to plot Figure 28. From Figure 28 it is seen that the occurrence of the 4 Natal Pulses from November 2009 to September 2010 is abnormally high. Further the same propagation trend down the coastline that was found in Figure 27 is seen in Figure 28 with the Pulses growing in diameter as they move southwards. Also noted is the slow velocity at which the pulses travel down the coast.

The found mean occurrence of Natal Pulses over all the datasets in Table 4 is 1.9 Pulses a year. This is higher than the average 1.6 pulses a year found by Rouault and Penven (2011). As seen in Figure 28 the years 2004 to 2008 saw less Natal Pulses than years 2008 to 2011. Since the majority of the datasets analysed in Table 4 are during the latter period, a higher average is expected.

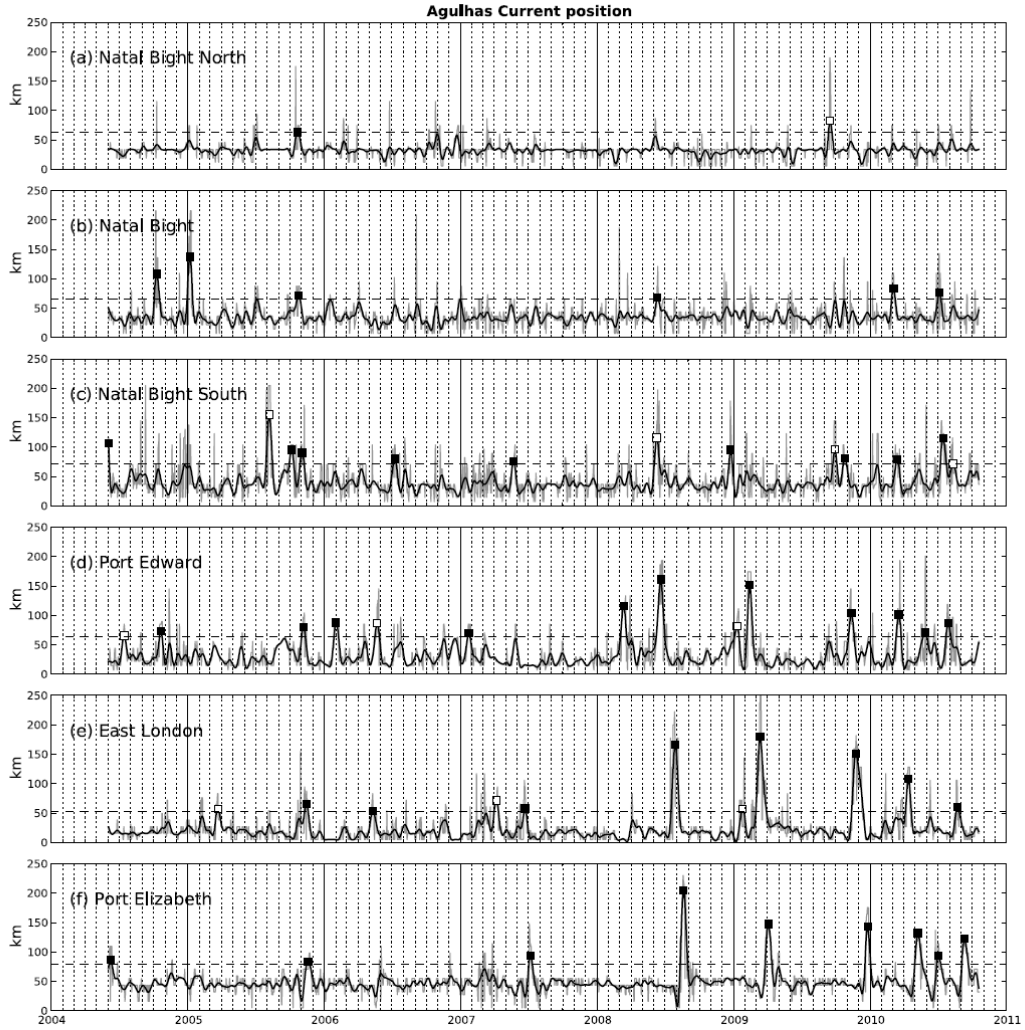

Figure 28: Position of the Agulhas current used to identify the presence of Natal Pulses. Natal Pulses indicated by black squares. (Rouault & Penven, 2011)

The lag between the locations shows the sluggish nature of the phenomenon but can be used to the advantage of grid planners. If an ocean current power plant were to be installed at Location 2 and the behaviour of the Agulhas Current was tracked further up the coast around Location 1, the presence of an approaching Natal Pulse can be predicted approximately a week to two weeks in advance. Such tracking can be done through remote sensing due to the strong correlation between *in situ* and altimetry results reducing the monitoring cost involved. This timely warning will allow operators to plan to use the period when the Natal Pulse is present for maintenance of the ocean current power plant. Furthermore grid planers can mobilise other capacity to ensure the demand of the country is met. However other available capacity may not be available during winter months when demand is high and since there is no seasonal trend in the occurrence of Natal Pulses there is risk associated around the firm capacity of an ocean current power plant. The lengthy presence of a Pulse (~20 days) in one location is a

concern for the technically possible capacity factor and the capability of ocean current energy to add to the base-load electricity supply of the country.

5.1.5. Summary of Deployment Series 1 results

Table 5: Results Deployment Series 1 at 20 m depth

At 30 m depth	**Location 1** *Port Edward*	**Location 2a** *Cape Morgan*	**Location 2b** *Cape Morgan*	**Location 3** *East London*	**Location 4** *Fish River*
Mean [m/s]	0.8	1.4	1.4	1.3	0.8
Maximum [m/s]	1.7	2.7	2.8	2.7	2.5
Mean Power Density [W/m^2]	404	1 934	1 891	1 725	658
Percentage [%] Current reversals	8.8	5.0	4.54	2.4	6.5
Number of Natal Pulses per year	2	1.3	2.6	1.5	2.3

From Table 5 it is deducted that the most promising area is Location 2. At Location 2, there are two sets of data available, collected at different time periods. During both time periods this location experienced the highest mean velocity of 1.4 m/s at 30 m depth. Location 3 has the second highest mean velocity of 1.3 m/s. Location 1 and Location 2 can be considered for turbine deployment but since Location 1 has a higher mean velocity, it shows greater potential for a consistent power yield. This analysis quantified directional variability through the percentage current reversal parameter. It was found that the directionality of the current is more consistent closer to the surface. The unusually high occurrence of Natal Pulses in the datasets captured during 2010 was highlighted and compared to satellite data in the region to confirm the findings. From the results of Deployment Series 1 a more detailed investigation into the area around Location 2 is required to determine the suitability of this region for turbine deployment and the practically extractable power.

5.2. Deployment Series 2

As discussed in section 3.1 the measurements taken in Deployment Series 2 consist of a mid-shelf and off-shore deployment in the Location 2 region. The following analysis compares the characteristics between the mid-shelf and off-shore locations. These characteristics will help formulate the suitable operating range for turbines designed to be deployed in the Agulhas Current. Further the potential capacity factor and capacity credit of a theoretical ocean current power plant at these locations is examined. These parameters will indicate the potential of ocean current power plants to contribute to the base-load of the South African electricity supply.

5.2.1. Current Magnitude

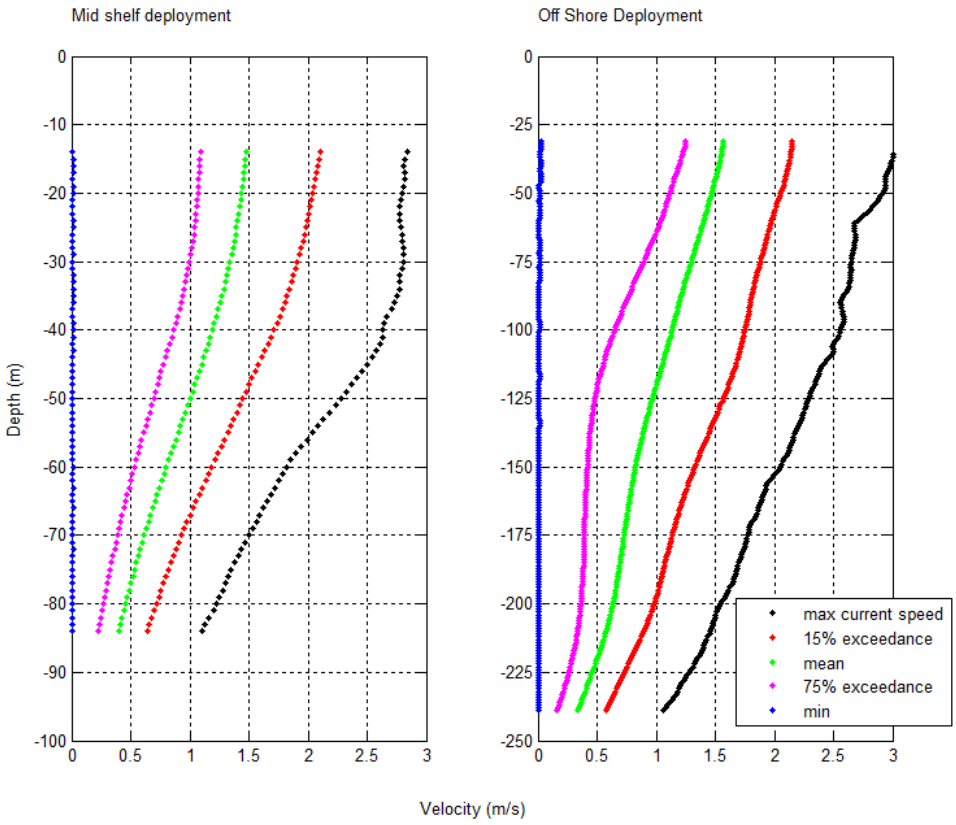

Figure 29: Current velocity (m/s) ADCP minimum (blue), 75% (magenta), mean (green), 15% (red), and maximum (black) flow speeds at the mid-shelf (left hand figure) and off-shore (right hand figure) locations

Figure 29 shows the current velocity versus depth. A minimum, 75% exceedance, 50% exceedance (mean), 15% exceedance and the current maximum is plotted. On comparison of the two sites, the presence of the Agulhas core is seen clearly at the off-shore location. At this location, at a water depth of 50 m the mean velocity is 1.49 m/s and at 30 m water depth, the mean velocity is 1.59 m/s. For the mid-shelf deployment the mean current velocity is 1.00 m/s at 50 m and 1.34 m/s at 30 m water depth. The mid-shelf mooring is thus placed at the core's edge. At 30 m water depth the off-shore current velocity is 1.2 times greater than the mid-shelf velocity, which when the cubed relationship between velocity and power is considered, results in a significant difference. The 75% exceedance values at 30 m depth are 1.0 m/s and 1.29 m/s for the mid-shelf and off-shore deployments, respectively and at 50 m are 0.69 m/s and 1.17 m/s. A similar trend is seen for the 15% exceedance plot with values at a 30 m depth of 1.91 m/s and 2.16 m/s for the mid-shelf and off-shore deployments, respectively, and at 50 m of 1.45 m/s and 2.06 m/s for the mid-shelf and off-shore deployments, respectively. These found ranges indicate that a turbine that is deployed in the Agulhas Current will need to operate at speeds between 0.6 m/s and 2 m/s.

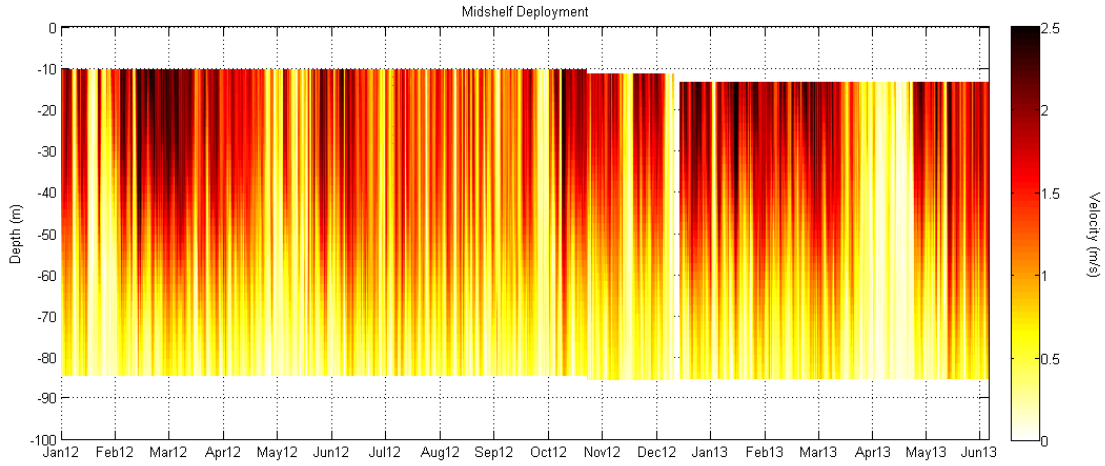

Figure 30: Temporal Plot at the Mid-shelf location. Time versus depth with the colour scale indicating current speed [m/s]

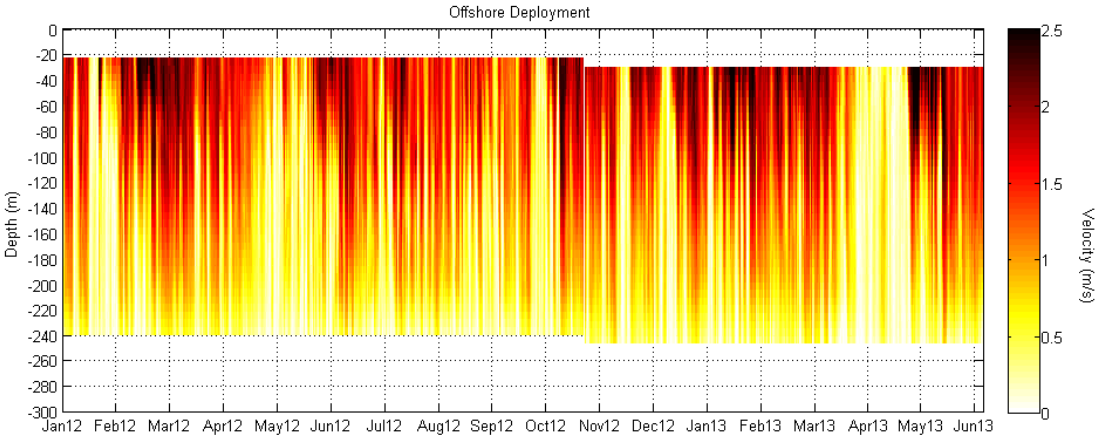

Figure 31: Temporal Plot at the Off-shore location. Time versus depth with the colour scale indicating current speed [m/s]

Figure 30 and Figure 31 are temporal time series plots of time versus depth with the colour scale indicating current velocity for each location. These plots highlight the variability of the current velocity showing the erratic presence of day long eddies and Natal Pulses. The distinct presence of a Natal Pulse is seen during April 2013, indicated by the entire water column velocity dropping to near zero. The size of these meanders are realised as both sites are affected by this occurrence. Both Figure 30 and Figure 31 show how problematic the presence of this phenomenon will be to potential power production from a turbine array as all power production will stop during the presence of a Natal Pulse. There are three other time periods of low velocity seen in these figures indicating the presence of eddies in the current core, namely during February 2012, May 2012 and October 2012. These eddies did not persist as long as the occurrence in April of 2013,

however these event will add to the variability of the current and lower the availability of the current.

As discussed in section 5.1.4 Rouault and Penven (2011) found an average of 1.6 Natal Pulses travel down the eastern coast of South Africa annually. The dataset evaluated here is 18 months long with only one distinct occurrence present that can result in a more optimist capacity factor for this period than in an average year. This shows that the measured *in situ* datasets cannot be used in isolation to quantify the performance of the current, but needs to be compared to longer datasets (10 years or more) obtained through satellite measurements. Such a comparison can be made because the presence of Natal Pulses is accurately predicted by remote sensing.

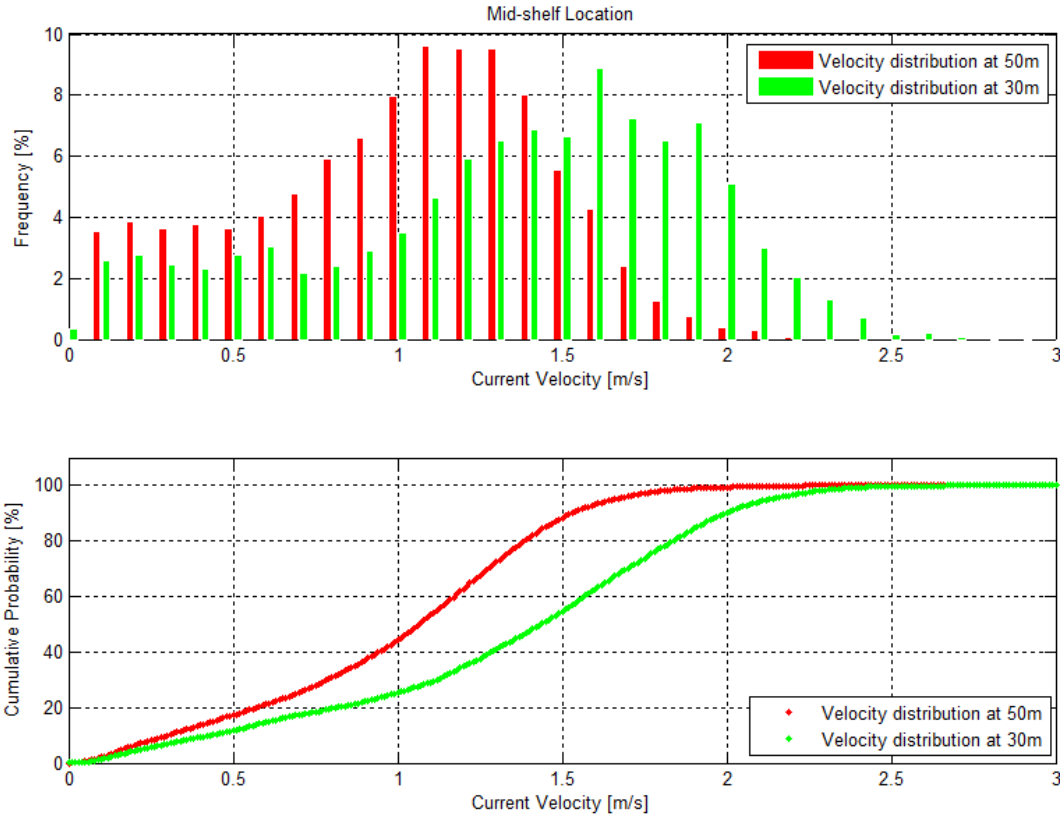

Figure 32: Velocity distribution at the mid-shelf location

Figure 32 and Figure 33 show the velocity distribution and cumulative frequency of occurrence at 30 m and 50 m depth for each of the locations. In both these figures in the frequency of plot, two district peaks are seen, one low velocity peak, indicating the velocity distribution during the presence of a Natal Pulse or weekly eddies and the second when no such phenomena are present. The second peak tends to a normal distribution curve but is skewed to the left by low velocity values. This seen distribution must be noted when the mean velocity or mean power density is evaluated throughout the water column as, if the periods

when Natal Pulses are present are treated as maintenance periods, thus excluded, then the average velocity or power density will be higher than represented. However, as seen in Figure 30 and Figure 31 there are periods of low velocity that do not persist as long as Natal Pulses but will negatively affect potential power production and cannot be discounted.

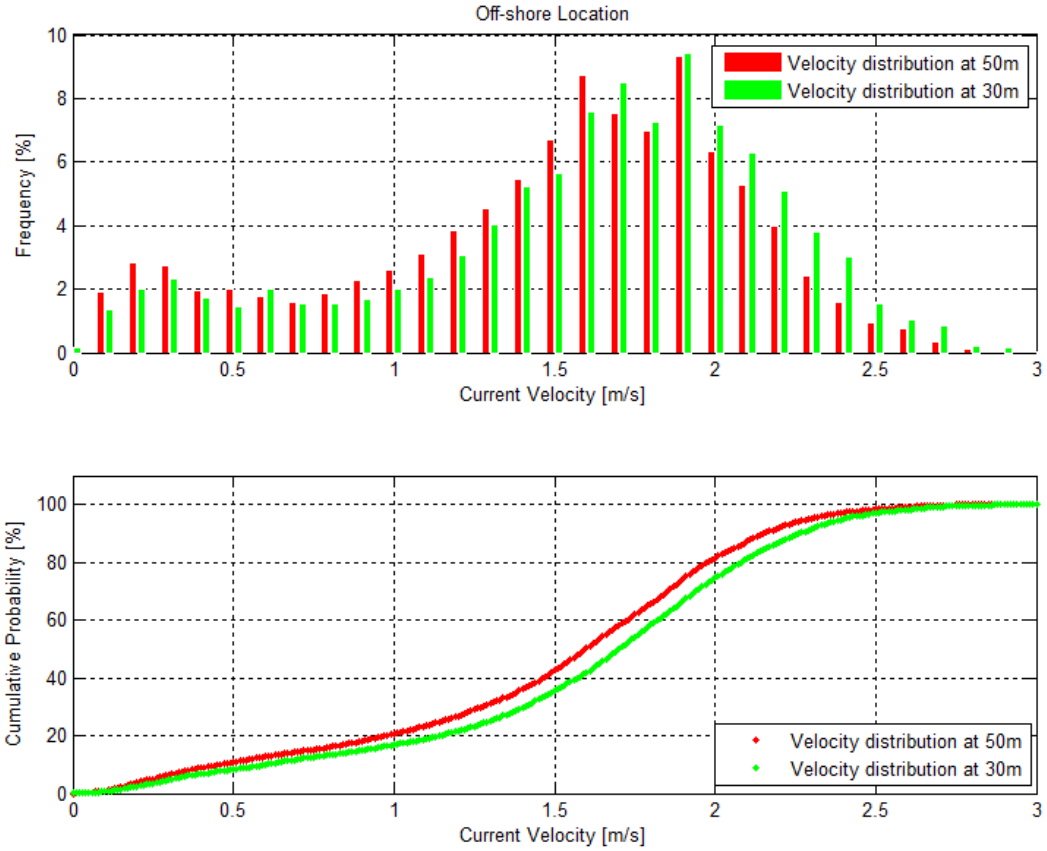

Figure 33: Velocity distribution at the off-shore location

The typical cut-in speed of marine turbines, as discussed in Table 3, is between 0.5 and 1 m/s. If the velocity distribution is compared to these velocity values for both the mid-shelf and off-shore location, it is noted that the low velocity peak present in the full distribution curve will result in non-operational turbines. Owing to this distribution, the variability of the velocity and power density of the current cannot be found through the use of standard deviation but variability should rather be examined once the power output from a turbine is found, through capacity factor and the time dependent capacity credit parameters.

Figure 32 and Figure 33 highlight the difference in velocity seen at 30 m depth compared to 50 m depth, by the shift in the histogram bars towards the higher velocities for the shallower measurement. There is less of a difference between the velocities at 30 m and 50 m depth at the off-shore location due to the deeper penetration of the current core at this site and lesser impact of seabed drag on

the current. Furthermore, velocities at a 60 m water depth at the off-shore location are comparable to the velocities at a 20 m depth at the mid-shelf location. This is important to note as deploying and mooring a turbine array at a sea bed depth of 255 m may prove challenging. Figure 29 to Figure 33 reiterate the importance of mooring the turbine array as close to the surface as possible for maximum power output.

5.2.2. Power Density

The mean power density versus depth is plotted in Figure 34. As noted in the velocity magnitude analysis, the power density at 20 m at the mid-shelf deployment (2 265 W/m^2) is similar to that at 60 m at the off shore deployment (2 180 W/m^2). At 30 m water depth the mean power density is 1 857 W/m^2 and 2 866 W/m^2 at the mid-shelf and off-shore locations, respectively. The power density at the off-shore location is 1.5 times greater than the power at the mid-shelf location at 30 m water depth. At 50 m water depth the mean power density is 813.6 W/m^2 and 2 440 W/m^2 at the mid-shelf and off-shore locations, respectively. This results in the power density at the off-shore location being 3 times larger than that of the mid-shelf deployment at 50 m water depth.

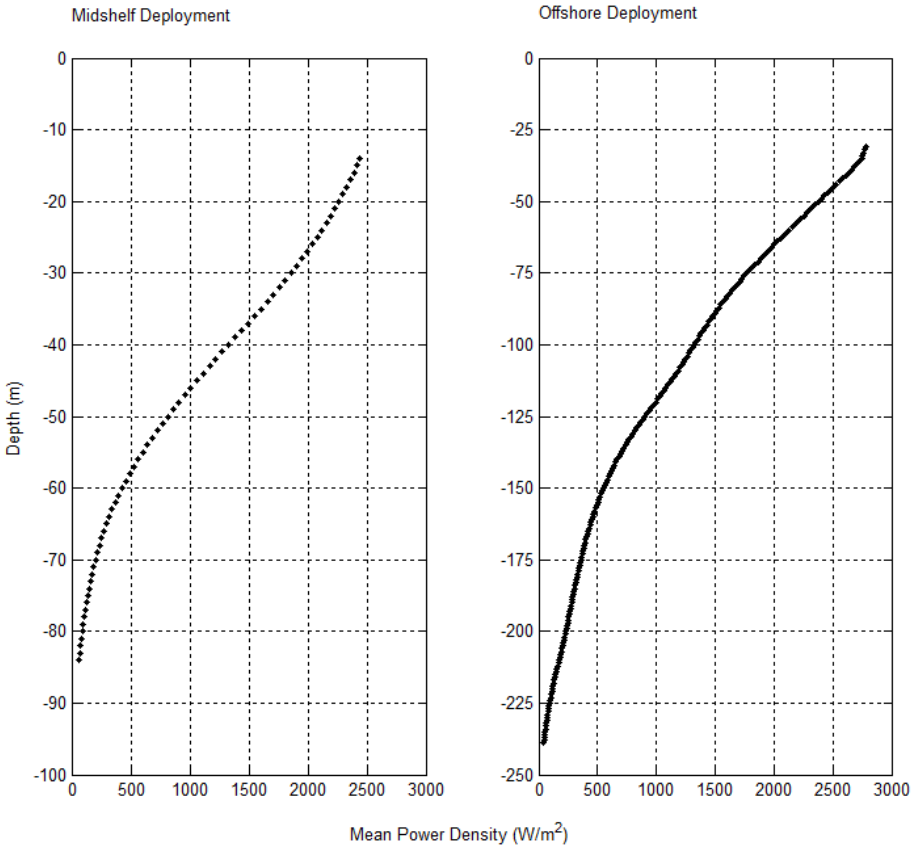

Figure 34: Mean power density (W/m^2)

5.2.3. Directional Analysis

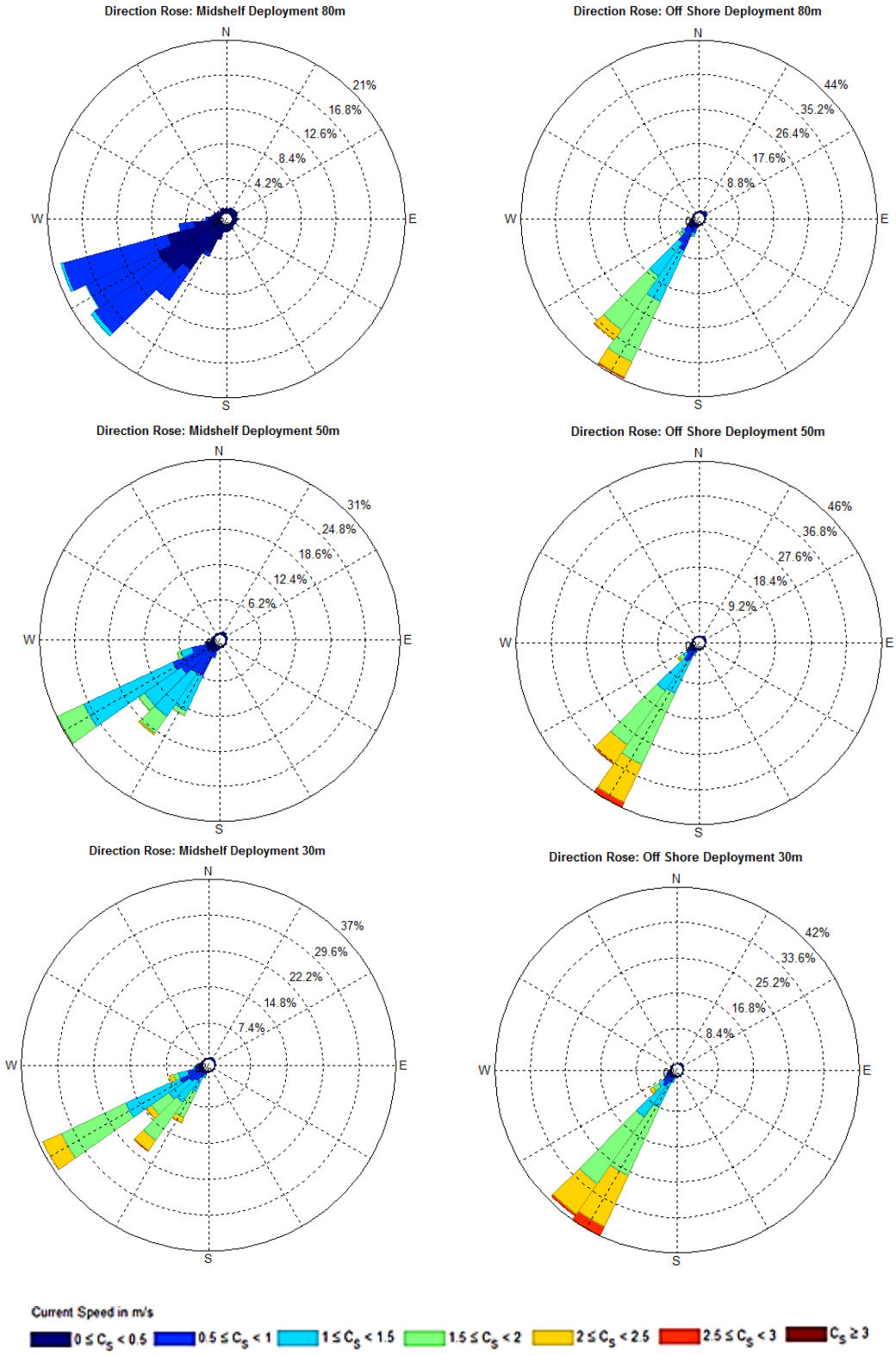

Figure 35: Mid-shelf location (left) and Off-shore location (right): Current directional Roses at 80 m (top), 50 m (centre), and 30 m (bottom) water depth

The direction at each location is described through directional roses plotted at 80 m, 50 m and 30 m in Figure 35. When the mid-shelf and offshore locations are compared a slight shift in the predominant current direction is seen as the current approaches the shore.

At the off-shore location the predominant current direction is approximately 195˚ from North where at the mid-shelf location, the predominant current direction is 210˚ from North. This directionality shows that the current flows in a general south westerly direction with onshore components.

At the mid-shelf location, at 80 m water depth, the onshore directional tendencies are seen, whereas at 50 m and 30 m water depth, the directionality ranges between 195˚ and 210˚ from North. The current directionality is more constant at the off-shore location with only two predominant directions seen, namely 195˚ and 200˚ from North. This is compared to the mid-shelf deployment that possesses five distinct directional components. This indicates the presence of the core at the offshore location, with the more swift flowing waters reducing the variability in the direction of the current

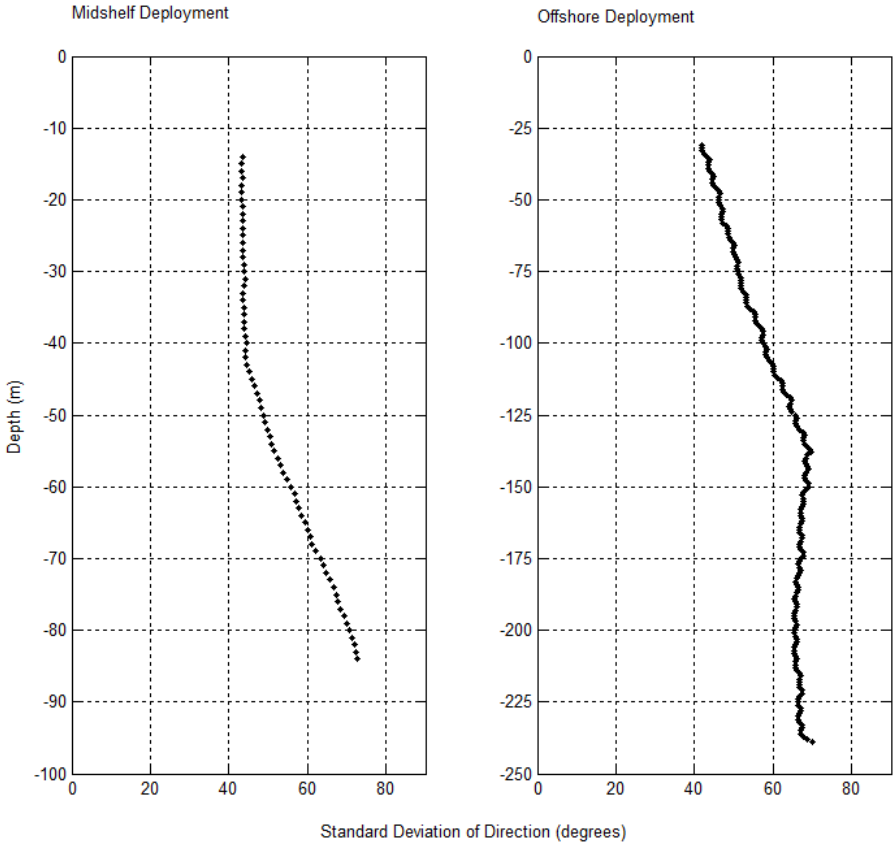

Figure 36: Standard deviation of flow direction in degrees

The directional roses do not show directionality when the velocity is zero, but the near zero velocity components can be seen to ring the centre of the rose, indicating that during eddies or Natal Pulses the directionality of the current is no longer in the south westerly direction and current reversals take place. This is further analysed in Figure 37.

Figure 36 and Figure 37 illustrates the relationship of the standard deviation of direction and the percentage current reversals with depth below sea surface. The standard deviation of the current's direction increases with depth in the upper water column as seen in both mid-shelf and off-shore locations. In the off-shore location the variability stabilises below a depth of 137 m. At 30 m depth the standard deviation is 43.98˚ and 40.08˚ for the mid-shelf and off-shore locations, respectively. At a depth of 50 m, the standard deviation is 48.66˚ and 44.85˚ for the mid-shelf and off-shore locations, respectively. This variability shows that the chosen turbine must be able to adapt to the change in flow direction in order to achieve a maximum power output.

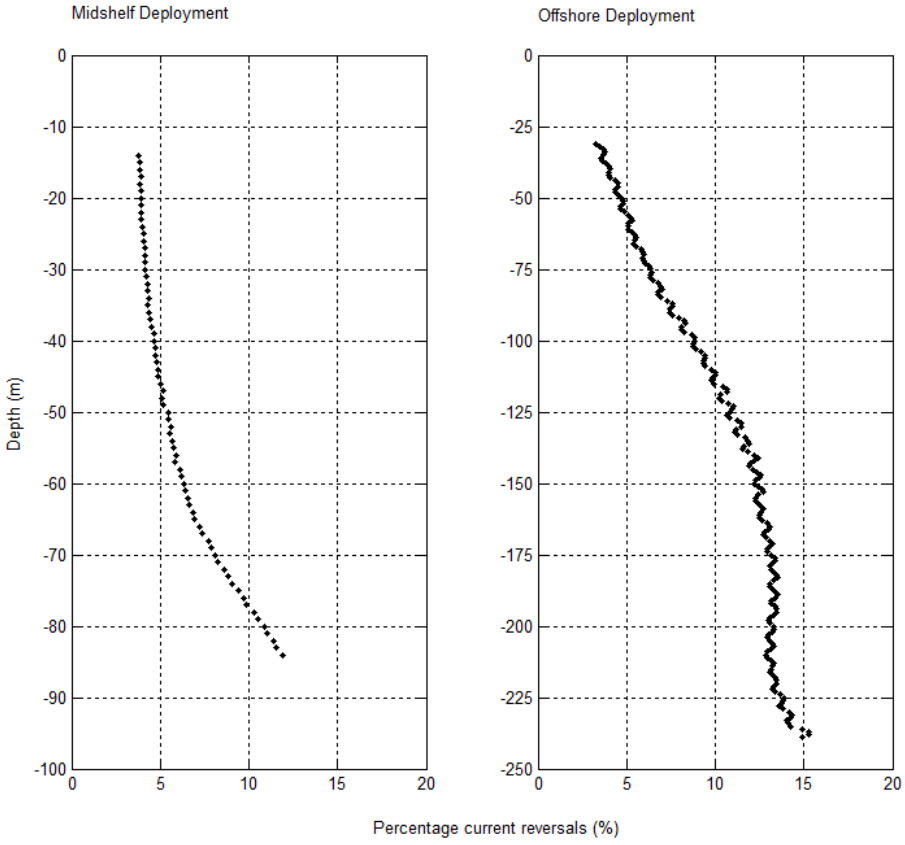

Figure 37: Percent of time that flow reversals occur at each location

The percentage current reversals show the same trend of directional variability increasing with depth. The area of interest for turbine deployment lies in the upper 50 m and at this depth the percentage current reversals for the mid-shelf

and off-shore location is 5.4% is it 4.4%, respectively. At a depth of 30 m, current reversals of 4.1% and 3.1% are realised at the mid-self and off-shore locations, respectively. At these water depths, this percentage of current reversals is low and will generally take place during the occurrence of Natal Pulses however; the selected turbine must be able to survive these events.

5.2.4. Capacity Factor

From the results of the current magnitude and directional analysis it is established that the required technology needs to operate in a flow range of 0.6 m/s and 2 m/s with the mean velocity occurring between 1 m/s and 1.5 m/s. Further, this technology must be adaptable to change in current direction and survive the presence of a Natal Pulse which results in a zero velocity period. From the analysed technology, Table 3, the Minesto Deep Green turbine will be the most suitable technology to use to determine the practically extractable power from the Agulhas Current. Although the published maximum mooring depth is 120 m, this will be increased as Minesto adjusts the mooring and tethering system to deploy in the Gulf Stream. The practicality of mooring the Minesto Deep Green turbine at depths comparable to the off-shore location will be determined at the FAU test site (280 m deep). The depth of the mid-shelf location is comparable to prospected tidal test sites for the deployment of the Minesto technology (consented 0.5 MW power plant in Holyhead Deep, Anglesey, UK). The power curves of the 500 kW (DG-12) and 850 kW (DG-14) Minesto turbines, used to find the capacity factors at the selected depths and locations, can be found in Appendix D on the full technical specification sheets of each turbine.

Table 6 and Table 7 show the found capacity factors for each location at a 30 m and 50 m water depth for the two different Minesto turbines. Table 6 presents the findings from the 850 kW Deep Green turbine with a rated speed of 1.73 m/s and optimal operating range of 1.4 m/s to 2.2 m/s and Table 7 presents the findings from the 500 kW Deep Green turbine with a rated speed of 1.6 m/s and optimal operating range of 1.4 m/s to 2.2 m/s. Similar to the wind turbine industry, the economics of the availability of power versus the magnitude of the power produced must be weighed up against one another to find the best suited turbine; however such an economic analysis is beyond the scope of this investigation.

Table 6: Found Capacity factor for the Minesto 850 kW Turbine

Minesto 850 kW Deep Green rated speed of 1.73 m/s		
Depth	**Mid-Shelf Location**	**Off-Shore Location**
30 m	56%	70%
50 m	30%	63%

Table 7: Found Capacity factor for the Minesto 500 kW Turbine

Minesto 500 kW Deep Green rated speed of 1.6 m/s		
Depth	**Mid-Shelf Location**	**Off-Shore Location**
30 m	62%	74%
50 m	37%	68%

On examination of Table 6 and Table 7, the capacity factor for the off-shore location is significantly higher than the mid-shelf location, with only a 5% drop in capacity factor between the 30 m and 50 m deployment depths. At the mid-shelf location a 25% drop in capacity factor is seen between the 30 m and 50 m deployment depths. Since the mid-shelf location is situated at the edge of the Agulhas Current, the core does not penetrate as deep as at the off-shore location, resulting in a drop in velocity which is amplified by the cubed power velocity relation and the subsequent drop in capacity factor.

The mid-shelf location performs better, in respect to capacity factor, when the 500 kW turbine is used as the energy extraction technology with capacity factors of 62% and 37% at a depth of 30 m and 50 m, respectively. These figures are reduced to 56% and 30% when the 850 kW turbine is deployed due to the higher rated operating speed of the specific turbine. At the off-shore location, capacity factors of 74% and 68% are seen when the 500 kW turbine is deployed at depths of 30 m and 50 m, respectively. Capacity factors of 70% and 63% are estimated when the 850 kW turbine is deployed at depths of 30 m and 50 m, respectively. With reference to the 850 kW turbine, these results indicate that the capacity factor of the off-shore site is 1.25 times greater at 30 m and 2.1 times greater at 50 m than that of the capacity factors found at the mid-shelf location at identical depths.

When comparing the found capacity factors at both locations to the values of other renewable energy resources, the Agulhas Current fairs well. Desktop analysis by Kritzinger in collaboration with Department of Energy's IPP-office, approved for publication in 2014 found for the South African wind resource, the capacity factor for the under-construction or installed wind farms greater than 80 MW range from 30% to 45%. If the turbines are installed at 50 m or shallower, the found capacity factors are greater than those generated by wind farms for both analysed turbines. A typical capacity factor found for tidal energy extraction ranges from 20% to 30% and for wave energy extraction devices, 15% to 22% (Boyle, 2012). The found capacity factors of the Agulhas Current point to a more constant resource in comparison to other renewable energy resources indicating a possible contribution to the base-load supply of electricity.

Although the capacity factor of the off-shore site is higher than that of the mid-shelf location, the economics of the longer sea cable and increased mooring challenges must be taken into consideration when deciding on an optimal deployment location. Furthermore the price of energy availability coupled with the price per kWh of generated electricity must also be examined when selecting the rated power size of the turbine. Table 8 shows the theoretical power output and specific yield from the 850 kW and 500 kW Minesto turbine respectively.

The annual electricity production from the 850 kW turbine at the off-shore site will be 5.20 GWh and 4.15 GWh at the mid-shelf location. For the 500 kW turbine the annual electricity production at the off-shore location is 3.26 GWh and 2.71 GWh at the mid-shelf location. For both the mid-shelf and off-shore locations the 500 kW turbine has a higher specific yield than the 850 kW turbine and higher capacity factors and thus a turbine with a lower rated speed is more suited for this application. However, the turbines used in the analysis are designed specifically for tidal applications, thus there is a need to optimise the chosen turbine for the Agulhas Current conditions to maximize turbine capacity factor and produced energy.

Table 8: Theoretical Power output at 30 m depth

	Minesto 850 kW (rated at 1.73 m/s)		**Minesto 500 kW** (rated at 1.6 m/s)	
	Annual Yield (MWh/annum)	**Specific yield (kWh per year /kW installed)**	Annual Yield (MWh/annum)	**Specific yield (kWh per year /kW installed)**
Mid-Shelf Location	4 153 MWh	**4 886 kWh/kW**	2 708 MWh	**5 416 kWh/kW**
Off-Shore Location	5 197 MWh	**6 114 kWh/kW**	3 258 MWh	**6 515 kWh/kW**

5.2.5. Capacity Credit:

Having found a suitable turbine for energy extraction (Minesto Deep Green -12, 500 kW) the availability of the Agulhas Current can be determined during peak hours. The power produced from the 500 kW turbine was simply scaled up to 1 000 MW with no regard for array placement, wake regions or overall cabling losses. Further the velocity at the measured ADCP point is used as the input to find the power for the 1 000 MW system, thus the spatial variation in velocity, as would be seen in an array configuration, is not taken into consideration. This simplified approach can be used as this analysis aims to illustrate the availability of a potential ocean current plant during peak periods. Figure 38 shows the possible contribution of a 1 000 MW ocean current plant at the offshore location to the overall system demand during the peak demand months of the year. During the month of May there are three instances of two days where the ocean

current plant drops off completely, during June two instances of four days of no production and during July one instance of three days of no production. This results in a capacity factor of 68% for this period. However, it is encouraging to see the persistent presence of the current throughout the peak evening periods during the time periods when the plant is online.

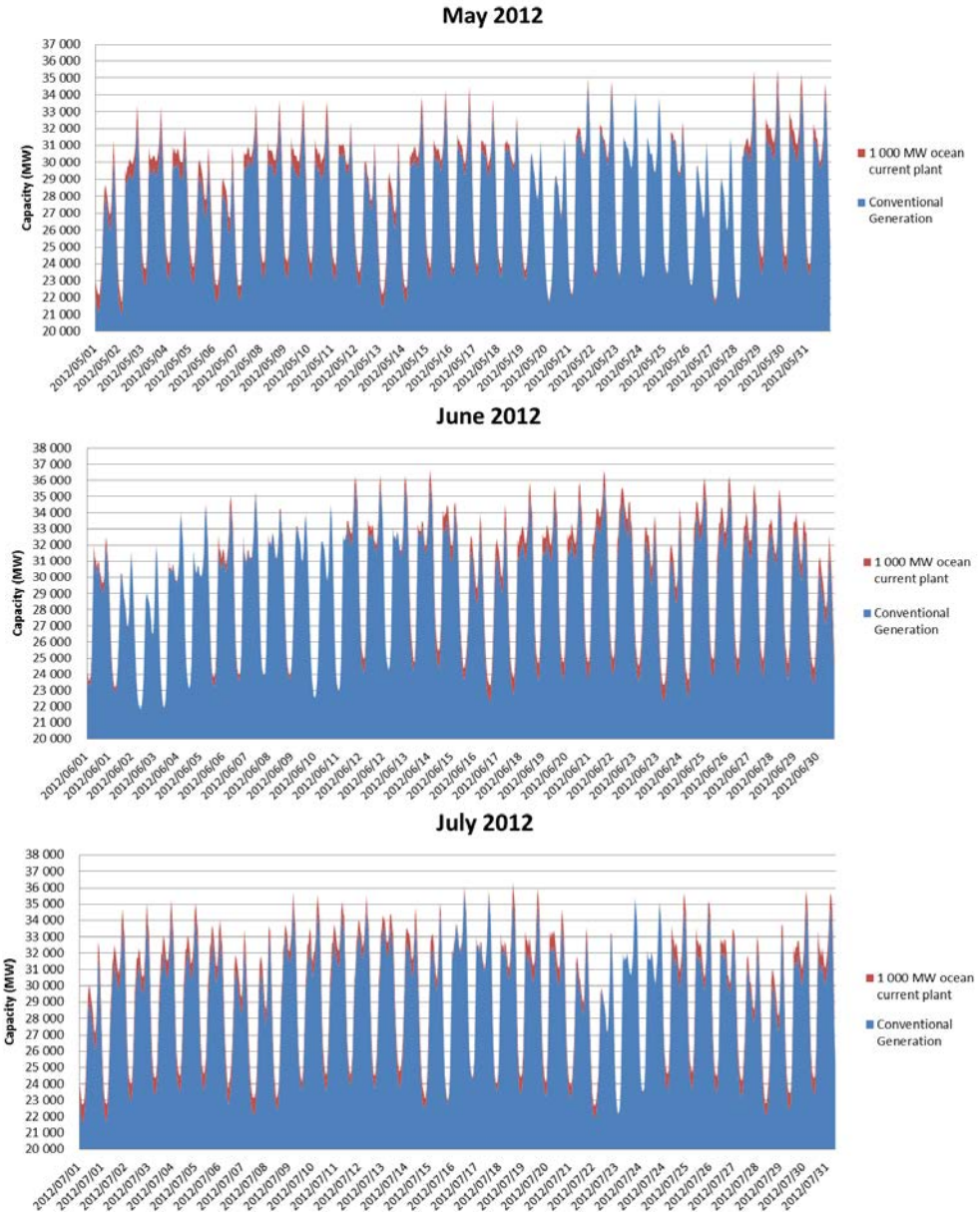

Figure 38: Possible contribution of a 1 000 MW ocean current power plant to the overall system demand

The capacity credit for varying sized plants is shown in Table 9 where the equivalent load carrying capacity is taken at 99% confidence interval. The found equivalent load carrying capacity shows what dispatchable conventional power plants investment can be deferred. The capacity credit for a 2 000 MW ocean

current plant is found to be 32% and 36% at the mid-shelf and off-shore locations respectively. The found capacity credit by Pöller (2011) for a dispersed wind power plant capacity of 2 000 MW is 27% (Pöller, 2011). Thus an ocean current plant compares well to the wind power plant performance in South Africa. Capacity credit decreases with installed renewable energy capacity as shown in Table 9 and this trend same trend was observed by Pöller (2011). There is an outlier in this trend at the off-shore location and this abnormality needs to be further investigated in future work. These results show that an ocean current power plant has the ability to reliably add to the energy mix of South Africa and supply electricity during peak demand periods with a reasonable confidence.

Table 9: Capacity Credit

Size of plant [MW]	Mid-shelf Location		Off-shore Location	
	Equivalent load carrying capacity	Capacity credit	Equivalent load carrying capacity	Capacity credit
100	60.7	61%	62.5	62%
200	104.7	52%	131.7	66%
500	232.6	47%	242.3	48%
1000	433.6	43%	450.8	45%
2000	647.6	32%	720.8	36%

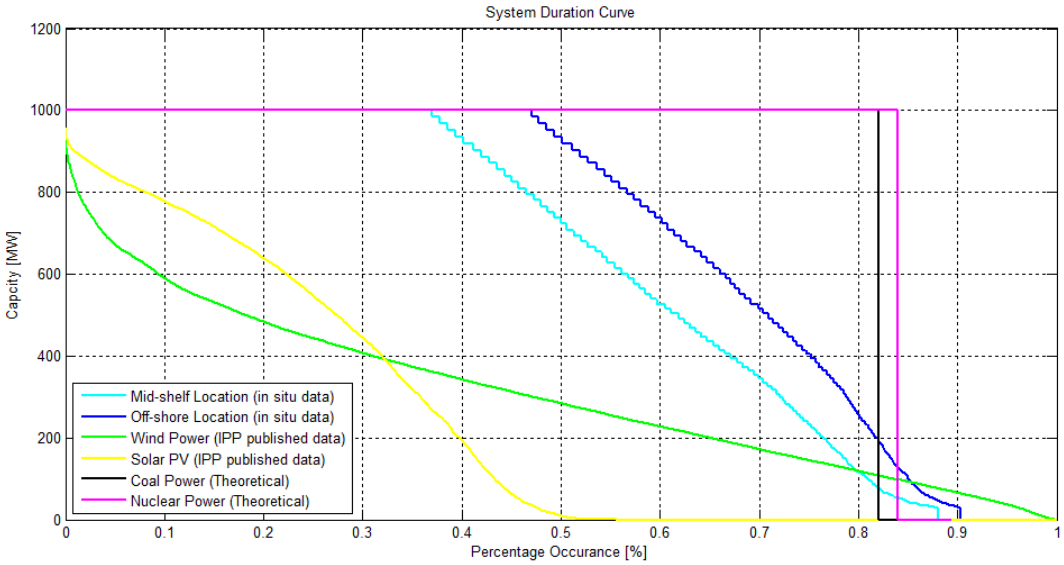

Figure 39: System duration curve for conventional and renewable energy power plants

System duration curves are presented in Figure 39 for all systems normalised to 1000 MW peak. Wind and solar photovoltaic systems are presented and conventional power systems of coal and nuclear are shown. The conventional

power systems' curves are based on single published availability figures from Eskom (Eskom , 2014). The renewable energy duration curves are produced from the online independent power producer plants published data. The ocean current plants are theoretical plants with practicalities such as maintenance down time and losses not accounted for, resulting in a more positive duration curve than possible. Although the performance of the ocean current power plants may be inflated, that ocean current plants are significantly more online than the wind and solar plants as illustrated by Figure 39. Furthermore the ocean current plant compares well to conventional power plant duration curves indicating the possibility that this source of renewable energy can add to the base-load electricity supply of the country.

5.3. Other Contributing Factors

The practically extractable power does not only depend on the selected power take-off technology and resource velocity and directionality but is also affected by a number of others factors. These factors are discussed below.

5.3.1. Geotechnical and Mooring Considerations:

The results found, with respect to the current magnitude and direction, indicate that a strong and constant flow of seawater takes place at the off-shore location. However this location has a sounding depth of 255 m which raises concerns surrounding the mooring challenges and the drag forces on the turbine tether in order to moor the turbine hub at 30 m below the surface. A stronger and more advanced mooring system will be required at the off-shore location and the economics of higher power production versus the cost of a more robust mooring system must be considered.

Most experience in the mooring of tidal energy extraction devices is in water depths of less than 100 m and since there is no oil drilling activity in this area off the eastern South African coast, there is a lack of practical engineering experience of working in the required water depths. The mid-shelf location has a sounding depth of 91 m thus some of the lessons learnt from the tidal industry will be transferable, however when working in a tidal resource there is a period of slack water as the tide changes between ebb and flow. The constant flow of the current may prove challenging during deployment and maintenance operations for ocean current power plants.

In order for successful mooring of turbines within the Agulhas current the engineering constraints with respect to the environment needs to be well understood. One aspect of this is the sedimentary and geotechnical properties of the seabed for mooring considerations. Limited information is available on these characteristics and properties of the subsurface ocean. Documentation of the ocean bed forms along the South East coast of South Africa occurred in the late

1970s and thus the information presented here is based on these maps and findings.

Figure 40 shows a schematic diagram of the shelf section between the latitudes of 28˚S and 34˚S. The region of focus, as shown in Figure 40, is section B and C, the outer shelf region which is dominated by the current. The Agulhas current dictates the sedimentary transport in this region. Here the presence of shifting subaqueous dunes and relict gravels are seen. Dune heights of up to 8 m, length of 200 m and dune field widths of a minimum of 10 km have been recorded. The outer-shelf gravels consist of relict sediments produced during the early Flandrain transgression by reworking of fossil algalreef bioherms (Flemming, 1978). There is a distinct change in bed form type between the inner-shelf and outer-shelf which consist of relict carbonate facies. The continental shelf has a very steep slope (~12˚ gradient) and is dissected by numerous submarine canyons. The outer shelf region consists of current-generated bed forms such as sand streamers, dunes and an exposed gravel pavement (Flemming, 1980).

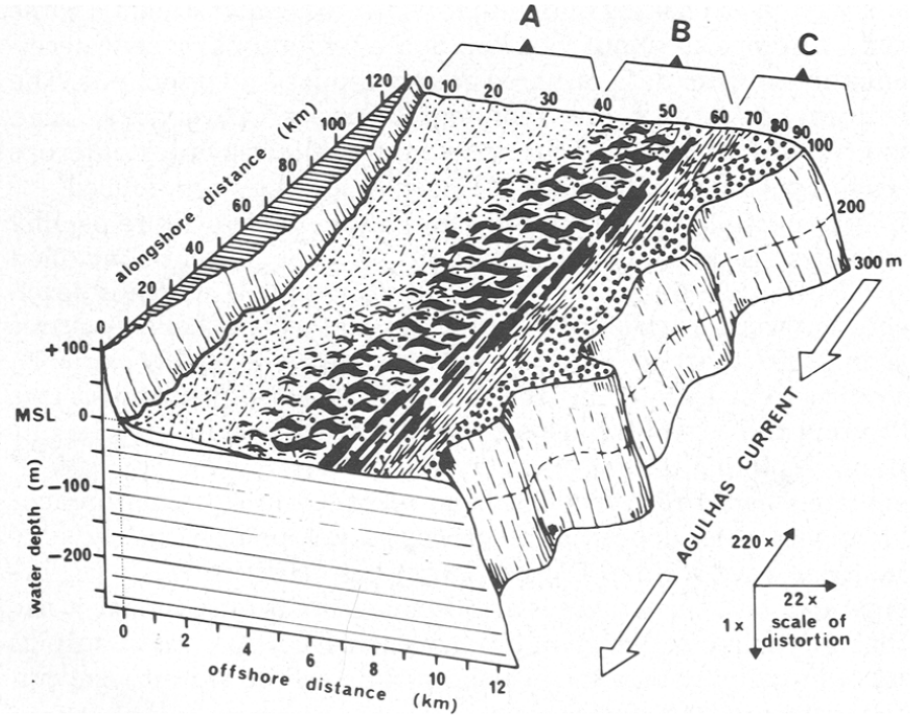

Figure 40: Schematic block diagram of the shelf section summarizing the sedimentary and structural (Flemming, 1980).

The shifting dunes can be problematic as cabling running ashore can be possibly exposed increasing risk of scour, indicating that more frequent maintenance on the cabling will have to be conducted. The presence of the dunes will also increase the amount of dredging that has to be done before bedrock is reached. These dunes are a continuous feature along the southeast margin of the African continent and thus will be encountered continuously along the coast. An array of

turbines will be tethered and anchored to the sea bed. The concerns surrounding this mooring method will be similar to those in other unidirectional currents with one main loading direction where vortices and vortex shedding may be problematic. The device will have to be robust and designed to withstand geological and environmental extremes whilst keeping the sophisticated equipment afloat, thus the anchoring foundation must be designed for dynamical loading. The anchors must be designed to resist high cyclic lateral loads with a good scour protection on the tethering cable (Dean, 2010).

Another phenomenon within the Agulhas current is the presence of “Giant Waves” these waves are unpredictable and have the ability to break large ships in two (Lutjeharms, 2006). These waves occur in the core of the current at the landward border, the same position investigated for device deployment. Although the energy extraction devices will be located at least 20 m below the surface such extreme conditions must be taken into account for maintenance concerns and the fatigue loading in the device and mooring system.

Very little experience has been gained in respect to mooring considerations in this region, thus extensive geotechnical surveys will have to be carried out if ocean current energy becomes a reality in this region.

5.3.2. Commercial Fishing Activities:

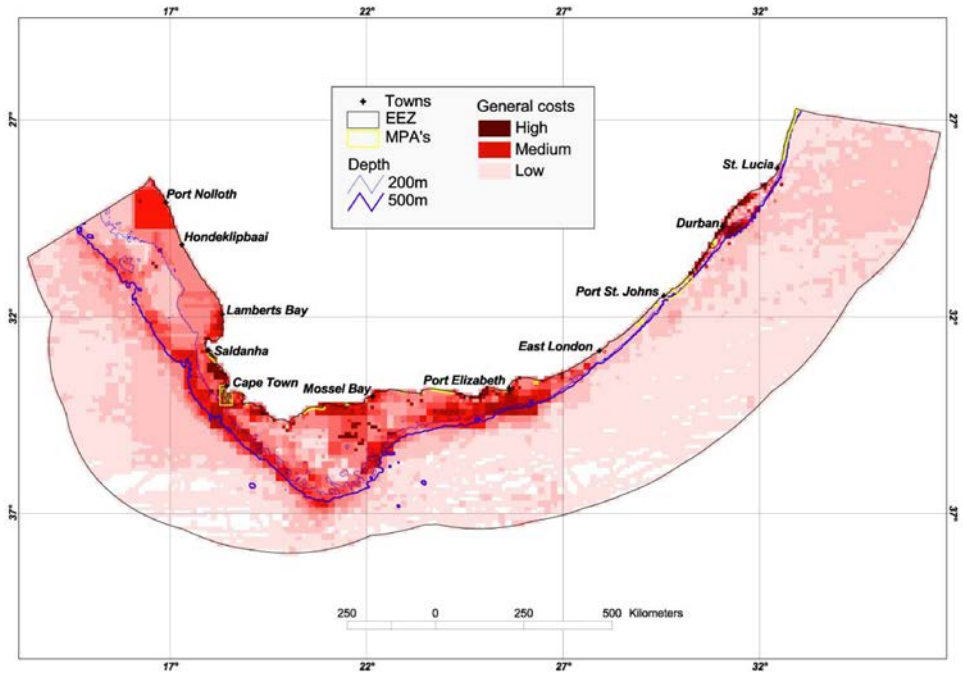

Figure 41: Map showing the cost benefit to the fisheries industry. The darker areas are of greater importance to the industry in both benthic and pelagic respects (Sink, et al., 2011).

Figure 41 shows areas of importance to the fisheries industry. The map shows a cost benefit analysis indicating the zones of high yield. The area of interest for current turbine development lies between East London and Port St John's and from Figure 41 it is seen that this is not a prime area for fishing activity. This finding is positive as placing a turbine array in this area will help unlock the economic potential of the ocean in this region without interfering with other economic activities or ocean users. This is a preliminary finding and the site specific effect of the turbine array on the commercial and subsistence fish farmers will need to be determined through an environmental impact assessment.

5.3.3. Shipping Routes:

The shipping route down the east coast of South Africa is an important trade route as illustrated in Figure 42 by the number of journeys travelled over a year period. The establishment of a turbine array must not hinder this economic activity and the appropriate depth below the surface must be established. Although the deployment depth of the turbines will take heed of ship wakes, exclusion zones may have to be considered in respect to ship anchoring concerns in the region of turbine deployment.

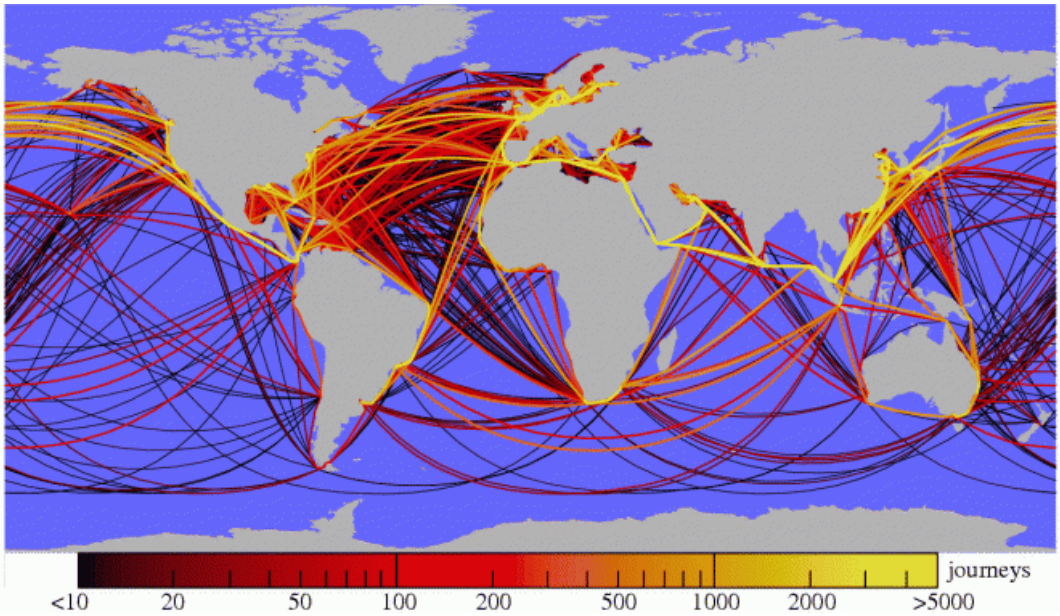

Figure 42: The trajectories of all cargo ships bigger than 10 000 GT during 2007 (Kaluza, et al., 2010).

5.3.4. Existing Infrastructure that can Consume the Generated Energy:

A schematic of the existing Eskom substations is seen in Figure 43. The mid-shelf site is located 14 km from the shore and a further 30 km from the nearest medium voltage station. The off-shore site is 18 km from shore and then a further 30 km from the nearest medium voltage station. This indicates that there is existing infrastructure to make use of the generated electricity, however an economic analysis must be carried out to determine whether the increased power generated at the off-shore location justifies the increase in sea cabling length. Such an assessment is beyond the scope of this project. The distances from the deployment sites to the nearest substation are significantly longer than that seen for tidal sites, but comparable to off-shore wind sites. For off-shore wind sites subsea AC cabling is used for projects located up to approximately 60 km off-shore (Norton, et al., 2011).

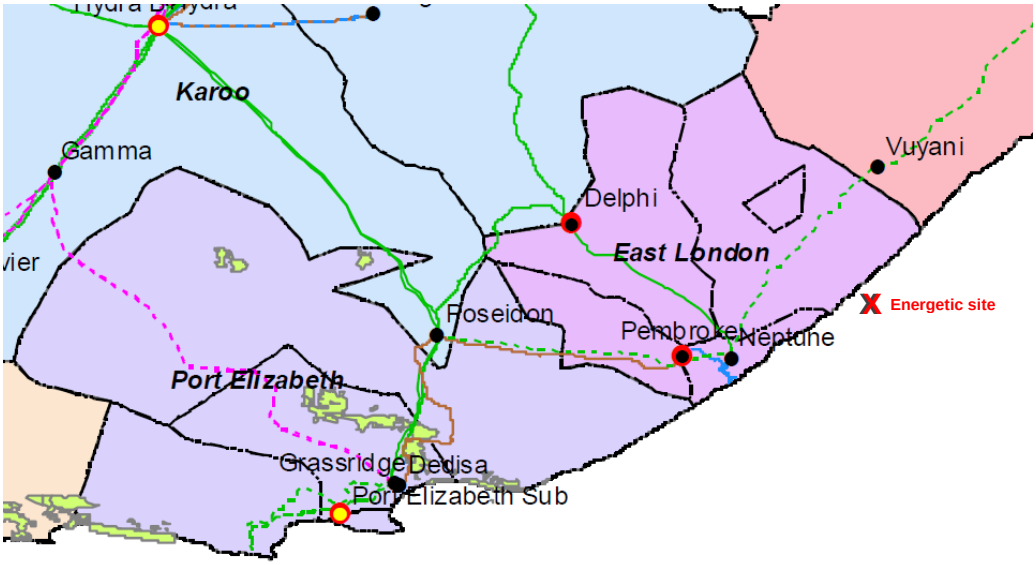

Figure 43: Position of existing Eskom substations in the region of interest (Eskom, 2015)

5.3.5. Environmental Impact:

The closest existing marine protected area lies 15 km north of the analysed sites. No marine protected areas lie between the selected sites and the closest harbour located on the coast of Port Elizabeth, 350 km south west of the chosen sites. The positions of the existing and proposed marine protected areas along the South African coastline are seen in Figure 44. The closest economic hub in this area is East London which lies south of the analysed sites, thus no cabling or vessels required for the deployment and maintenance of the devices will pass through marine protected areas. It is also encouraging to notice that the

proposed marine protected areas will also not cause obstacles in this regard. Furthermore the chosen turbines are shrouded, therefore decreasing the impact of these devices on marine mammals.

On a larger scale, the environmental impact on meridional overturning circulation of placing turbines that extract energy from the Agulhas current has not yet been investigated and the maximum size of a potential power plant is yet to be established. In 2007 the Bureau of Ocean Energy Management published an Environmental Impact Statement (U.S. Department of the Interior Minerals Management Service, 2007) in which the effects of deployment of ocean current turbines in the Gulf Stream are considered. The impacts will depend on the technology and array configuration chosen but typical impacts include reduction in current velocity and energy and possible reduction in wave height in the vicinity of the devices (U.S. Department of the Interior Minerals Management Service, 2007). Reduction of wave height will be localised, but the reduction in current energy can impact larger systems namely weather patterns, and the interactions of current with near shore waters. Such impacts within the Agulhas Current will need to be determined through large scale ocean modelling. The impacts of ocean current turbine systems can be limited through restricting the quantity of energy extracted from the current and maximising the efficiency of the systems deployed. If such mitigations are put in place this environmental challenge should not result in the discontinuation of ocean current projects.

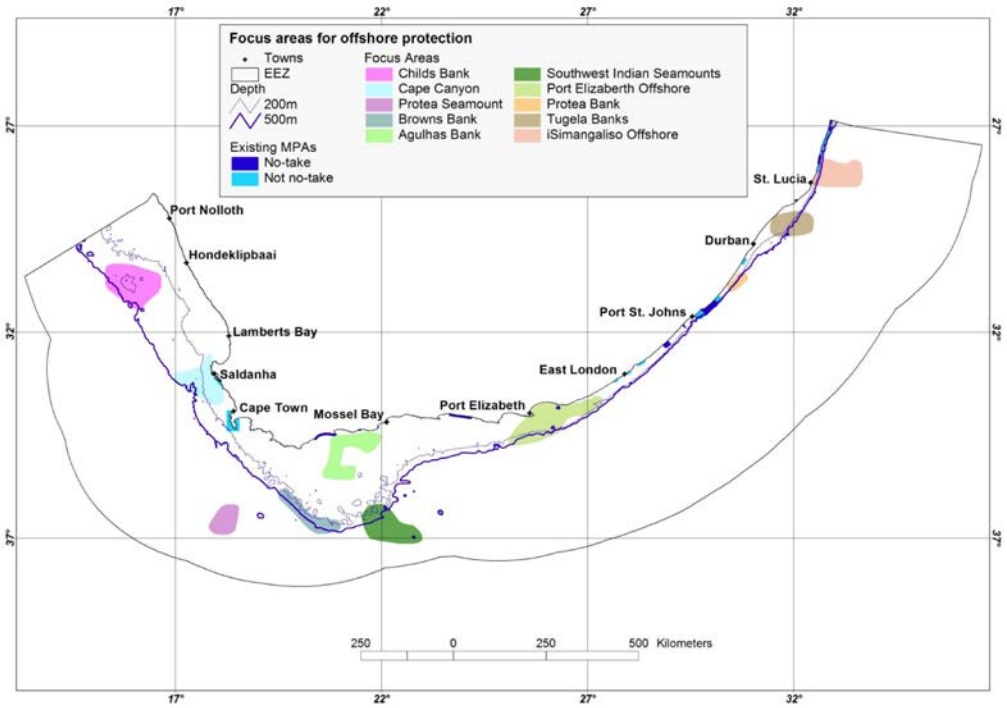

Figure 44: Existing and proposed marine protected areas around the South African coast (Sink, et al., 2011).

5.3.6. Regulatory Environment

South Africa has a well-established National Environmental Management: Integrated Coastal Management Act (2008) (ICMA) which regulates the activities along the coastline. Prior to any construction on the coastline an environmental impact assessment will need to be carried out in regulation with this act. However there is a lack of Marine Spatial Planning within the EEZ zones of South Africa to regulate marine usage between the various stakeholders in the marine environment. The launch of Operation Phakisa has seen the establishment of a formal Maritime Spatial Planning (MSP) process for South Africa. The National Coastal Management Programme of South Africa that falls under the ICMA act and is valid for the period of 2013 to 2015 aims to resolve current management problems and user-conflicts (due to the wide variety of activities and uses of the coast), and outline the long-term development and management of the coastline (Department of Environmetal Affairs , 2014). The focus areas for the MSP are as follows: aquaculture, mining, shipping, fisheries and conservation (Marine Protection Services and Governance , 2014). Renewable energy has been excluded from this plan, and this can result in uncertainty surrounding the consenting process for marine renewable projects.

Other formal permits which will need to be considered in order to obtain consent for a marine renewable project include: National Environmental Management Biodiversity Act, Sea Birds and Seals Protection Act and NERSA Electricity Regulation Act. This is not necessarily a comprehensive list as each project's permitting will need to be approached on a site to site basis.

From the preliminary analysis of other contribution factors, there is no one factor that will cause such a project to be a no-go. The economics of such an endeavour are still a challenge and the environmental concerns will need to be addressed so that renewable energy stakeholders become well established and welcomed users of the marine environment.

6. CONCLUSION

Through the analysis of ADCP datasets along the eastern South African coastline, an area of swift, stable flow in the Agulhas Current has been identified. This area is approximately 100 km northeast from East London, the closet economic hub. One mid-shelf and one off-shore site in this area is analysed and it has been found that the off-shore site holds more energy with higher velocities and reduced directional variability. This analysis indicates that the current core is located in the proximity of the off-shore site and only boarders on the mid-shelf site. The mean velocities found at 30 m depth at the offshore location is 1.59 m/s and at the mid-shelf location is 1.34 m/s. Ideally a turbine will operate at rated speed in this velocity range.

From a technology survey of devices that are currently undergoing sea trials or have undergone sea trials, the Minesto Deep Green (DG-12) turbine has been identified as the most appropriate developed technology for potential deployment in the Agulhas Current. The Minesto DG-12 has a rated power of 500 kW at 1.6 m/s and for a single turbine the achievable capacity factor at the off-shore site at 30 m below the surface is 74% and the mid-shelf site 62%. The found estimated capacity factors compare well to other renewable energy resources with the mid-shelf site being higher or comparable to off-shore wind and the off-shore site being significantly higher than all renewable energy technology without storage. Although promising capacity factors can be achieved with the Minesto Deep Green turbines, there is great uncertainty surrounding the survivability and mooring challenges of this technology.

It has been found that the presence of Natal Pulses can be predicated by approximately 15 days if tacked from a location higher up the coast. This prediction helps in minimising the effects of this phenomenon as such periods of no production can be used for scheduled maintenance and grid planners will have warning enough to mobilise other forms of generation.

The capacity credit of a potential ocean current power plant was evaluated to determine the ability of such a plant to add to the base-load electricity supply of the country. For a 2 000 MW system at the off-shore location the capacity credit was found to be 47% which is significantly higher than the 27% for wind power plants of the same magnitude. This figure indicates that an ocean current plant can add to the base-load electricity supply of the country increasing the reliability of the system as it supplies power during peak demand periods. With South Africa’s present electricity crisis this found result is encouraging. South Africa’s renewable energy mix consists of mostly solar PV and wind with some concentrating solar power and biomass plants. Currently wind and solar PV plants are very cost effective and being rolled out in South Africa but do not reliably add to the system capacity during peak or constrained hours of the day.

Owing to the immature nature of ocean current technology the cost of such a power plant is high; however the more stable nature of this resource sets it apart from other intermittent renewable energy resources.

The Minesto Deep Green turbine is the only suitable, developed technology found at the time of this study, however there is still scope for further technology development that performs at rated power within average water speeds of 1.5 m/s and can survive the occurrence of current reversals in the form of Natal Pulses. It is recommended that further technology development be carried out with specific focus on suitable technology for ocean current applications. Together with this technology analysis, it is recommended that a detailed economic assessment be carried out to determine whether the increased mooring challenges and longer length of undersea cabling is justified by the increased power output at the off-shore site.

Although there are a number of engineering and financial challenges in deploying a turbine array in the Agulhas Current, it has been shown that this current holds potential to make a significant contribution to the South African electricity grid.

7. REFERENCES

Beal, L. 2003. *The Agulhas Undercurrent Experiment* [Online]. Available: http://www.po.gso.uri.edu/wbc/Fall_Beal/ [2013, February 20].

Beal, L. M. & Bryden, H. L. 1999. The Velocity and Vorticity Structure of the Agulhas Current at 32 S. *Journal of Geophysical Research*, 104(C3): 5151-5176.

Bowen, K. 2015. *IPP System Data.* Email. 22 July [Author in possession of email].

Boyle, G. 2012. *Renewable Energy*. 3 ed. Oxford: Oxford University Press.

Bryden, H. L., Beal, L. M. & Duncan, L. M., 2005. Structure and Transport of the Agulhas Current and its Temporal Variability*. Journal of Oceanography*, 61: 479 - 492.

Chen, F. 2010. Kuroshio Power Plant Development Plan*. Renewable and Sustainable Energy Reviews*, 14: 2655-2668.

Couch, S. & Bryden, I. 2006. Tidal Current Energy Extraction: Hydrodynamic Resource Characteristics. *Journal of Engineering for the Maritime Environment*, 220(M): 185-194.

Dean, E. 2010. *Offshore Geotechnical Engineering*. London: Thomas Telford Limited.

Department of Environmental Affairs. 2014. *The National Coastal Management Programme of South Africa*, Cape Town: Department of Environmental Affairs.

Duerr, A. E. S. & Dhanak, M. R. 2012. An Assessment of the Hydrokinetic Energy Resource of the Florida Current. *Journal of Oceanic Engineering*, 37(2): 281-293.

Ecomerit Technologies, 2012. *Aquantis* [Online]. Available: http://www.ecomerittech.com/aquantis.php [2015, February 7].

Eskom. 2014. *Generation* [Online]. Available: http://integratedreport.eskom.co.za/supplementary/lin-generation.php [2015 July 27].

Eskom. 2015. *Generation Connection Capacity Assessment of the 2022 Transmission Network*, Johannesburg: Eskom [Online]. Available:

http://www.eskom.co.za/Whatweredoing/GCCAReport/Documents/GCCA2022Document%20Jun2015.pdf

Flemming, B. 1978. Underwater Sand Dunes along the Southeast African Continental Margin-Observations and Implications. *Marine Geology*, 26: 177-198.

Flemming, B. 1980. Sand Transport and Bedform Patterns on the Continental Shelf between Durban and Port Elizabeth (Southeast African Continental Margin). *Sedimentary Geology*, 26: 179-205.

Gyory, J., Mariano, A. J. & Ryan, E. H. 2012. *The Benguela Current* [Online]. Available: http://oceancurrents.rsmas.miami.edu/atlantic/benguela.html [2013, March 11].

Ingram, D., Smith, G., Bittencourt-Ferriera, C. & Smith, H. 2011*. Protocols for the Equitable Assessment of Marine Energy Converters*. Edinburgh: The University of Edinburgh on behalf of EquiMar project consortium.

Joubert, J. R. 2008. *An Investigation of the wave energy resource on the South African Coast, focusing on the spatial distribution of the South West Coast*. Master's thesis. Stellenbosch: Stellenbosch University.

Kabir, A. & Lemongo, I. J. 2014*.* Hydrokinetic Energy Resource Assessment of the Gulf Stream Near Cape Hatteras, North Carolina*, Proceedings of the ASME 2014 33rd International Conference on Ocean, Offshore and Arctic Engineering*: San Francisco.

Kaluza, P, Kolzsch, A, Gastner, M. T. & Blasius, B. 2010. The Complex Network of Gloabal Cargo Ship Movements. *Journal of The Royal Society ,* 7: 1093-1103.

Kane, D. 2014. The Next 90: Using Vortex Power to Extract Energy from Ocean Currents Flowing below 3 Meters per Second. *Proceedings of the 5th International Conference on Ocean Energy,* Halifax.

Kempener, R. & Neumann, F., 2014. *Tidal Energy Technology Brief*, Bonn: International Renewable Energy Agency [Online]. Available: http://www.irena.org/DocumentDownloads/Publications/Tidal_Energy_V4_WEB.pdf

Kritzinger, K. 2015. Personal Interview. 23 February, Stellenbosch.

Krug, M. & Tournadre, J. 2012. Satellite Observations of an Annual Cycle in the Agulhas Current. *Geophysical Research Letters,* 39: L15607.

Lutjeharms, J. 2006. *The Agulhas Current*. Berlin: Springer.

Marais, E., Chowdhury, S. & Chowdhury, S. P. 2011. Theoretical Resource Assessment of Marine Current Energy in the Agulhas Current along South Africa's East Coast. *Paper presented at Power and Energy Society General Meeting, IEEE*, San Diego [Electronic]. Available: http://ieeexplore.ieee.org/xpl/articleDetails.jsp?arnumber=6039502&tag=1

Marine Protection Services and Governance. 2014. *Unlocking the Economic Potential of South Africa's Oceans,* Durban: Operation Phakisa.

Meyer, I., Reinecke, J., Roberts, M. & Niekerk, J. V. 2013. *Assessment of the Ocean Energy Resources off the South African Coast*, Stellenbosch: Centre for Renewable and Sustainable Energy Studies, Stellenbosch University.

MeyGen. 2015. *Technology* [Online]. Available: http://www.meygen.com/technology/ [2015, July 10].

Minesto. 2011. *DG-12 Technical Specifications*, Sweden: Minesto.

Minesto. 2011. *DG-14 Technical Specifications*, Sweden: Minesto.

Minesto. 2015*. Minesto* [Online]. Available at: http://minesto.com/ [2015, July 5].

Mofor, L., Goldsmith, J. & Jones, F. 2014. *Ocean Energy: Technology Readiness, Patents, Development Status and Outlook,* Bonn: International Renewable Energy Agency [Online]. Available: http://www.irena.org/DocumentDownloads/Publications/IRENA_Ocean_Energy_report_2014.pdf

Norton, M., Mansoldo, A. & Rivera, A. 2011. *Offshore Grid Study: Analysis of the Appropriate Architecture of an Irish Offshore Network*, Dublin: EirGrid Plc [Online]. Available: http://www.eirgrid.com/media/2257_Offshore_Grid_Study_FA.pdf

Pidwirny, M. 2006. *Surface and Subsurface Ocean Currents: Ocean Current Map* [Online]. Available: http://www.physicalgeography.net/fundamentals/8q_1.html [2015, July 3].

Pöller, M., 2011. *Capacity Credit of Wind Generation in South Africa*, Pretoria: Deutsche Gesellschaft für Internationale Zusammenarbeit (GIZ) GmbH [Online]. Available: http://www.wasaproject.info/docs/WindCapacityCreditFeb2011.pdf

Rouault, M. 2011. *Agulhas Current variability determined from space: a multi-sensor approach.* Doctoral dissertation. Cape Town: University of Cape Town.

Rouault, M. J. & Penven, P. 2011. New Perspectives on the Natal Pulse from Satellite Observations. *Journal of Geophysical Research*, 116: C07013.

Sink, K. et al. 2011. *Spatial planning to identify focus areas for offshore biodiversity protection in South Africa: Final Report for the Offshore Marine Protected Area Project*. Cape Town: South African National Biodiversity Institute.

Subsea World News. 2014. IHI, *Toshiba Conduct Tidal Turbine Demonstration Research* [Online]. Available: http://subseaworldnews.com/2014/12/26/ihi-toshiba-conduct-tidal-turbine-demonstration-research/ [2015, July 3].

Tethys. 2015*. MeyGen Tidal Energy Project - Phase I* [Online]. Available: http://tethys.pnnl.gov/annex-iv-sites/meygen-tidal-energy-project-phase-i [2015, July 3].

Tidal Energy Today. 2015. *VIDEO: SeaGen S 1.2 MW tidal turbine* [Online]. Available: http://tidalenergytoday.com/2015/05/01/video-seagen-s-1-2-mw-tidal-turbine/ [2015, July 3].

U.S. Department of the Interior Minerals Management Service. 2007. *Programmatic Environmental Impact Statement for Alternative Energy Development and Production and Alternate Use of Facilities on the Outer Continental Shelf: Final Environmental Impact Statement*, USA: Bureau of Ocean Energy Management.

Van Zwieten, J. H., Meyer, I. & Alsenas, G. M. 2014. Evaluation of HYCOM as a Tool for Ocean Current Energy Assessment. *Proceeding of Marine Energy Technology Conference*, Seattle.

Vortex Power Drive. 2014. *Vortex Power Drive* [Online]. Available: http://www.vortexpowerdrive.com/ [2015, July 3].

Wright, S. H., Chowdhury, S. & Chowdhury, S. P. 2011. A Feasibility Study for Marine Energy. *Paper presented at Power and Energy Society General Meeting, IEEE*, San Diego [Electronic]. Available: http://ieeexplore.ieee.org/xpls/abs_all.jsp?arnumber=6039896

APPENDIX A.METADATA ADCP DEPLOYMENTS

A total of 51 deployments were made between September 2005 and September 2010. The details of each deployment, including deployment date and time, GPS position and instrument type are given in Table 10.

The data is given in bins that divide the water column into horizontal sections.

- only bins where less than 25 % of the current measurements were labelled as ‘bad data’ are included.
- Bin 1 is always closest to the ADCP, with consecutive numbers moving away from the ADCP.
- Depth is the actual or calculated depth in meters of the centre of that bin.
- Range is the distance in meters from the ADCPs transducer to the centre of that bin.

Table 10: Deployment details for ADCP current meter deployments made on the east coast of South Africa.

SQ	Filename	ADCP type	Pressure sensor	Latitude (S)	Longitude (E)	Deployment date	Recovery date	Ship sounding (m)	Position
1	PE751	RDI 75	yes	-31.22263	30.20273	8-Sep-2005 16:44	11-Dec-2005 10:25	156	offshore
2	PE301	RDI 300 + waves	yes	-31.19722	30.17517	8-Sep-2005 17:06	11-Dec-2005 11:20	60	midshelf
3	PE601	RDI 600	yes	-31.17855	30.15253	8-Sep-2005 17:30	11-Dec-2005 12:05	31.8	inshore
4	PE602	RDI 600	**no**	-31.17860	30.15263	11-Dec-2005 13:58	10-Apr-2006 10:40	32.98	inshore
5	PE302	RDI 300 + waves	yes	-31.19732	30.17480	11-Dec-2005 14:54	10-Apr-2006 09:36	61.74	midshelf
6	PE752	RDI 75	yes	-31.22303	30.20270	13-Dec-2005 17:02	06-Apr-2006 08:22	173.4	offshore
7	EL1901	Nortek	yes	-32.50997	28.83000	14-Dec-2005 02:15	07-Apr-2006 09:10	83.25	midshelf
8	PE603	RDI 600	yes	-31.17865	30.15245	10-Apr-2006 17:30	09-Sep-2006 09:00	32.11	inshore
9	PEM03	RDI 600	**no**	-31.19753	30.17460	10-Apr-2006 17:50	09-Sep-2006 08:30	62.11	midshelf
10	EL201	Nortek	yes	-32.50717	28.83242	11-Apr-2006 14:45	02-Sep-2006 16:00	82.95	midshelf
11	EL303	RDI 300 + waves	yes	-32.32363	29.02225	11-Apr-2006 17:10	02-Sep-2006 07:00	96	midshelf
12	EL403	RDI 75	yes	-32.96595	28.30622	1-May-2006 19:06	08-Sep-2006 06:45	96	midshelf
13	EL754	RDI 75	yes	-32.57633	28.75208	8-Sep-2006 14:55	12-Dec-2006 08:40	91.99	midshelf
14	EL301	Nortek	yes	-32.50763	28.83210	8-Sep-2006 15:55	12-Dec-2006 10:45	84.78	midshelf
15	EL304	RDI 300	yes	-32.47545	28.79237	8-Sep-2006 16:27	12-Dec-2006 11:45	90	midshelf
16	EL401	Nortek	yes	-32.50753	28.83292	13-Dec-2006 11:28	07-Mar-2007 13:26	81.3	midshelf
17	EL755	RDI 75	yes	-32.64985	28.69545	13-Dec-2006 14:57	07-Mar-2007 15:25	102	offshore
18	EL305	RDI 300	yes	-32.87433	28.43367	13-Dec-2006 20:26	07-Mar-2007 18:02	88.8	midshelf
19	EL501	Nortek	yes	-32.50743	28.83293	8-Mar-2007 06:29	17-Aug-2007 15:34	85.5	midshelf
20	EL756	RDI 75	yes	-32.43732	28.94465	8-Mar-2007 08:45	17-Aug-2007 17:05	196	offshore
21	EL306	RDI 300	yes	-33.15012	28.11602	8-Mar-2007 14:49	14-Aug-2007 11:26	98.7	midshelf
22	EL601	Nortek	yes	-32.50735	28.83287	18-Aug-2007 10:20	06-Dec-2007 15:40	84.84	midshelf
23	EL757	RDI 75	yes	-32.51000	28.83287	18-Aug-2007 10:37	06-Dec-2007 14:52	83.86	midshelf
24	EL307	RDI 300	yes	-33.15005	28.09953	18-Aug-2007 15:19	06-Dec-2007 06:45	83.5	midshelf
25	FR301	RDI 300	yes	-33.85170	27.08120	18-Aug-2007 21:33	05-Dec-2007 16:44	89.6	midshelf

26	EL701	Nortek	yes	-32.50802	28.83293	07-Dec-2007 17:47	30-Mar-2008 08:20	85	midshelf
27	EL308	RDI 300	yes	-33.14983	28.09905	07-Dec-2007 21:07	30-Mar-2008 16:00	85	midshelf
28	FR752	RDI 75	yes	-33.85070	27.08023	08-Dec-2007 01:30	29-Mar-2008 08:30	88	midshelf
29	EL801	Nortek	yes	-32.50754	28.83314	01-Apr-2008 06:05	12-Jul-2008 07:30	87	midshelf
30	EL309	RDI 300	no	-33.14990	28.09933	01-Apr-2008 11:24	11-Jul-2008 15:03	88.7	midshelf
31	FR303	RDI 300	yes	-33.70283	27.29817	1-Apr-2008 16:01	13-Jul-2008 07:24	97	midshelf
32	EL310	RDI 300	yes	-33.14970	28.09903	11-Jul-2008 16:32	10-Dec-2008 17:30	82	midshelf
33	EL901	Nortek	yes	-32.50495	28.83143	12-Jul-2008 13:45	13-Dec-2008 06:50	84.5	midshelf
34	CM301	RDI 300	yes	-32.50737	28.83185	12-Jul-2008 14:06	13-Dec-2008 06:05	82.7	midshelf
35	FR304	RDI 300	no	-33.70290	27.29782	13-Jul-2008 09:41	09-Dec-2008 08:30	96	midshelf
36	FR305	RDI 300	no	-33.70310	27.29803	12-Dec-2008 09:38	4-Feb-2009 03:57	91.72	midshelf
37	EL311	RDI 300	yes	-33.15115	28.09700	12-Dec-2008 17:25	22-Mar-2009 08:30	83.12	midshelf
38	EL1910	Nortek	yes	-32.50560	28.83183	13-Dec-2008 13:23	23-Mar-2009 09:20	86	midshelf
39	CM302	RDI 300	yes	-32.49923	28.82348	13-Dec-2008 13:41	23-Mar-2009 10:10	86	midshelf
40	FR306	RDI 300	yes	-33.70322	27.29727	21-Mar-2009 14:20	24-Aug-2009 08:20	91.5	midshelf
41	EL312	RDI 300	yes	-33.15160	28.08072	23-Mar-2009 11:10	26-Aug-2009 07:20	86.6	midshelf
42	CM303	RDI 300	yes	-32.50638	28.83150	23-Mar-2009 11:10	25-Aug-2009 08:07	83.7	midshelf
43	CM304	RDI 300	no	-32.50790	28.83100	25-Aug-2009 09:15	5-Dec-2009 10:37	83	midshelf
44	EL313	RDI 300	yes	-33.15203	28.08727	26-Aug-2009 08:54	4-Dec-2009 14:30	82.7	midshelf
45	FR307	RDI 300	yes	-33.70333	27.29677	26-Aug-2009 15:24	4-Dec-2009 06:20	84	midshelf
46	EL314	RDI 300	yes	-33.15145	28.00866	4-Dec-2009 14:58	3-Mar-2010 13:15	89.02	midshelf
47	FR308	RDI 300	yes	-33.70335	27.29750	4-Dec-2009 20:06	4-Mar-2010 06:50	93.3	midshelf
48	CM305	RDI 300	no	-32.50733	28.83183	5-Dec-2009 13:39	3-Mar-2010 06:20	85.94	midshelf
49	CM306	RDI 300	no	-32.50725	28.83179	3-Mar-2010 09:10	13-Sep-2010 06:45	84	midshelf
50	EL315	RDI 300	yes	-33.15140	28.08651	3-Mar-2010 15:25	13-Sep-2010 11:30	88	midshelf
51	FR309	RDI 300	yes	-33.71332	27.29745	4-Mar-2010 08:15	3-Sep-2010 15:50	93.2	midshelf

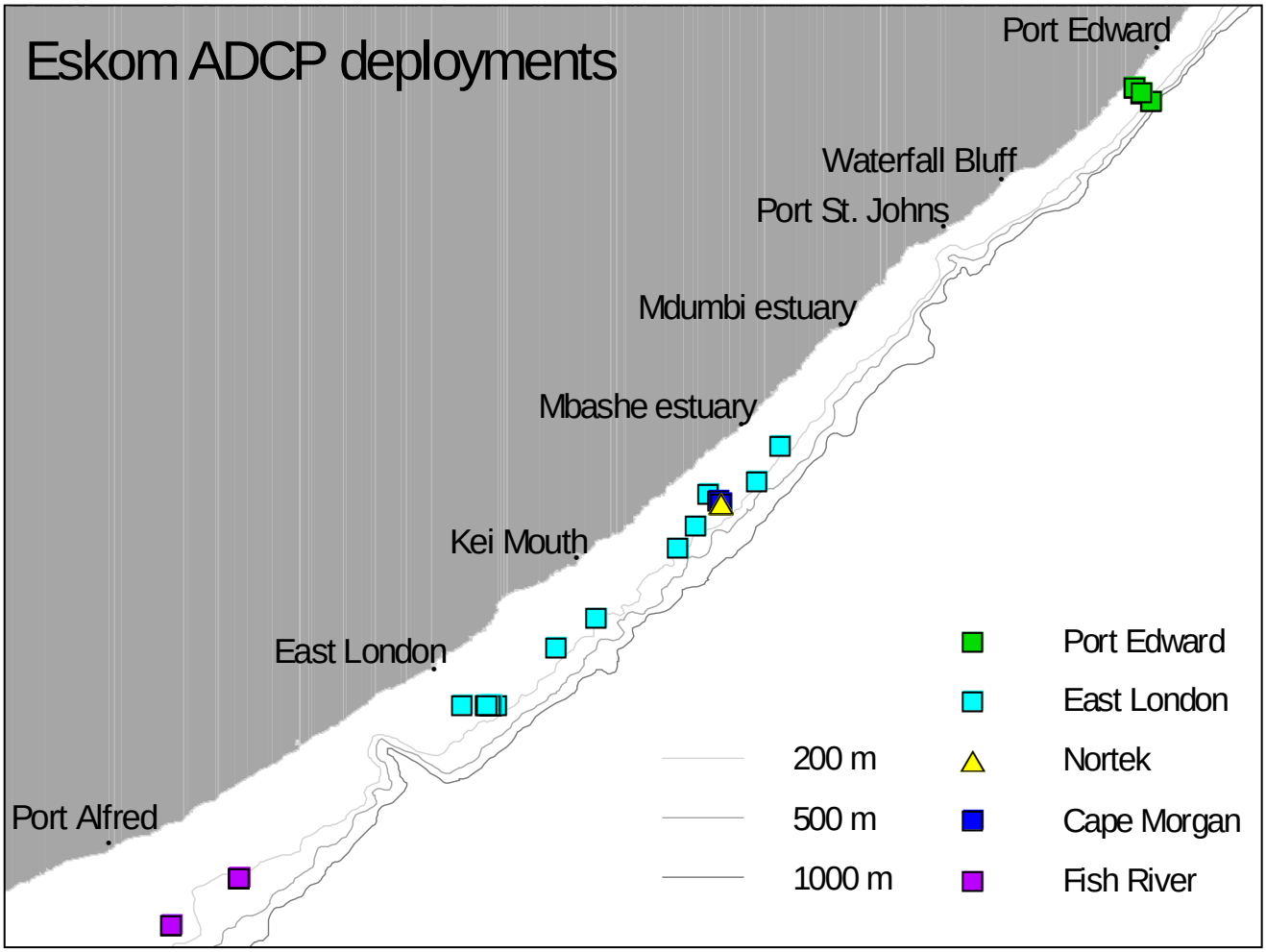

Figure 45: Map of ADCP deployments made on the south coast of South Africa between September 2005 and September 2010.

APPENDIX B. TECHNOLOGY READINESS LEVELS

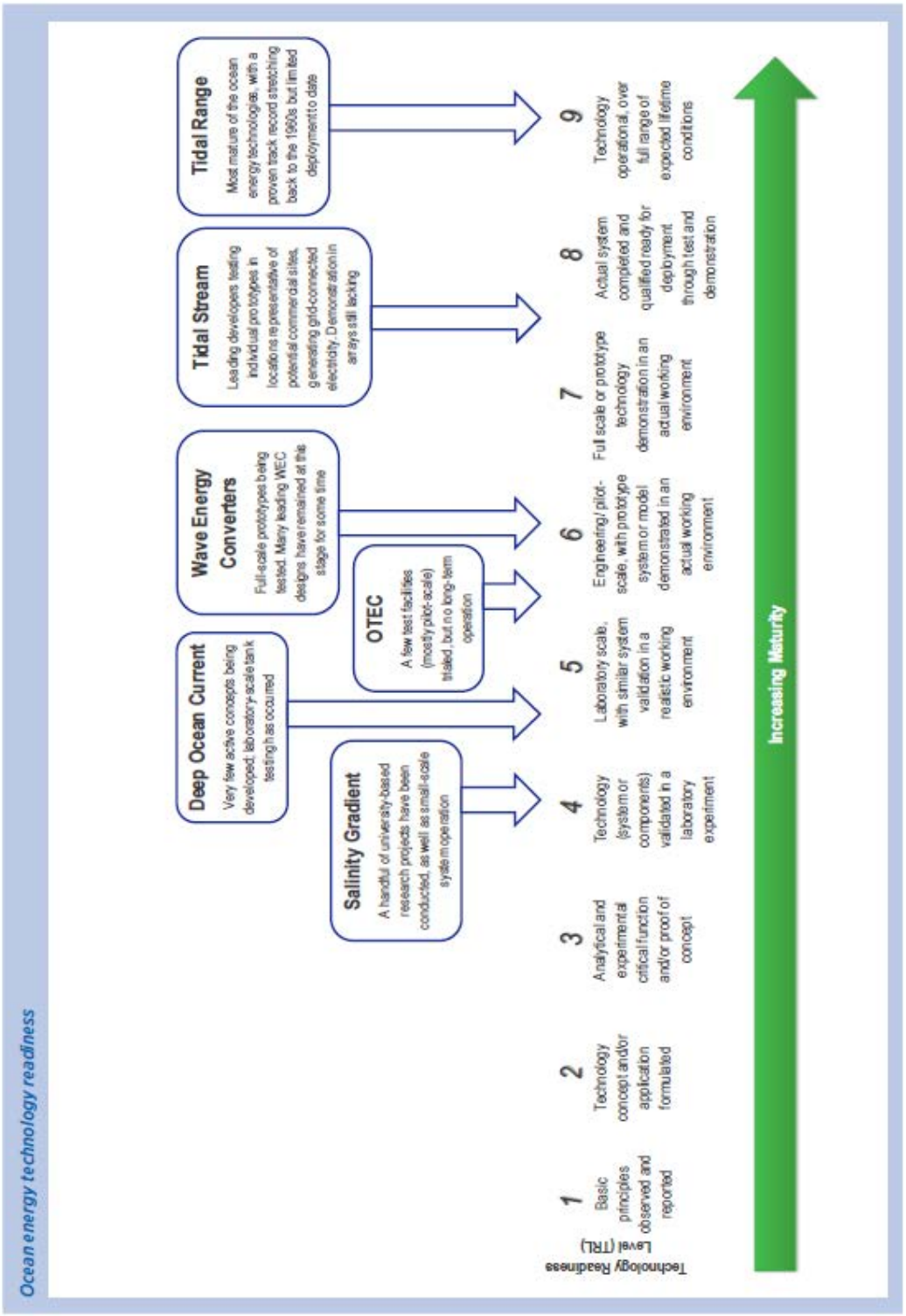

APPENDIX C. INDIVIDUAL MOORING ANALYSIS

The details of the data can be found in Appendix A. The raw data that is useful is found in 3 to 5 month periods of ADCP deployment. Different ADCP types have been used at different sites, which will be noted where applicable. It must also be mentioned that consecutive deployments of ADCP's have not necessarily occurred at the same location, which can prove problematic when attempting annual analysis for one site. The tables below contain basic statistical analysis for each site at a depth of 20 m from the ocean surface. Figure 46 is a schematic of this explanation.

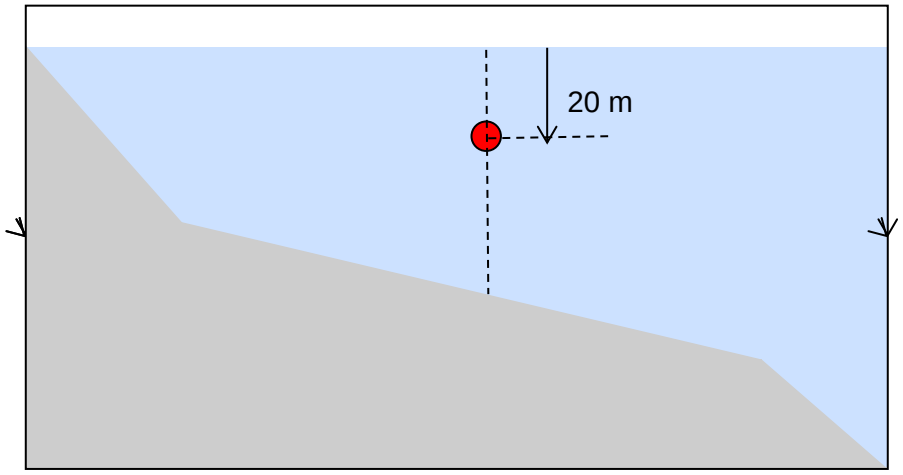

Figure 46: Schematic illustration of where the data measurements are taken (not to scale)

In Table 11 to Table 17, it is seen that some values have been highlighted. These values are where a mean velocity of greater than 1.2 m/s has been observed. A mean value of 1.2 m/s has been chosen, for this indicates that the current will flow at speeds applicable for marine turbines for a large portion of the operating time.

Table 11: Cape Morgan evaluation

At 20 m depth	CM301	CM302	CM303	CM304	CM305	CM306
Sea bed depth	82.7 m	86 m	83.7 m	83 m	85.9 m	84 m
Mean	1.40	0.93	1.64	1.28	1.70	1.37
Median	1.57	0.86	1.70	1.45	1.75	1.58
Standard Deviation	0.60	0.63	0.48	0.52	0.48	0.65
Kurtosis	-0.57	-0.94	0.26	-0.86	1.28	-0.73
Skewness	-0.71	0.39	-0.67	-0.60	-0.93	-0.75
Maximum	2.43	2.60	2.74	2.23	2.82	2.49

Table 12: Port Edward evaluation

at 20 m depth	Midshelf			Offshore	
	PE301	PE302	PEM03	PE751	PE752
Sea bed depth	60 m	61 m	62 m	156 m	173 m
Mean	0.84	1.05	0.86	1.21	1.30
Median	0.87	1.20	0.87	1.32	1.44
Standard Deviation	0.36	0.44	0.36	0.56	0.57
Kurtosis	-0.65	-0.52	-0.29	-0.86	-0.55
Skewness	-0.23	-0.77	-0.04	-0.35	-0.69
Maximum	1.80	1.92	1.92	2.38	2.38

Table 13: Fish River evaluation

at 20 m depth	FR301	FR752	FR303	FR304	FR305	FR306	FR307	FR308	FR309
Sea bed depth	89 m	88 m	97 m	96 m	91 m	91 m	84 m	93 m	93 m
Mean	1.18	1.39	1.01	0.85	1.12	0.88	1.00	1.02	0.98
Median	1.22	1.42	0.94	0.78	1.14	0.77	0.99	1.02	1.00
Standard Deviation	0.48	0.51	0.59	0.51	0.54	0.55	0.50	0.55	0.58
Kurtosis	-0.47	-0.72	-1.02	-0.06	-0.98	-0.68	-0.64	-0.82	-1.04
Skewness	-0.22	-0.13	0.28	0.61	-0.12	0.50	0.20	0.13	0.18
Maximum	2.48	2.73	2.44	2.67	2.19	2.55	2.44	2.77	2.33

Table 14: East London evaluation using the Nortek Sensor

at 20 m depth	EL 1901	EL 201	EL 301	EL 401	EL 501	EL 601	EL 701	EL 801	EL 901	EL 1910
Sea bed depth	83 m	82 m	84 m	81 m	85 m	84 m	85 m	87 m	84 m	84 m
Mean	1.61	1.44	1.57	1.38	1.37	1.55	1.66	1.49	0.60	0.92
Median	1.75	1.59	1.67	1.56	1.46	1.57	1.81	1.82	0.43	0.90
Standard Deviation	0.50	0.54	0.47	0.59	0.57	0.31	0.55	0.76	0.50	0.60
Kurtosis	1.18	-0.07	1.04	-0.88	-0.37	0.52	1.11	-1.30	0.32	-1.18
Skewness	-1.26	-0.91	-1.01	-0.58	-0.46	-0.48	-1.29	-0.40	1.13	0.26
Maximum	2.62	2.39	2.52	2.48	2.70	2.48	2.58	2.58	2.10	2.30

Table 15: East London (scattered) evaluation using the RDI 75 Sensor

at 20 m depth	EL403	EL754	EL755	EL756	EL757
Sea bed depth	96 m	91.99 m	102 m	196 m	83.86 m
Mean	1.23	1.51	1.43	1.48	1.78
Median	1.33	1.61	1.63	1.56	1.79
Standard Deviation	0.54	0.48	0.61	0.59	0.33
Kurtosis	-0.76	0.72	-0.73	0.08	0.32
Skewness	-0.49	-0.95	-0.65	-0.52	-0.43
Maximum	2.31	2.48	2.60	3.22	2.73

Table 16: East London evaluation using the RDI 300

at 20 m depth	EL 303	EL 304	EL 305	EL 306	EL 307	EL 308	EL 309
Sea bed depth	96 m	90 m	88.8 m	98.7 m	83.5 m	85 m	88.7 m
Mean	1.41	1.11	1.48	1.38	1.58	1.84	1.36
Median	1.53	1.16	1.67	1.54	1.63	1.88	1.57
Standard Deviation	0.55	0.45	0.62	0.65	0.44	0.38	0.75
Kurtosis	-0.24	-0.51	-0.40	-0.93	0.21	-0.20	-1.22
Skewness	-0.75	-0.33	-0.80	-0.50	-0.61	-0.43	-0.34
Maximum	2.58	2.13	2.73	2.58	2.83	2.78	2.75

Table 17: East London evaluation using the RDI 300 cont.

at 20 m depth	EL 310	EL 311	EL 312	EL 313	EL 314	EL 315
Sea bed depth	82 m	83.1 m	86 m	82.7 m	89.0 m	88 m
Mean	0.88	1.22	1.39	1.19	1.30	1.16
Median	0.83	1.42	1.48	1.20	1.45	1.31
Standard Deviation	0.51	0.72	0.51	0.51	0.59	0.69
Kurtosis	-0.92	-1.30	-0.60	-0.89	-0.60	-1.28
Skewness	0.25	-0.32	-0.56	-0.05	-0.65	-0.10
Maximum	2.22	2.62	2.37	2.30	2.67	2.79

APPENDIX D. MINESTO TURBINE SPECIFICATIONS

Technical Specifications

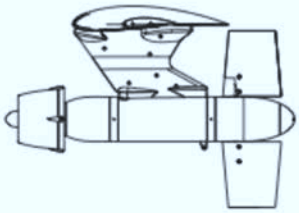

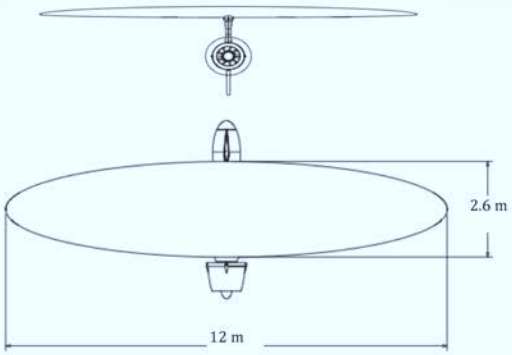

Wing Span	12m
Rated Power	500 kW
Tether Length	85-120m
Depth	75-100m
Desired Speed	1.4-2.2 m/s
Lower/Upper Cut off current	0.5/2.5 m/s
Weight	7 tons
Devices/km²	25
Clearance (tip to surface)	12-16m
Rotor diameter	1m
Swept area	2000m²
Nacelle diameter	0.75m
Nacelle length	4.5m
Nacelle weight	4 tons

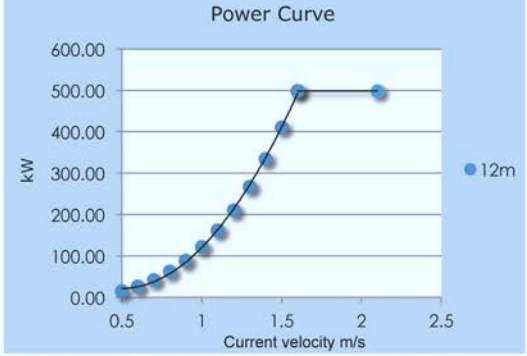

Specifications and operating data are for informational purposes only and do not represent any warranty or promise; data is subject to change without prior notice. © 2011 Minesto

Technical Specifications

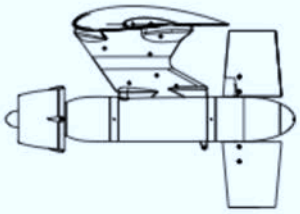

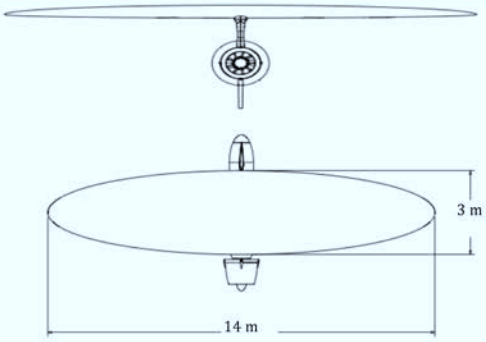

Wing Span	14m
Rated Power (@m/s)	850 kW@1.7
Tether Length	110-140m
Depth	90-120m
Desired Speed	1.4-2.2 m/s
Lower/Upper Cut off current	0.5/2.5 m/s
Weight	11 tons
Devices/km²	16
Clearance (tip to surface)	14-18m
Rotor diameter	1.15m
Swept area	2700m²
Nacelle diameter	0.875m
Nacelle length	5.25m
Nacelle weight	6.35 tons

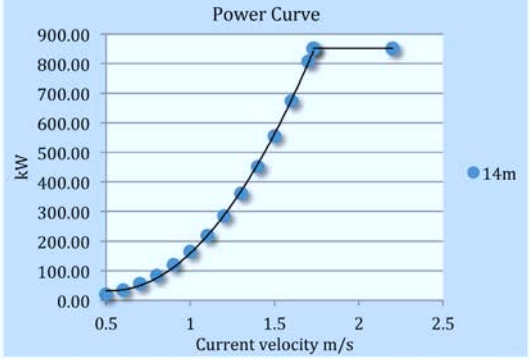

Specifications and operating data are for informational purposes only and do not represent any warranty or promise; data is subject to change without prior notice. © 2011